The Advanced Centre for Biochemical Engineering
Department of Biochemical Engineering
University College London

Growth of Mesenchymal Stromal Cells in Automated Microwell Cultures: Influence of the Engineering Environment on Cell Growth Kinetics and Non-Directed Differentiation

Thesis submitted for the degree of Doctor of Philosophy

Rosario Scott
September 2008

I, Rosario Scott, confirm that the work presented in this thesis is my own. Where information has been derived from other sources, I confirm that this has been indicated in the thesis.

Rosario Scott

02-September-2008

ABSTRACT

Human Mesenchymal Stromal Cells (hMSC) have the potential to differentiate into lineages of mesoderm origin, such as osteogenic, chondrogenic, and adipogenic lineages, presenting a promising potential for autologous regenerative medicine applications. However, one of the major challenges associated with delivering hMSC to the clinic is the propagation of undifferentiated cells *in vitro* in order to reach the quantity required for therapeutic applications. This thesis investigates the effect of environmental parameters that impact cell growth characteristics of hMSC in microwell plates, for the design of an automated cell expansion process in a robotic platform. As a result of this work, the main parameters that can be used to control the growth rate and differentiation potential of hMSC at all stages of the cell expansion process have been identified. A mathematical model has also been developed to forward predict the cell growth characteristic of hMSC for an individual donor, allowing for a patient specific bioprocess design that will ensure enough cells can be supplied back to the patient in a timely manner while assuring the quality of the final product.

Process parameters for the cell expansion process of hMSC in automated microwells have been characterised. Optimum values for inoculation cell density and medium exchange strategies have been proven to reduce the overall time of the cell expansion process for hMSC in an undifferentiated state for their use in regenerative medicine therapies. These parameters were implemented in the cell expansion in an automated platform for the duration of one passage, proving the potential of such technology for the delivery of hMSC to the clinic.

ACKNOWLEDGEMENTS

Being given the opportunity to study for a Ph.D. is a privilege. It is not something I could have undertaken without the support of a number of individuals and institutions.

First, I would like to thank University College London (UCL) for providing the facilities for my studies. I would also like to thank Professor Gary Lye and Dr Chris Mason for their advice and support during my three years at UCL. Special thanks go to Professor Gary Lye for his useful advice and criticism during the review phase of this thesis. I would also like to acknowledge the useful discussion and contributions made by Professor Michael Hoare and Professor Peter Dunhill.

Secondly, I would like to thank Merck Inc. for awarding a three year scholarship which provided me with the time and funds to support my studies. In particular I would like to thank Barry Buckland for taking and interest in my progress throughout my career.

I would also like to thank my fellow Ph.D. and post doctoral students at UCL, the university staff, the university administration, and the laboratory staff for their support. In particular I would like Dr. Waqar Hussain, Dr. Farlan Veraitch, Spyridon Gerontas, Ioannis Papantoniou, Alfred Ding, and Ju-Wei Wong for their discussions, camaraderie, and support. Unlike a Ph.D. which deals with inanimate objects, cell cultures have the annoying habit of requiring attention at all times of the night and day, seven days a week. Without co-workers prepared to cover for each other on occasions I would have got even less sleep than I did during my three years at UCL.

Finally I would like to thank my friends and family for their support throughout my Ph.D. and indeed my entire life. Whatever we achieve in life is nothing if we do not have people with whom to share the highs and lows. I would particularly like to thank my Mother 'Rosario', my Brother 'Rafael', my father 'Rafael', and specially Dr. Jon Poynter for his help, support, and for sharing the highs and lows throughout the completion of this thesis. I would also like to thank Kevin Darbyshire, Monica de la Cruz, Viky Barrios, and Mari-Pierre Gentile for their friendship and support.

TABLE OF CONTENTS

TABLE OF FIGURES

TABLE OF TABLES

CHAPTER ONE

INTRODUCTION

1 INTRODUCTION

Stem cells are undifferentiated cells that have the ability to generate multiple cell lineages and the potential to contribute to tissue homeostasis by replenishment of cells or regeneration of tissue after injury (Woodward et al., 2005; Liu et al., 2005; Li et al., 2005). Biological advances in the last decade have made it possible to study the path of differentiation and the effect of different parameters in stem cell proliferation for regenerative medicine applications. Regenerative medicine is an emerging field, aiming at the study of restoration of tissues and organs that have been injured or diseased. These can be achieved by constructing tissue-engineered organs *in vitro* for transplantation, by transplanting stem cells into the patient to regenerate the tissue *in vivo*, or by using stem cells as gene delivery carriers (Haseltine, 2001; Mironov et al., 2004).

With an increasingly aging population, the demand for regenerative medicine has been rising in the last few years and it is expected to increase in the coming decades. The lack of donors for transplantation and the limited existing therapies to treat degenerative diseases such as cancer, Parkinsons, or Alzheimer, is driving extensive research in the use of stem cells as an alternative source of therapy. The advantage of the use of stem cells versus drug therapies is that stem cell treatments aim at the replacement of diseased tissue with healthy new cells, while drug therapies tend to alleviate the symptoms of the illness without eliminating the damaged tissue or recovering normal function in abnormally behaving cells, tissues, or organs.

Because of their capacity for sustained self-renewal with the potential to differentiate into specialized cell types, stem cells promise a renewable source of human tissue for research, pharmaceutical testing, and cell-based therapies (Mineault et al., 2006). Adult or embryonic stem cells can be used for regenerative medicine applications. Although adult stem cells are not as versatile as embryonic stem cells in terms of differentiation and proliferation potential, they present some advantages over the selection of embryonic stem cells. They can be obtained from the patient, making them autologous and eliminating the need for immune suppressors. Also, the isolation process for adult stem cells is

more robust, and there are no ethical problems posed by the use of cells coming from adult donors.

The main challenge for the success of the use of stem cells in clinical applications is the ability to produce enough material to satisfy the demand (Mason et al., 2006). There are still no effective technological approaches to cultivate stem cells *in vitro*, or to direct differentiation towards a desired lineage. The development of a cell expansion process to proliferate stem cells *in vitro* is complicated by the intrinsic variability of the cell source, difficulty of isolation from the donor, spontaneous differentiation, and the sensitivity of stem cells to micro-environmental conditions.

1.1 Stem Cells

There are three basic categories of cells in the human body: germ cells, somatic cells and stem cells. Germ cells give rise to gametes (eggs and sperm), somatic cells include the bulk of the cells that make-up the human body in their differentiated state, and stem cells have the potential to give rise to cells of different lineages. Stem cells posses three main characteristics that differentiate them from somatic cells (Weissman, 2000):

- self-renewal, or the ability to generate at least one daughter cell after mitosis with identical characteristics to the mother cell
- multi-lineage differentiation of a single cell into one of the three germ layer cells that form an organism
- *in vivo* functional reconstitution of a given tissue

Proliferating stem cells *in vitro* have the unique capacity to renew themselves and the potential to differentiate into cells of different lineages under specific stimuli. Unlike a somatic cell, they can divide symmetrically into two identical daughter cells or asymmetrically generating an identical daughter cell and a differentiated cell.

Depending on their differential potential, stem cells can be classified as totipotent, pluripotent and multipotent. Totipotent stem cells have the ability to

form all cell types, and the capability to form a whole organism. Pluripotent stem cells have the ability to differentiate into cells of all three germ layers (ectoderm, mesoderm and endoderm) but cannot form a whole organism. Multipotent stem cells have the potential of giving rise to a limited range of cells and tissues, and are lineage committed. Therefore, a multipotent stem cell such skin stem cell would give rise to the various types of skin cells (Bongso et al., 2004). Stem cells can also be classified into two categories according to their origin: embryonic and adult.

1.1.1 Embryonic Stem Cells

Embryonic stem cell lines are derived from the inner cell mass of the blastocyst that originates five days after the fertilization of a female egg with a spermatozoid. These cells can be propagated *in vitro* while maintaining pluripotency for extended periods of time. Their differentiation potential is characterised by their ability to transform into cells of the three germ layers that give rise to an organism: endoderm, ectoderm, and mesoderm. Embryonic cells were first obtained from mouse, but it was not until 1998 when J. Thomson derived the first line of human embryonic stem cells (Thomson et al., 1998). Human embryonic stem cells cultured *in vitro* possess the three characteristics that define stem cells (Weissman, 2000), and have been maintained in culture for more than 300 doublings. However, embryonic stem cell lines are an artefact of tissue engineering techniques, since they do not remain as such *in vivo*. The cells that constitute the blastocyst differentiate quickly into different lineages to form tissues and organs for the development of an organism. Embryonic stem cells can also be propagated *in vitro* for months while retaining self-renewal potential and pluripotent characteristics. However, the conditions that regulate the cell propagation and differentiation process of embryonic stem cells is not well understood. As a result of the culture conditions for the propagation of embryonic stem cells *in vitro*, changes in karyotype and gene expression have been reported recently such as mitotic errors in chromosome 21 (Katz-Jaffe et al., 2004) and gain of chromosomes 17 and 12 (Drapper et al., 2004). Until we understand the cues that make an embryonic stem cell decide its fate, being division,

differentiation, apoptosis, or adaptation, it will not be possible to implement clinical applications for cell or tissue replacement.

1.1.2 Adult Stem Cells

Adult stem cells of limited differentiation potential are found in many organs and tissues in the body including brain, bone marrow, peripheral blood, blood vessels, skeletal muscle, skin, teeth, heart, gut, liver, ovarian epithelium, and testis. They are thought to reside in a specific area of each tissue, called a "stem cell niche". They still possess stem cell characteristics of self-renewal and differentiation, but they have limited proliferation potential *in vitro* (DiGirolamo et al., 1999). Their self-renewal potential is maintained in the body, since these cells are involved in the maintenance and repair of tissues and organs throughout the life span of the individual (Young et al., 2004). Typically, there is a very small number of stem cells in each tissue, and once removed from the body, their capacity to divide is limited, making generation of large quantities of stem cells difficult.

Some examples of differentiation pathways of adult stem cells are hematopoietic stem cells that give rise to all type of blood cells, mesenchymal stem cells that mature into cells of mesoderm lineage, epithelial stem cells that give rise to cells in the lining of the digestive tract, and neural stem cells that give rise to neurons, astrocytes and oligodendrocytes (D'Amour et al., 2005).

Stem cells that mature into cells of mesoderm origin have been isolated following different techniques which has given rise to the discovery of several cell lines with particular characteristics such as mesenchymal stromal cells, MIAMI cells and MAPC.

1.1.2.1 Human Mesenchymal Stromal Cells

Human Mesenchymal Stromal Cells (hMSC) are the precursors for cells of mesoderm origin such as osteocytes, adipocytes, and chondrocytes (Pittenger et al., 1999; Jaiswal et al., 2000). Although the richest source of hMSC in the adult body is the bone marrow (Wexler et al., 2003), they have been isolated from a variety of tissues including umbilical cord (Romanov et al., 2003), peripheral

blood (Wexler et al., 2003), placenta (in't Anker et al., 2004), adipose tissue (Zuk et al., 2001), and skeletal muscle (Sinanan et al., 2004).

hMSC were isolated initially by Friedenstein et al. in 1976 based on their adherence to tissue culture surfaces. Following a bone marrow extraction from the patient through the iliac crest, mononucleated cells can be isolated from the mixture of blood, adipose tissue and bone marrow obtained from the extraction. The mononucleated cells can be isolated from this bone marrow sample by a density gradient centrifugation. Red blood cells sediment at the bottom, platelets at the top, and the mononucleated portion of cells remains in the inter-phase. The mononucleated cells are plated in a T-flask, and hMSC are isolated on the basis of their adherence to the plastic culture (Gronthos et al, 1994). hMSC have been expanded *in vitro* for up to 50 population doublings before senescing, showing average telomere lengths and normal karyotype but exhibiting poor proliferation beyond 30 population doublings (Reyes et al., 2001). In spite of not losing their normal karyotype and telomerase activity after extensive subcultivation, other results have shown that hMSC can only be expanded for 15 doublings, while others cease replicating after four cell doublings after which signs of senesce and/or apoptosis appear (Conget et al., 1999; Bruder et al., 1997; DiGirolamo et al., 1999; Phinney et al., 1999).

While the terminology of human Mesenchymal Stem Cells (hMSC) has been used to describe the plastic-adherent cells isolated from bone marrow with multipotent differentiation capacity, some investigators decided to omit any reference to stem cells when publishing clinical and pre-clinical studies due to the difficulty in their characterisation as stem cells and the scientific implications of use of such a term (Pereira et al., 1998; Keating et al., 1998, Horwitz et al., 1999). The term 'Mesenchymal Stromal Cells' was proposed by Horwitz in 2003 and it has been widely used since, with the advantage of having the same acronym for the continuation of the scientific discourse.

One of the major challenges for the expansion of hMSC remains the fact that they have not yet been fully characterised. It is difficult to determine if the cell population remains as a homogeneous culture of hMSC after isolation and

extensive subcultivation, or if a mixed population of committed progenitors together with hMSC from the bone marrow aspirates are present in the culture. Many molecular markers expressed in hMSC are also found on other cell types such as fibroblast with which they share identical morphology (Ishii et al., 2005), and a combination of different markers is normally used to determine the identity of the population. In spite of the biological challenges still unresolved in order to fully characterise hMSC during routine subcultivation and extrapolate such analysis to future functional success in the clinic, these cells provide a promising alternative for the use in regenerative medicine applications.

1.1.2.2 MIAMI

A novel way to isolate and proliferate adherent dependent cells from bone marrow has been reported to produce a new population of progenitor cells, named MIAMI for marrow-isolated adult multilineage inducible cells. This population of progenitor cells express Oct-4, SSEA4, and Rex-1, which are embryonic stem cell markers, and differentiate into germ layers of mesodermal, ectodermal, and endodermal origin. They also differ from hMSC in that they show self-renewal capability *in vitro* for up to more than 50 population doublings, with doubling times ranging from 20 to 36 hour as indicated in the International Patent WO 2004/06172A2 describing the derivation and uses of MIAMI cells (Schiller et al., 2004). MIAMI cells are identified by the unique set of markers shown in Table 1.1. Interestingly, these cells do not express HLA markers, which would make them potentially resistant to immune rejection and an attractive source of readily-available pluripotent cells for regenerative medicine applications with no need for patient-specific cell expansion processes. Worth noticing is that the isolation process by which MIAMI cells are selected only on the basis of their adherence to a culture surface plate, does not prove that a heterogeneous population is the result of this isolation. As with hMSC, it remains to be determined if a mix population of progenitor cells carried over from the isolation from bone marrow may be responsible for the pluripotent behaviour of these cells. Single-cell derived colonies or retroviral marking strategies should be completed to address the homogeneity and clonal identity of MIAMI cells.

Table 1.1. Representative MIAMI Cell Markers (Schiller et al., 2004, p. 18).

Marker	MIAMI Cell Expression	Marker	MIAMI Cell Expression
CD10	+	CD117 (cKit)	-
CD13	-	CD122 (IL-2Rβ)	+
CD29	+	CD133	-
CD34	-	CD156	+
CD36	-	CD164	+
CD44	+	BMP-receptor 1B	+
CD45	-	CNTFR	+
CD49b	-	HGF Receptor (c-Met)	+
CD49e	+	Class I-HLA	-
CD54(ICAM-1)	-	HLA-DR	-
CD56 (NCAM)	-	hTERT	+
CD63	+	NTRK3	+
CD71	-	POU4F1 (Oct-4)	+
CD81 (TAPA-1)	+	Rex-1	+
CD90	+	SSEA4	+

The isolation and culture conditions used to select MIAMI cells, mimics the microenvironment of adult stem cells in their original niche, including low oxygen levels (3-5% O2), co-culture with non-adherent cells from bone marrow, and fibronectin-coated culture surfaces. The cells isolated under physiological conditions were later selected according to their adherence to the culture plate, resulting in this new population named MIAMI cells (D'Ippolito et al., 2004).

Their differential potential, extended proliferation life *in vitro*, and fast doubling time, demonstrate these cells to be a promising cell source for regenerative medicine applications. However, this work has not been reproduced by any other group yet, and the clinical performance of MIAMI cells remains to be proven.

1.1.2.3 MAPC

Catherine Verfaille's group in the University of Minnesota, isolated a new population of adult stem cells while attempting to isolate MSC from human and rat bone marrow. This distinct cell population, named multipotent adult progenitor cells or MAPC, differ from MSC in that they appear to proliferate

without senescence and in their pluripotent differentiation ability *in vitro* and *in vivo*. They have been shown to expand *in vitro* for up to 150 population doublings, and to differentiate into cells of not just mesenchymal lineage, but also endothelium and endoderm (Jiang et al., 2002).

Some modifications to the well-established protocol for the isolation of hMSC from bone marrow resulted in the discovery of this new population of progenitor cells. The main change to this protocol consists in an antibody negative selection for CD45 and glycophorin A (hematopoietic markers) expressing cells by means of micromagnetic beads, after the density gradient centrifugation step that separates mononucleated cells from the bone marrow sample. The cell expansion of these cells play a crucial role on the maintenance of the characteristic of MAPC, and it is based on tight control over cell density at inoculation and harvest, CO_2 concentration, and pH of the medium. Unlike hMSC, MAPC do not express major histocompability (MHC) class I antigens, and are CD105 (or SH2) negative, but as hMSC they do not express any of the hematopoietic markers (Jiang et al., 2002; Reyes et al., 2002; Schwartz et al, 2002).

From the work published up to now, MAPC show great potential as a cell source for regenerative medicine. However, there is no evidence that these cells exist as such *in vivo*, and further studies on the mechanism of isolation of MAPC need to be done since no other group has been able to reproduce this work. The implications of transplanting these cells into patients before further characterisation of karyotype changes, functionality, and gene expression over time *in vitro* and *in vivo* need to be addressed before a clinical application can be envisaged.

1.1.3 Clinical Applications of hMSC

Mesenchymal stem cells can be isolated, expanded in culture, and differentiated into bone, cartilage, muscle, tendon, fat, and a variety of other connective tissues. This, together with the fact that the cells can be isolated from the patient eliminating the risk of immune rejection, makes hMSC an ideal candidate for stem cell therapy and tissue-engineered organs for implantation (Ishii et al., 2005).

Stem cell transplantation has been used a routine therapy for leukemia patients, where bone marrow mononucleated cells are injected from a donor to a patient to replenish hematopoietic stem cells. For mesenchymal stem cells, a few clinical studies show promise of safety and efficacy for future applications. Allogeneic bone marrow transplantation in osteogenesis imperfecta patients resulted in 1.5% to 2.0% engraftment of donor osteoblasts, suggesting that mesenchymal precursors present in the marrow may have a potential therapeutic role (Horwitz et al., 1999). In a canine model of chronic myocardial ischemia, canine MSC injected intravenously caused a reversal of reduced left ventricular ejection fraction, which was fatal in control animals. In a goat model, injected MSC into the knee joint appeared to slow development of osteoarthritis. In humans, co-transplantation of hMSC with HLA-identical sibling hematopoietic stem cells appeared to decrease the incidence of graft-versus-host disease and to improve disease-free survival (Deans et al., 2000). hMSC have also been propagated *in vitro* together with amnion epithelial cells to develop a tissue-engineered membrane to restore the fetal membrane integrity after spontaneous premature rupture of membranes, which complicates 1% of all pregnancies (Ochsenbien-Kolble et al., 2003).

One of the most promising studies is the use of MSC to remodel and restore performance of infracted hearts. To overcome the poor cell viability associated with transplantation *in vivo,* Mangi et al. in 2003 genetically engineered rat mesenchymal stem cells using *ex vivo* retroviral transduction to over express the pro-survival gene Akt1. Transplantation of $5x10^6$ cells into the ischemic rat myocardium repaired the infracted myocardium, and nearly normalized cardiac performance.

The discovery of differentiation of hMSC into astrocytes and neurons shows the potential clinical applications in treating a variety of central nervous system disorders, such as brain injury, stroke, Parkinson's disease, and other neurodegenerative disorders (Kopen et al., 1999; Sanchez-Ramos et al., 2000; Mezey et al., 2000). Other applications for hMSC are being explored, including their use as feeder layers for the cell expansion of human embryonic stem cells (Cheng et al., 2003) as a replacement for mouse fibroblast. Further studies

ensuring the homogeneity of the hMSC population implanted for these studies must follow in order to prove that these findings are reproducible and not an artefact of precursors present after isolation or phenotypic changes due to uncontrolled environmental manipulations during cell expansion.

Safety considerations while expanding hMSC for clinical application must be taken into account. With the current cell expansion process that is being used by most researchers, hMSC can undergo spontaneous transformations such as mutations in their tumorogenic check points during cell division, that support the hypothesis that cancer stem cells originate from adult stem cells, as shown by Rubio et al. (2005) and Bapat et al. (2005). The potential of hMSC for different clinical applications suggests that in the coming years the demand for processes that can successfully propagate these cells *in vitro* will increase considerably.

1.1.4 Characterisation of hMSC

One of the main challenges in the study of stem cells is to be able to characterise the population at different stages of proliferation under different experimental conditions. The reason being it is the lack of information on specific markers that define the cell types as hMSC, with the sole definition being their ability to differentiate along specific lineages when induced to do so (Tuan et al., 2003). Because of the lack of a definitive set of surface markers that would determine the identity of hMSC, several analyses are needed to determine the characteristics of the population as a stem cell population. Most analyses are sacrificial, and require large amounts of cells to collect statistically significant data. Considering the limited number of stem cells obtained after isolation, it is a major challenge to acquire enough data throughout the cell expansion life of a stem cell population, especially for those with limited proliferation potential. Because the cells are the product and the number of cells obtained from one isolation is limited, there is frequently not enough cellular material from a given donor to characterise the phenotype of the population, nor to determine the karyotype, tumorogenicity, and functionality *in vivo* after undergoing a cell expansion in the laboratory.

At the moment, the minimum analyses required to characterise and analyse a population of stem cells include flow cytometry for surface markers (Table 1.2),

Q-PCR for gene expression, telomerase activity, telomere length, karyotype, and functionality test to differentiate stem cells into different germ layers. Not as widely used, but in need of further studies are cell cycle analysis, metabolism, apoptosis, and senesce of the population over the extent of the cell expansion process.

At present, characterisation of hMSC is widely accomplished by flow-cytometry analysis of surface markers. They are positive for CD34 upon bone marrow extraction, although they lose the expression of this marker soon after isolation and during subcultivation. Stro-1 has been identified as a marker for cells that can differentiate into multiple mesenchymal lineages by Gronthos et al. (1995). However, findings by Ishii et al., (2005) suggested that Stro-1 was not essential for the differentiation potential of hMSC. Furthermore, Fickert et al. (2004) showed that a CD9/CD90/CD166 triple positive subpopulation of hMSC showed multipotency for chondrogenic, osteogenic and adipogenic differentiation providing a basis for identification of hMSC. Expression of CD166 is indicative of multipotency in hMCS. However, the level of expression has been shown to decrease with increasing cell density in culture and regained during inoculation of successive passages (Yeh et al., 2005). Expression levels of CD90 and CD105 (SH2) are maintained over sequential passages and they can be important for validating cultures of hMSC intended for therapy (Honczarenkoa et al., 2006). A good indication of hMSC identity can be reached by expression of CD90, CD105 and CD166 as a minimum set of surface markers. A more extensive list has been compiled from results obtained by different groups (Table 1.2), showing the different surface marker expression in three adult progenitor cell populations. This table of surface marker expression across hMSC-like stem cells highlights the differences in surface marker expression for different populations derived from bone marrow: human mesenchymal stem cells, multipotent adult progenitor cells (discussed in 1.1.2.3), and a subpopulation of agranualar rapidly dividing cells isolated from hMSC identified by Prockop et al. (1997) and named RS-1.

Table 1.2. Surface Antigen Comparison Among hMSC-like Cells: Mesenchymal Stromal Cells (MSCs), Multipotent Adult Progenitor Cells (MAPCs), Recycling Stem (RS-1) Cells - small agranular and rapidly dividing subpopulation of hMSC (modified from Pittenger et al, 2004)

Surface antigen	MSCs	MAPCs	RS-1	Surface antigen	MSCs	MAPCs	RS-1
CD9	+			CD50 ICAM3	-	-	
CD10		-	-	CD54 ICAM1	+		
CD11a,b	-		-	CD62E E-selectin	-	-	
CD13	+	+		CD71 trasferrin rec	+		+
CD14	-		-	CD73 SH3	+		
CD18 integrin β2	-			CD90 Thy-1	+	+	+/-
CD29	+			CD105 SH2	+		
CD31 PECAM	-	-	-/+	CD106 VCAM	+	-	
CD34	-	-	-	CD117	-	-	
CD44	+		+	CD133	-	+	-
CD45	-	-	-	CD166 ALCAM	+		
CD49b integrin α2	+	+		HLA ABC	+	-	+/-
CD49d integrin α4	-			HLA DR	-	-	-
CD49e integrin α5	+		+	SSEA-4	+	+	

1.1.5 Plasticity and Reprograming

The term 'plasticity' has been introduced recently in the adult stem cell research community to indicate the greater differentiation potential in post-natal adult progenitor cells than previously thought (Verfaillie, 2002). Up to now, it was believed that stem cells followed one direction of differentiation from pluripotent or multipotent to a lineage-committed precursor, and from there to a somatic cell type. However, different investigators have shown that adult stem cells may have the potential to differentiate into cells of different lineage than the one they are precursors for (Krause et al., 2001; Horwitz, 2003) or that they can change their phenotype according to microenvironment conditions (Ferrari et al., 1998; Sanchez-Ramos et al, 2000).

Stem cell plasticity has been defined as “the ability of a stem cell from a specific tissue or organ to acquire the phenotype of another cell from a different tissue or organ, and in some cases, to switch between somatic mesodermal, ectodermal,

neural crest and endodermal lineages" (Martin-Rendon et al., 2003). Cell plasticity has been shown for hematopoietic cells, indicating that they can trans-differentiate into different lineages and that their engraftment and progenitor phenotypes vary inversely with cell cycle transit (Quesenberry et al., 2002).

Possible explanations for the perceived plasticity of adult stem cells include: the heterogeneity of the population, cell fusion of transplanted cells with host cells, trans de-/re-differentiation of cells when removed from their niche, and conservation of pluripotency during adulthood (Verfaillie, 2002).

The argument that plasticity is an artefact of a non homogeneous population of stem cells, where tissue committed cells within the cell population are responsible for the differentiation into different lineages, and not the plasticity of lineage-committed stem cells has been studied by single progeny populations for neural stem cells but not for hMSC. It has been suggested that bone marrow contains not just hematopoietic and mesenchymal stem cells, but also endothelial stem cells (ESC), multipotent adult progenitor cells (MAPC), pluripotent stem cells (PCS) as well as tissue committed stem cells (TCSC), identifying the isolation process one of the main causes for perceived plasticity (Ratajczad et al., 2004).

The difficulty in isolation and characterisation of specific stem cell and progenitor cell populations from bone marrow makes either argument difficult to prove until further studies are able to show clear characterisation and development of cell fate from bone marrow *in vitro* and *in vivo*.

Pluripotency can also be induced in somatic adult cells by retroviral transduction of defined transcription factors such as Oct3/4, Sox2, Klf4, and c-Myc expressed in embryonic stem cells (Takahashi et al, 2007). The direct reprogramming of somatic cells to give rise to stem cells with induced pluripotency is of great interest and it has the potential to generate a source of patient-specific cells. Other strategies of reprogramming somatic cells such as nuclear transplantation, cellular fusion, and culture induced reprogramming have been reported previously and have been extensively reviewed (Jaenisch et al., 2008), although the advantages of viral-mediated transduction of stem-characteristic transcription factors for

therapeutic applications is drawing a lot of attention towards improving the yield as well as the safety of this technology.

1.2 Bioprocess Conditions for Cell Expansion of hMSC

In vitro expansion of hMSC allows cell proliferation in an undifferentiated state for a limited number of passages before senesce occurs, dependent upon the source of the cells (Hayflick, 1965; DiGirolamo et al.,, 1999; Sekiya et al., 2001). Different parameters intrinsic to the nature of the cells affect the proliferation potential of hMSC and the quality of the cells produced. Because of the variability of cell growth kinetics according to age, sex, health, (Stolzing et al., 2006, Phinney et al., 1999) and the isolation technique used to separate cells from bone marrow, it is a challenge to design a robust expansion protocol that ensures enough cells are produced for further clinical applications.

To date, not much effort has been directed towards controlling physical parameters during the cell expansion process. Most of the research in adult stem cells has been targeted towards differentiation potential with the aid of chemical additives. Recently Zhao and coworkers have discovered the sensitivity of hMSC when cultured under hypoxic conditions that mimic the microenvironment within the bone marrow (Zhao et al, 2005). Studies such as this one on hMSC as well as in embryonic stem cells investigating the effect of environmental conditions on growth kinetics and differentiation has turned attention to the importance of controlled environmental conditions during proliferation of stem cells (Veraitch et al., 2008).

1.2.1 Isolation of hMSC From Bone Marrow Aspirates

Mesenchymal stem cells can be isolated from bone marrow, blood, umbilical cord, and muscle. Only 1 in $1x10^7$ to $1x10^8$ cells in bone marrow is a mesenchymal stem cell (Reyes et al., 2001; Silva et al., 2003), therefore the isolation technique used to recover such a small amount of cells is a crucial step in the cell expansion protocol.

Different methods to select for hMSC within a tissue have been reported in literature, such as immunomagnetic selection (Largar'kova et al, 2006) or size-sieved isolation (Hung et al., 2002) or flow cytometry (Zohar et al., 1997). However, the results from different studies with hMSC are variable because there is no standardized protocol for preparing and characterising hMSC, and this is hindering the development of cell and gene therapies using adult stem cells from bone marrow (Smith et al., 2004). A widely used method of isolation is by density gradient centrifugation over a bed of Ficoll (Caplan, 1991; Clark et al., 1995; Bruder et al, 1997). This separation is not highly selective, recovering all mononucleated cells from a mixture of blood and bone marrow. The isolation is completed during the first passage on the basis that hMSC are the only cells that attach to the surface of a culture vessel. Removal of supernatant after seeding the isolate into a culture flask separates hMSC from all other cells. There are several variations in this protocol that can make the separation more efficient or can produce cells with better propagation and differentiation potential.

The process involves several aseptic manipulations and at least two centrifugation steps. Considering that the crude sample contains granulocytes, debris, bone fragments, adipose tissue, and macrophages, it is important to minimise the processing time to avoid further damage of hMSC during the process. Released DNA will bind and make the mixture more viscous making it hard to separate, ubiquitin, granulocytes, and macrophages can degrade or engulf other cells as well. Also, for samples that have been cryopreserved with DMSO, processing time is of importance since this chemical is toxic to the cells at room temperature (Horita et al., 1964).

1.2.2 Culture Vessels for the Cell Expansion Process of hMSC: T-flasks, Bioreactors, and Microcarries

Mesenchymal stem cells are adherent dependent, in that they need a surface to adhere to, for survival and proliferation. They are also contact inhibited (Ball et al., 2004), which means that they will only grow until they form a monolayer and are in contact with other hMSC cells, after which they stop proliferating and apoptosis or senesce occurs. These characteristics make the cell expansion

process more challenging than suspension cultures from an engineering perspective, since large surface areas are needed to scale up the process.

1.2.2.1 T-flasks

Laboratory techniques used to expand hMSC are based upon passages in T-flasks, which are convenient for research purposes since they are easy to manipulate and can provide enough cellular material for characterisation analysis. However, T-flasks are a batch culture technique and do not allow online monitoring and control of metabolites, cell concentration, dissolved gasses, or pH, all of which are critical parameters in the development of a robust cell expansion process. T-flasks can easily be scaled up to Nunc Cell Factories, which range from one to forty trays of 1250 cm^2 per tray. These culture vessels have been used for production of large number of cells for vaccine and protein production e.g. Chu et al., 2001. For the purpose of scaling up production of hMSC, this technology is impractical, since not so many cells are available from an individual patient as to inoculate such large culture surfaces.

1.2.2.2 Bioreactors

A bioreactor is a closed system that allows cell expansion of animal cells without the need for open aseptic manipulations with their inherent risk of contamination. For the propagation of mammalian cells on a large scale, there have been more studies undertaken with stirred-tank bioreactors designed for the propagation of suspension cultures than for adherence-dependent cell cultures. The main reason for this is that there are many more biological products derived from mammalian cells cultured in suspension than for those cultured on surfaces. For example, the biotechnology industry has thrived in the last twenty years from the production of monoclonal antibodies in CHO or NSO cells, and most vaccines are also produced in suspension cultures. However, stirred-tank bioreactors can also be used for adherent cell lines if they are cultured using microcarriers or by cell adaptation to suspension culture as demonstrated by Baksh et al. (2003).

The recent discovery of stem cells, (embryonic and adult), as a new technology for regenerative medicine has driven interest in the design of alternative

bioreactors for the cell expansion of adherent cells. An example of this is the automated bioreactor designed by Kino-Oka et al. (2005) that can perform a series of manipulations such as medium exchanges and passages while providing process control capabilities. Also, Koller et al. (1993) developed a perfusion culture bioreactor for the expansion of hMSC and optimised the process for maximum cell growth. Bioreactor as well as automated cultures will enable a tighter control of the cell expansion process for hMSC, resulting in a more robust process for the commercialisation of adult stem cells for therapeutic applications.

1.2.2.3 Microcarriers

Microcarries are commonly used in the cell expansion of adherent dependent cells. These are porous or non porous particles, which can be spherical or flat, that allow attachment of cells on the surface while being kept in suspension in a shake flask or stirred-tank bioreactor. Nunc has recently designed flat microcarriers with the same polystyrene surface used in T-flasks (Lenglois et al., 2004; Kenda-Ropson et al., 2001), with the advantage that the surface of the microcarriers can be activated by electron beam irradiation allowing the cells to detach by lowering the temperature to 20˚C (Kenda-Ropson et al., 2002). The principle advantage of microcarriers over T-flask is the larger surface area per unit volume of media in the system. The cells have easier access to nutrients and oxygen because mass transfer is driven by convection in microcarriers cultures, instead of diffusion in T-flasks. Because microcarries are maintained in suspension, the culture can be expanded in bioreactors which allows tighter control over culture conditions. Process conditions can be optimised for cell growth using fed batch or perfusion techniques. Cell sampling is also easier and the process can be readily scaled up. Shan et al. (2004) demonstrated that hMSC proliferation rate was three to five times higher in Cytodex3 microcarriers than in T-flasks. Similar improvement in proliferation rates were also observed by Wu et al. (2003) while growing hMSC on macroporous CultiSher G microcarriers in spinner flasks as opposed to T-flasks. One of the disadvantages of using microcarriers as a means to extend the surface area for anchorage dependent cell cultures is the difficulty on dissociating cells from the surface and the subsequent separation of dislodged cells from the microcarriers. The process that is already

troublesome to accomplish in the laboratory scale results in yield loses of cells that remained entrapped in the higher density microcarrier pellet that settles at the bottom of the flask or bioreactor. This difficulty is not of major importance for somatic cell lines used in the biotechnology industry since the product is secreted from the cells or extracted by cell lysis. For tissue engineering applications where the cells are the product, cell yield losses as well as deterioration of cell quality due to separation and recovery from microcarrier cultures must be studied and optimised further before this technology can be considered as a viable process for the expansion of stem cells.

1.2.3 Effect of Dissolved Oxygen on hMSC Cultures

hMSC are cultured *in vitro* at atmospheric pressure and oxygen levels, whilst regulating % CO_2 to 5% (v/v) to maintain the pH of the media. Temperature is the only parameter that mimics physiological conditions at 37˚C. The loss of proliferative and differential potential of hMSC *in vitro* versus *in vivo* is in part due to this change of physical parameters.

hMSC environmental conditions *in vivo* include 2-5% dissolved oxygen instead of the 20% oxygen that is currently used for culture *in vitro*. It has been suspected that cell proliferation at higher oxygen concentrations has a detrimental effect on the growth and differentiation of hMSC *in vitro*. As an example of the loss of differentiation potential due to higher oxygen concentration for osteoblast, it has been shown that transient changes in oxygen tension inhibit osteogenic differentiation (Salim et al., 2004). Also, Fink et al. (2004) found that hMSC exhibited adipocyte-like phenotype when cultured at 1% oxygen, but they did not show adipocyte-specific transcription patterns, indicating a change in phenotype but not true adipogenic differentiation.

Growth of hMSC with 20% oxygen may cause oxidative stress and be responsible for rapid erosion of the telomere length that determines the population doubling limit of the cells. To corroborate this theory, oxidative stress, telomere length and telomerase activity have been measured for hMSC expanded under different oxygen concentrations. Results have shown that cells can reach 60 population doublings (PD) under 5% oxygen versus 40 PD with 20% oxygen

before entering cell arrest. More intracellular oxidants were also found for the high oxygen condition, although they were not responsible for telomere erosion since telomere length and telomerase activity were found to be similar for both conditions (Martin et al., 2004, Moussavi-Harami et al., 2004). In a more recent study, it has been shown that hMSC do not exhibit telomerase activity unless transfected with hTERT (Zimmermann et al., 2003, Abdallah et al., 2005).

Studies to date have shown that maintaining hMSC cultures under physiological oxygen concentrations result in a higher population doubling limit. However, further studies are needed to determine the effect of oxygen in metabolic rates, growth rates, viability, gene expression, differentiation potential, and phenotype of hMSC.

1.2.4 Effect of Extracellular pH on hMSC Cultures

Most media formulations contain sodium bicarbonate as a buffering agent to maintain the pH close to 7.5. Mammalian cell growth starts to decrease below pH 6.9 and above pH 7.7, but each cell line has an optimum pH within this range that maximises growth rate and viability. Optimum pH has been shown for different cell lines not just in terms of cell growth, but also in terms of product formation. Sometimes optimum pH for cell growth does not correlate with optimum pH for antibody production or virus infectivity, and adjustments need to be made to achieve maximum yield of the desired product (Miller et al., 1988).

For a given population of stem cells in culture, optimum pH is determined by maximum cell growth and viability whilst maintaining desired differentiation patterns. For instance, for neural stem cells, it has been shown that manipulation of environmental pH levels, results in 40% higher densities and 15-20% higher viabilities during the dissociation of cells in bioreactors (Sen et al., 2004). Variations of environmental pH can also affect functionality and differentiation patterns of stem cells, as shown for trophoblast which increase fibronectin secretion for ranging from 6 to 8. The study has also been performed for hMSC showing no effect on fibronectin secretion due to changes in pH, however, the effect on cell growth or differentiation was not studied (Gaus et al., 2002). Analysis of optimum pH has not be published for hMSC or embryonic stem cells,

but as shown for other stem cell populations it may affect cell characteristics and needs to be addressed in the near future.

1.2.5 Effect of Agitation and Shear on hMSC Cultures

Mechanical forces also have an impact on stem cell growth and differentiation. Mesenchymal stem cells are adherent dependent and only grow once attached to a surface. After initial attachment to the culture surface, they can be exposed to agitation and shear if grown on microcarriers and during the centrifugation step at harvest to remove trypsin before inoculation into a new vessel. The sensitivity of hMSC to agitation and shear stress has not been studied.

Agitation and shear can disrupt the cytoskeleton and plasma membrane of the cells, and can also be a trigger for differentiation or gene expression. There are studies on the sensitivity of mammalian cells to agitation and shear. However, it is well know that stem cells are more sensitive to physical conditions than other cell lines, and it is important to understand the impact of such conditions on cell growth and differentiation. For example, one study on the effect of mechanical strain on hMSC differentiation indicated that strain levels modulate differentiation to osteogenic but not chondrogenic lineages (Taboas et al., 2003). Quantitative assessment of strain and stress levels applied to hMSC during routine subcultivation have not received much attention, and the effect of such environmental manipulations on the cells are unknown.

Currently subculturing techniques used for the propagation of hMSC tend to mimic the protocols that have historically been used for other cell lines such as fibroblast, but it is not understood if these protocols utilise the best conditions for the proliferation of hMSC.

1.2.6 Effect of Inoculation Cell Density of hMSC Static Cultures

Inoculation cell density (ICD) in the context of adherent-dependent cells is the number of cells per centimetre squared seeded onto the vessel at the beginning of the propagation step into a new culture vessel. If the initial number of cells per centimetre square is too high the time taken to cover the surface decreases whilst

the frequency of harvest and aseptic manipulations increases for the overall cell expansion process. However, if the ICD is too low the cells will not be able to sense the cytokines secreted by nearby cells and cell growth may be arrested. Most researchers studying hMSC have published results based on an ICD of $5x10^3$ cells/cm^2 which has been established as customary for cell propagation of hMSC (Friendstein et al., 1976).

The distance between cells on the culture surface at inoculation is expected to have an impact on the time to harvest and length of the passage, but recent studies show that it also affects the doubling time of hMSC. Sekiya et al. (2002) demonstrated that the lower the ICD, the lower the doubling time for hMSC. The mechanism for why this happens is not well understood, and more studies need to be done to observe the implications of ICD in conjunction with other parameters on the population doubling limit and differentiation potential of hMSC.

1.3 Culture Media for the Proliferation of hMSC

Cell expansions of stem cells in the laboratory have tended to follow the same techniques historically used in tissue culture of other adherent cells. The reason being because the main focus of study up to now has been the directed differentiation of mesenchymal stem cells and maintenance of the culture in an undifferentiated state. To date not much research has been conducted in the development of a media formulation that would satisfy the requirements of growth for hMSC. Media development is a cost intensive effort that is normally undertaken by suppliers to commercialize the product, but most academic research laboratories do not focus their attention on this topic.

1.3.1 Basal medium

Basal medium is a solution that provides basic nutrients such as amino acids, vitamins, inorganic salts, and a carbon source such as glucose, to support environmental and nutritional requirements for the proliferation of a given cell line. Commercial media formulations are available for cell proliferation of mammalian cell cultures, and are widely used in all research laboratories for an extended range of cell lines. Only a few industrial companies can afford to

develop and produce a custom-made media for a specific process. The performance of different commercially available media has been studied and found to affect growth rates, yields, and differentiation potential of hMSC (Sotiropoulou et al., 2006).

Storage and handling of basal medium is extremely important, since some of the component ingredients degrade after exposure to light and temperatures higher than 4˚C. It has been shown that DMEM generates reactive oxygen species when exposed to light in a time-dependent manner. The main components responsible for generation of reactive oxygen species are riboflavin, tryptophan, tyrosine, pyridoxine, and folic acid (Grzelak et al., 2001). Most laboratory practices do not control the time exposure of media to light, and results generated from experiments using this media may generate erroneous conclusions.

These media formulations are chemically defined and contain no animal-derived products. However, some additions to the basic media are needed to support growth of hMSC and to increase productivity of the culture by reducing doubling times. Most studies for hMSC employ media with different supplements added prior to use. The most common supplements added are L-glutamine, antibiotics, growth factors, and serum.

L-glutamine needs to be added immediately prior to use, because otherwise it degrades rapidly and it would significantly decrease the shelf-life of the media. Studies have shown that the chemical decomposition of glutamine to ammonia and pyrrolidonecarboxylic acid is influenced not just by temperature, but by media type and pH (Ozturk et al., 1990).

Some growth factors are added to improve proliferation rates and also to trigger differentiation of hMSC to a desired lineage. An example of this is the addition of 1 ng/ml FGF (fibroblast growth factor) that has been proven to prolong the life-span of hMSC to more than 50 doublings whilst maintaining their differentiation potential (Bianchi et al., 2003). This effect seems to be dose dependent, and other observations show that higher doses of bFGF (3 ng/ml) induce adipogenic differentiation (Nerbauer et al., 2004).

Most cell lines cannot sustain growth for consecutive passages without the addition of serum in the media. Serum is an animal derived component that improves cell growth. Most researchers report the addition of 10% serum to their media formulation for the proliferation of hMSC. Although serum addition improves growth kinetics, there are several disadvantages for the use of serum as discussed in Section 1.3.2, and major efforts are underway to eliminate this supplement and to replace it by chemically defined components.

1.3.2 Serum

Serum is the fluid component that remains after centrifugation of blood that has been allowed to clot slowly and lacks the clotting factors and other elements which plasma includes. Its addition to culture media allows cells to proliferate faster and eliminates some susceptibility to environmental conditions. Serum contains over 1,000 compounds including proteins, electrolytes, lipids, carbohydrates, hormones and enzymes, but it has never been fully characterised. It also contains growth factors that improve cell proliferation and differentiation and other factors that bind and inactivate toxic products such as proteases and free radicals. Serum also serves as a carrier for lipids, enzymes, micronutrients, and trace elements, improving transport across the cell membrane. Other proteins in serum, such as albumin and fetuin, influence physical conditions of the culture such as viscosity, osmolality, pH, and gas delivery rates (Bodziak et al., 1985).

In spite of the advantages of adding serum to culture medium there are several adverse implications from a process control and safety point of view that are gearing the tissue and cell culture community to shift towards a serum-free medium, and ideally a chemically defined medium.

Serum is the most expensive additive to basal medium for cell culture applications, after some specialized components such as growth factors. Addition of serum to the culture media raises the production cost significantly, making process changes such as perfusion culture which normally improves yield and quality of the product uneconomical. The composition of each lot of serum also depends widely on the pool of cattle used for the batch, and consequently have an impact on the performance of the cell expansion process. For most commercial

bioprocesses still using serum in their media formulation, different lots of serum are screened for the cell line of interest. In addition to a certificate of analysis demonstrating that no adventitious agents are present in the particular batch of serum, the screening of a batch includes plating efficiency, growth promotion, colony morphology, and toxicity tests for a particular cell line (Evans, 2006). Once a lot is identified for optimum performance in cell growth and product yield, the complete lot is purchased to complete several batches of production. For research at small scale this is not always an option, and the addition of different lots of serum to the media may be responsible for difficulties in the interpretation and reproducibility of results (Stute et al., 2004).

Serum can be obtained from humans, but not in quantities large enough to be used in the production of cells for most therapeutic applications. Normally serum from animal origins is used for the cell proliferation of mammalian cells, and FBS (fetal bovine serum) or FCS (fetal calf serum) is used for cell expansion of hMSC. However, animal serum has the potential of carrying infectious agents, such as mycoplasma, viruses and prions.

Recently, a group of researchers in San Diego reported expression of immunogenic nonhuman sialic acid on the surface of human embryonic stem cells (Martin et al., 2005). This discovery revolutionized the field of embryonic stem cell science, since it represented a risk for all future therapeutic applications of stem cells. Currently, human embryonic stem cells are subcultured over a feeder layer of mouse fibroblasts, and the possibility that this protein may have come from the feeder layer was examined first. However, a titration experiment reducing the amount of serum in medium indicated a dose dependency in the levels of expression of this particular nonhuman sialic acid on the cell membrane. Many groups are currently working on subculture techniques to propagate human embryonic stem cells in chemically defined media with animal-free raw materials and without feeder layers. As with all production of biologics, elimination of animal-derived components is of great importance in order to reduce the risk of transmission of adventicious agents into the product as well as to increase robustness of the process.

Similar problems can be expected with the culture of adult stem cells, although so far reports have not shown evidence of the presence of nonhuman sialic acid due to the presence of serum in media.

1.3.3 Trypsin

Cell detachment of anchorage dependent cells from a culture surface is achieved by enzymatic dissociation. Trypsin is an enzyme commonly used to detach adherent dependent cells for further use or for subcultivation. The most commonly used trypsin is porcine derived, although alternative sources of non animal-derived trypsin are becoming available such as recombinant rTrypsin or Trypzean. Trypsin can also be replaced by non animal-derived proteases such as No-zyme or rProtease produced in yeast or bacteria (Keenan et al., 2006). These trypsin replacement products are important when culturing cells intended for human use, given the risk associated with any animal-derived raw material. As for serum, any animal-derived product carries the risk of transmitting TSE (transmissible spongiform encephalopathies) and other adventitious agents into the biological product, and eventually the recipient of the therapy.

This enzyme cleaves focal points formed between the cell membrane and the surface achieving detachment in a contact time of 5 to 10 minutes. Longer contact times are detrimental for the plasma membrane, as trypsin starts to degrade surface proteins (Cole and Paul, 1966; Phillips, 1972). As a result, cell death and loss of characterisation surface markers occurs after long exposure to trypsin.

No studies to date have revealed the limiting time of exposure of hMSC to trypsin and the detrimental effect of traces of the enzyme in culture due to carry over during passaging. Some cell culture processes are designed to remove trypsin prior to inoculation in a new vessel by centrifugation, whilst others carry over traces of trypsin diluted with culture media. No investigations have been undertaken to determine if the carry over of trypsin is more detrimental to the cells than the additional centrifugation step to remove it. However, considering the sensitivity of hMSC to external conditions, it may be an important parameter to be addressed in future studies.

1.4 Process Control, Optimisation, and Quality Assurance in the Production of hMSC in an Un-Differentiated State

When designing a process for the cell expansion of hMSC it is important to consider reproducibility, quality, and compliance with regulatory agencies for each step of the proliferation scheme. Just as important as the discovery of therapeutic applications for stem cells is the ability to produce enough clinical grade material to satisfy large demands in a timely manner.

Several parameters must be controlled and understood in order to design a successful process for the production of stem cells as the end product. The main possible sources of variability, the impact of process controlled parameters, and automation of a cell expansion process are further discussed in this section.

1.4.1 Sources of Variability in the Expansion of hMSC

There are some sources of variability in all cell culture processes that need to be accounted for when designing a cell expansion that would provide equally acceptable quality material as the end product. There are ways to minimise such variations between lots produced by controlling process parameters and by screening the raw materials that will be in contact with the cells. There are other non controllable parameters such as the source of the cells, which is a challenge for regenerative medicine applications for which there is not an established cell line for all batches of material. Each cell expansion is produced with cells from a different patient, with intrinsic characteristics that result in variations of cell growth patterns and differentiation.

1.4.1.1 Cell Source

It is well known that the doubling time of hMSC varies according to the age of the patient and the tissues from which they were derived. Some variation on the differentiation potential and the population doubling limit is also expected according to the donor (Phinney et al., 1999). Other factors such as sample to sample variability, sex, age, smoking habits, and other medical conditions of the donor will have an effect on the cell growth and differentiation potential of hMSC isolated from different tissues of the patient.

Understanding the range of variations expected in the growth and differentiation potential of hMSC *in vitro* due to the cell source is important when determining ranges for all other controllable parameters in the process. A degree of flexibility must be built into the cell expansion process to accommodate longer processing times in cases of slower growing cell line, or where larger number of cells may be needed to accomplish desired differentiation outcomes.

1.4.1.2 Raw Materials

Lot to lot variability of some raw materials can change cell growth rates significantly and alter other characteristics of the cells such as metabolic rates, surface markers, and gene expression. Some raw materials are more variable than others, and some measures can be taken into account to alleviate disruptions in the process due to raw material variability. Most variable raw materials for a cell expansion process are those that are not chemically defined and specially those which are animal-derived, such as serum. Basal media also varies from lot to lot due to the source of individual components from which is formulated, or from changes in the production process such as water supply or sterilisation techniques. Individual additives that are chemically defined or that have undergone more intense separation processes before formulation such as growth factors, trace elements, amino acids, vitamins, are expected to be more consistent between lots.

An approach to minimise variations between lots is to screen the individual components before incorporation into the process. Once the material is found acceptable for the cell expansion process, the entire lot is purchased. This will at least minimise the variability of media within a single consignment and assure reproducibility of the process within a given consignment for a large number of batches of desired product.

Something else to consider is the availability of vendors for a given raw material. Some variability may be expected from raw materials coming from different vendors, such is the case for surface culture vessels such as T-flasks from Nunc versus Corning. However, it is important to consider an alternative source for a critical material in case quality or supply problems are encountered.

Understanding the variability between products from different vendors and the effect on the process is important for the successful production of cell derived products.

1.4.1.3 Manual Operations

When manual operations are needed for the execution of a process, hiring qualified staff and providing them with appropriate training is important to achieve consistency in the cell expansion process. Even when trained technicians are in charge of the cell culture manipulations, there are usually some variations in the way particular steps are carried out by each operator. There is also a human error factor to be considered. Small variations in the aseptic manipulations conducted under a biosafety cabinet include; (i) the time of operation and consequently exposure of the cells to atmospheric conditions; (ii) pippeting errors and (iii) the shaking of the T-flasks during cell harvest, that may cause damage to cells or aggregation.

Process variability due to manual operations can be eliminated by automation. A robot can conduct the same operations with the same precision every time, eliminating human error or variability on each step of the process. Although implementing an automated process requires a large capital investment and initial research in process development, it is more cost effective than paying for the training and salaries of a larger number of technicians over a long period of time.

1.4.1.4 Utilities

Utilities include deionised water, clean steam, electric power, piping, and the valves needed to run a process. Changes in any of the utility systems in a laboratory may affect the process resulting in unexpected results and in some instances the source of the variability may be unclear. Examples of such utility issues which may affect the results are as follows:

- Contamination or residues in the pipes may affect the metal content in the water or stem, translating into changes in cell growth.

- Malfunction of a valve or a gas regulator may supply an incorrect concentration of a gas to an incubator resulting in an unregulated pH environment.
- Power shortages if not well controlled my result in loss of material in refrigerators and freezers, and subsequently decrease the rate of cell growth during incubation.

Although mechanical problems cannot always be avoided, an appropriate maintenance plan and careful placement of controllers and alarms will minimise the disruption caused by abnormalities in the utility systems. Maintaining accurate records of utilities, components and operators will also make indentifying the source of problem easier minimising the need for long atypical process report investigations to determine the source of error.

1.4.2 Measured Process Parameters for Process Control

Several parameters must be monitored during the expansion of hMSC to properly characterise the quality of the product, as per any other biological product. For autologous therapies, the cells being proliferated *in vitro* are the product. Consequently it is the process that becomes the product when manufacturing under cGMP regulations. Tight control of the quality of the cells at different stages of the cell expansion process becomes an important issue not just to ensure robustness, but also to comply with regulatory agencies.

1.4.2.1 Experimental and Routine in Process Analysis

The quality of the cells at different stages of the cell expansion process can be monitored by using an array of assays as detailed in Table 1.3. Some of the assays available are appropriate and necessary to gain a good understanding of the process and to develop a robust cell expansion protocol for clinical applications. A well characterised process in an automated platform for clinical applications will also required the completion of process characterisation and process validation studies to satisfy cGMP regulations. For such purpose, a detailed understanding of the quality of the cells at different stages of growth will require more extensive tests than for routine in-process characterisation. In

addition to the assays highlighted in Table 1.3, these tests should include functionality assays to determine the differentiation potential of the cells at different stages of growth. Functionality assays prove that a population of stem cells maintains the potential of differentiating into different cell types.

However, for routine analysis of an established process, the number of sampling events and number of cells utilised for such purposes must be reduced in order to minimise the risk of contamination and excessive loss of final product, in this case of hMSC. Regardless of such considerations, the minimum number of assays selected for routine manufacturing of hMSC have to be sufficient to prove that the quality of the cells delivered to the clinic comply with the requirements of safety and quality for their intended use.

With the currently on-going research in the field of biologic analytical sciences, new assays as well as improved analytical equipment will facilitate on-line monitoring of stem cell cultures with non-invasive methods.

Table 1.3 In-process characterisation assays required for the development of a cell expansion protocol for hMSC and for routine analysis of an established process.

(overleaf…..)

Parameter	Experimental - Characterisation of cell line			Routine - Process Analysis	
	Assay	Description	Sample size	Assay	Sample size
Oxidative Stress	Dihydroehtidine	Stains peroxide mediated rxns CONFOCAL	0.5 cm^2 slide		
	p53	Detect presence of checkpoint p53 in the cell cycle (absent results in lack of control for cell division - tumorogenicity) WESTERN BLOT or RT-PCR	~1 ml		
	FLARE	Comet assay that measures 8-oxoguanine damaged nucleotides (known mutation due to oxidative damage) CONFOCAL	0.5 cm^2 slide		
Telomere length	TRAP	Telomere repeat amplification protocol OD	Depends on cell densities (min $2.5x10^6$ cells)	TRAP	Depends on cell densities (min 2.5 $x10^6$ cells)
Cell characterisation	Histology	Stains cells and view through microscope	0.5 cm^2 slide		
	FACS	Stain surface markers characteristic of cell type with flourecent dyes	$2x10^6$ cells per surface marker	FACS	$2x10^6$ cells per surface marker
	CONFOCAL	Stain alpha actin, some surface markers.	0.5 cm^2 slide	CONFOCAL	0.5 cm^2 slide
	Stem cell functionality kit	Differentiation into adipocytes, chondrocytes and osteocytes.	Enough to inoculate new culture (depends on selected vessel)		
Cell Population	Hemocytometer	trypan blue exclusion	20 ul	Hemocytometer	20 ul
	Guava cell counter	viability, size distribution, cell cycle, apoptosis, other markers	100 ul	Guava cell counter	20 ul
	Cedex	viability, cell density			
Metabolic activity and process conditions	Bioprofiler	Glucose, lactate, glutamine, glutamate, NH4, pO2, CO2, osmolality, Mg, Ca, Na, K	30 ul	Bioprofiler	30 ul
	YSI	glucose/lactate	30 ul or 1 ml for turntable	YSI	30 ul or 1 ml for turntable
		glutamine/glutamate	30 ul or 1 ml for turntable		
	Other sensors	O2 sensors	none	O2 sensors	none
		pH sensors	none	pH sensors	none

1.4.2.2 Quantitative Indicators of Cell Growth Kinetics

There are some control parameters that need to be calculated in order to characterise the process of cell expansion. These calculations are done routinely in the cell proliferation steps for the production of biological products in order to monitor the robustness of the process. Mathematical growth models derived from this data play a key role in developing a biological process, since they can be predictive tools for expansion potential and for the characterisation and measure of kinetic parameters of a stem cell population (Deasy et al., 2003). Such growth kinetic parameters that characterise the growth of a cell population are cell growth rate, duration of the lag phase, time to reach stationary phase, and maximum cell density obtained at the stationary phase.

1.4.2.3 Surface Markers as Indicators of Product Quality

Routine characterisation is important for the expansion of stem cells, since they can differentiate spontaneously while maintaining the same morphology and cell growth characteristics. Surface marker expression can provide a good indication of the identity of the cell population as well as the degree of differentiation. Considering the limited amount of stem cells obtained from a donor and the large amount of cells needed for flow cytometry analysis of cell markers, this is not a test that can be done frequently for routine processing. However, new technologies are being developed that require fewer cells ($2\text{-}5x10^3$ cells) to obtain an accurate measurement for surface markers, such as a high throughput flow cytometer developed by Guava Technologies. Although cell surface marker expression alone cannot be used to ensure the ability of a cell to behave as stem cell and exhibit all characteristics of such *in vivo* as well as *in vitro*, it provides a good estimate of the identity and quality of the cell population at a given time in the cell expansion process. Loss of expression of surface markers characteristics of a specific progenitor population can be interpreted as changes in the phenotype of the cell population, and possible decrease in differentiation potential.

1.5 Automation for the Cell Expansion Process of hMSC

In spite of the initial capital investment and development cost to implement an automated process, there are several advantages over a manual process and some companies have already chosen to automate cell culture operations (Chapman, 2003; Kempner et al., 2002). The advantages of automation are:

- Better control over process parameters
- Less variability between batches
- Cost effectiveness through reduced staff, training and process operation time
- Time efficiency since more manipulations can be achieved in a given timeframe

The main reason why many processes are not automated is time to market. Most processes are a scale-up of the laboratory techniques used during the discovery phase of a new product. The extra time required to implement automation in a process may jeopardize the time lines dictated by market strategies and the ability to be 'first to market' with a new product.

The best way to overcome the challenge of reaching the market first whilst realising the benefits of an automated process that may be cost effective down the line, is to create a platform technology that could be transferable to different products. Once the platform technology has been developed, it can be implemented earlier at the research and development stage of a process. The purpose of this project is to develop a platform technology for the cell expansion and differentiation of hMSC in microwell reactors that could be applied to any process for the use of stem cells in any regenerative medicine applications.

1.6 Aims and Objectives of Thesis

hMSC have the potential to differentiate into lineages of mesoderm origin, such as osteogenic, chondrogenic, and adipogenic lineages, presenting a promising potential for autologous cell and gene therapy (Prockop, 1997), and regenerative medicine applications (Jaiswal et al., 2000). Research in the last decades has been focused in the understanding of directed differentiation of these cells into desired lineages for the construction of tissue-engineered organs for implantation or for

cell therapy applications as shown in Section 1.1.3. However, one of the main challenges in designing a robust expansion protocol that would ensure provision of enough cells of the desired quality for clinical applications is the ability to account for the inherent variability of the cell source. In order for autologous hMSC therapy to become available and to satisfy market needs, the variability of cell growth kinetics according to age, sex, and health of the bone marrow donor (Phinney et al., 1999) must be taken into consideration. Also, controlling physical parameters during the cell expansion process for hMSC and understanding the effect of these environmental factors on cell growth in an undifferentiated state is imperative when designing a robust process for the manufacture of biological material.

To ensure production of sufficient cells to satisfy market needs, bioprocess conditions and equipment for the expansion of hMSC need to be investigated and adopted, ensuring optimum growth in an undifferentiated state. The use of an automated platform will potentially facilitate higher output capabilities, whilst reducing variability due to operator manipulations (Terstegge et al., 2006, Joannides et al., 2006, Bernard et al., 2004). In addition, rigid control of determining parameters for growth will result in a robust cell expansion process for industrial applications in the emerging regenerative medicine sector. Study of the effect of physical conditions experienced by the cultures during automated manipulations will generate a set of Standard Operating Procedures (SOP) for an appropriate range of conditions, aimed at ensuring cells are maintained in an undifferentiated and still multipotent state.

The aim of this thesis is to investigate hMSC growth characteristics under different processing conditions, and to define the optimal culture conditions for the effective clinical scale production in an automated platform of large numbers of hMSC. It is also the aim of this thesis to develop a mathematical model that could describe the kinetics of growth for cells from each donor with the intention of forward predicting the overall cell expansion process time for each individual patient

The specific objectives of this thesis are:

- To characterise growth kinetics over sequential passages with the objective of establishing a baseline cell expansion process for future optimisation. Chapter 3 evaluates different isolation techniques for the separation of hMSC from bone marrow, as well as the effect of cell banking on cell growth, and the effect of culture surfaces and sequential cultivation on hMSC growth kinetics.
- To evaluate the controlled parameters for an automated hMSC expansion process. Chapter 4 assess the impact of inoculation seeding densities, feeding strategy, and pH and temperature excursions in hMSC expanded in an automated platform.
- To establish a mathematical model for hMSC growth kinetics. Chapter 5 demonstrates the accuracy of a mathematical model to forward predict the growth rate of cells from different donors over multiple passages as well as examines the surface marker expression of hMSC throughout the expansion process.

In addition to these chapters, Chapter 2 details all materials and methods that were used throughout the work and Chapter 6 gives a summary of the main observations and conclusions of the study as well as suggestions for future work.

CHAPTER TWO

Materials and Methods

2 MATERIALS AND METHODS

2.1 Isolation of hMSC from Bone Marrow Aspirates

Two methods were used to isolate hMSC from frozen bone marrow samples, Ficoll-Paque density gradient centrifugation and direct isolation.

2.1.1 Ficoll-Paque Density Gradient Centrifugation

Human bone marrow aspirates were collected from the iliac crest of volunteer donors after informed consent and stored in 250 ml sterile bags, at -140 to -170˚C in liquid nitrogen after addition of DMSO and heparin (in quantities not provided by the source) to prevent cell membrane breakage and clotting when thawed. The frozen samples were provided by the Department of Haematology, University College London Hospital, ranging in volume from 74 ml to 120 ml per bag. This isolation technique was performed on five bone marrow samples from different patients.

Frozen bone marrow samples were initially thawed at 37˚C and filtered through a 40 μm cell strainer (Falcon, Bibby Sterilin, Stone, UK) inside a class II biosafety cabinet to remove bone particles and aggregates of adipose tissue. Mononucleated cells were isolated from the filtered material by Ficoll-Paque density gradient centrifugation (StemCell Technologies, Vancouver, British Columbia, Canada). Ficoll-Paque solution is a mixture of Ficoll™ PM400 and sodium diatrizoate at a density of 1.077 g/ml, developed for purification of mononuclear cells from anti-coagulant treated human peripheral blood (Minami et al., 1978; Elequin et al., 1977; Arkin et al., 1991; Deguch et at. 1991). Differential migration after centrifugation of a blood sample deposited over an equal amount of Ficoll-Paque, results in the formation of layers of different cell types. This method required initial dilution of the filtered sample with an equal amount of Dulbecco's phosphate buffered saline (DPBS, Sigma Chemical Co., St. Louis, Missouri, USA). This solution was slowly poured over an equal volume of Ficoll-Paque in a 50 ml Falcon centrifuge tube to avoid any mixing between the two phases prior to centrifugation at 650g and 21˚C, for 30 minutes (Eppendorf 5810R AG, Hamburg, Germany). After centrifugation, several layers

were visible along the centrifuge tube. From the bottom of the tube up there was a lower layer containing erythrocytes and granulocytes, a layer of Ficoll-Paque, an interface of mononuclear cells in the middle of the tube, and a top layer of plasma as shown in Figure 2.1.

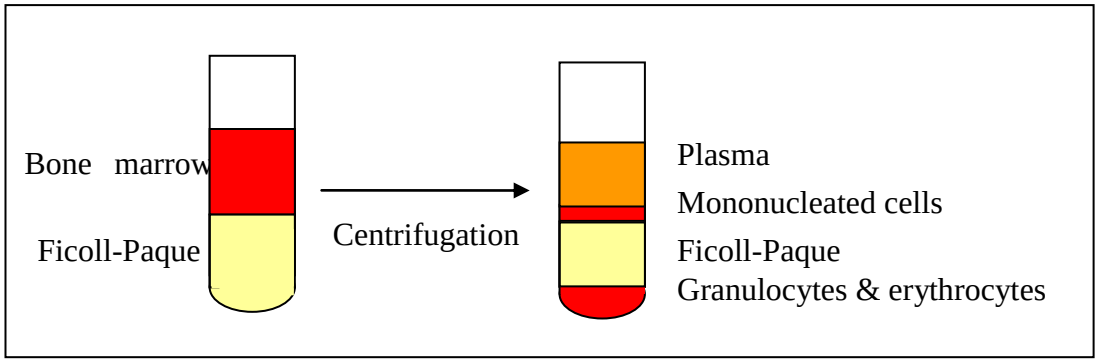

Figure 2.1 Schematic representation of Ficoll-Paque and bone marrow samples pre- and post-centrifugation. Bone marrow sample is poured over an equal volume of Ficoll-Paque and centrifuged. Different layers are formed after Ficoll-Paque density gradient centrifugation to separate mononucleated cells from bone marrow as described in section 2.1.1.

After centrifugation, the 50 ml falcon tube was taken into a class II biosafety cabinet. The plasma phase was carefully removed with a sterile pipette without disturbing the mononuclear cell interface, which was then collected for further processing. In order to remove any possible plasma and Ficoll-Paque solution aspirated along with the mononuclear cells, approximately 5 to 6 ml of the collected interface sample was mixed with 35 ml of DPBS in a 50 ml Falcon tube and centrifuged at 650 g and 21˚C, for 15 minutes. The resulting pellet was resuspended in hMSC culture medium, which consists of low-glucose DMEM (BioWhittaker, Walkersville, Maryland, USA) supplemented with 10 % (v/v) FBS (StemCell Technologies), 2 mM L-glutamine (BioWhittaker) and 100 U/ml penicillin and streptomycin (BioWhittaker). This medium formulation has been used in all experiments in this thesis for the cell expansion of hMSC, and will be referred to hereafter as culture medium. In order to minimise possible variability due to different lots of FBS as discussed in Section 1.3.2, only two lots of serum pre-selected for hMSC growth by the vendor (lot #05B14288 and lot #05B14286 from StemCell Technologies) were used for all experiments in this thesis. Cell viability was assessed by Trypan Blue exclusion method as described in section

2.6.1, by which the permeable cytoplasmic membrane of dead cells is penetrated by Trypan (BioWhittaker) staining the whole cell dark blue in contrast with the unstained life cells. Cell density was determined using a haemocytometer as described in section 2.6.1.

A second separation step was needed to extract hMSC from the suspension of mononuclear cells. This was achieved on the basis that hMSC are the only cells from the bone marrow extract that would adhere to a treated culture surface (Friedenstein et al., 1970; Friedenstein et al., 1976). Isolated mononuclear cells were seeded into T-25 or T-150 culture flasks (Corning Life Sciences, Corning, New York, USA) at inoculation cell densities ranging from $1x10^4$ to $1x10^7$ cells/cm^2, in culture medium, and incubated at 37˚C in a humid 5% (v/v) CO_2 atmosphere. Non-adherent cells were removed from the culture three days after initial isolation by performing a medium exchange. Fourteen to twenty days later, with medium exchanges every three to four days, adherent cells showing mesenchymal stromal phenotype covered 80% of the surface of the culture flask and were removed by enzymatic exposure to 0.25% trypsin in 1 mM EDTA solution (Sigma) for subsequent cell expansion (Section 2.4) or for the generation of a cell bank (Section 2.2).

2.1.2 Direct Isolation

Eighteen bone marrow sample bags from different patients were used to optimise and perform isolations using a novel Direct isolation technique that would facilitate automation. Sterile bags of frozen bone marrow aspirates (source indicated in Section 2.1.1) were thawed at 37˚C and the content of the bag was mixed with culture medium to achieve the desired inoculation cell density prior to seeding. In order to optimise the procedure, bone marrow samples were diluted with culture medium in different volume ratios ranging from 1:0 to 1:4 bone marrow in medium, as well as at different cell density concentrations ranging from $1x10^4$ to $1x10^6$ cells/cm^2. The mixed suspension of bone marrow with medium was then seeded into T-25 or T-150 Corning flasks, with a working volume ranging from 0.2 to 0.53 ml/cm^2. The medium was exchanged after 24 hr to remove the cells in suspension, and from then on it was exchanged at a

frequency ranging from once every three days to daily until 80% confluency of hMSC was reached. The cells were then detached from the surface of the flask by exposure to 0.25% trypsin in 1 mM EDTA for subsequent cell expansion (section 2.4) or for the generation of a cell bank (section 2.2).

2.2 Cell Banking

Cells were detached from the surface of the culture vessel (T-150, T-75, or T-25 flasks) by exposure to 0.04 ml/cm^2 of 0.25% trypsin in 1 mM EDTA solution for no less than 5 minutes and no longer than 10 minutes at 37˚C, after removing the spent medium and washing the cell monolayer with DPBS. Trypsin activity was inhibited by addition of 0.04 to 0.08 ml/cm^2 of culture medium. The content of each flask seeded from a single bone marrow donor was pooled into a common sterile container (Nalgene Nunc International, Rochester, New York, USA) and mixed by slowly pipetting up and down a minimum of ten times with gentle swirling. Two independent 0.5 ml samples of this concentrated cell suspension were taken for cell density measurements (Section 2.6). The cell viability and density of the concentrated cell suspension were determined by the Trypan Blue exclusion (Section 2.6.1).

A diluted cell suspension was then prepared to achieve 1x10^6 cells/ml in a final formulation of freezing medium. Freezing medium was prepared with 90% (v/v) culture medium and 10% (v/v) of the total volume of DMSO (Sigma). The concentrated cell suspension in freezing medium was dispensed into 1.5 ml Nalgene internal thread cryovials (Nalgene Nunc International) with 1 ml of cell suspension (or 1x10^6 cells) per vial, placed in a 5100 Cryo 1˚C Freezing Container widely known as ‘Mr. Frosty’ (Nalgene Nunc International) and left in a -70˚C freezer for 24 to 48 hours. A ‘Mr. Frosty’ is a polycarbonate container with a foam insert. After soaking the foam with 100% isopropyl alcohol, Mr. Frosty allows for control rate freezing of the cells at a cooling rate of 1˚C per min required for successful cell cryopreservation. After 24 to 48 hours in a -70˚C freezer, the vials of hMSC were transferred into a liquid nitrogen freezer.

For one of the banks created, the vials were placed inside a Nunc CryoFlex™ tubing (Nalgene Nunc International), a heat sealable polyethylene tubing

designed for CryoTube Vial encasement to reduce possible hazards, prior to immersion of the vials in a liquid nitrogen freezer. The time required to encapsulate individual vials, and the difficulty involved while removing them from the tubing did not justified the use of Nunc CryoFlex™ tubing for any other cell banks.

A total of six cell banks were created, each from a different donor at passages ranging from passage zero (P0 is considered to be the first hMSC collected from T-flasks seeded directly from bone marrow samples (Section 2.1.2)), or mononucleated cells isolated from a Ficoll-Paque density gradient centrifugation, (Section 2.1.1)) to passage four (P4). The number of vials per cell bank created ranged from 5 to 34 vials.

2.3 Culture Surfaces and Vessels

Different culture vessels and surfaces were used for the expansion of undifferentiated hMSC. Culture treated surfaces from Corning were used for static attachment cultures while ultra-low attachment plates from Corning were used for microcarrier suspension cultures of hMSC. Microcarrier cultures were performed with MicroHex (Corning) and with Cytodex 1, and Cytodex 3 (Pharmacia, Uppsala, Sweden).

2.3.1 T-flasks

T-flasks used for the expansion of hMSC were standard tissue culture treated polystyrene surfaces by Corning. The surfaces are modified using a corona discharge that generates highly energetic oxygen ions which graft onto the surface polystyrene chains, so that the surface becomes hydrophilic and negatively charged to optimise cell attachment (Hudis, 1974; Amstein and Hartman, 1975; Ramsey et. al., 1984). T-flasks had vent caps with a 0.2 µm membrane sealed into the cap, allowing sterile gas exchange from the CO_2 controlled incubators to regulate the pH of the culture medium. Different culture surface sizes used were 25 (T-25), 75 (T-75) and 150 (T-150) cm^2.

2.3.2 Microwell Plates

Flat-bottom, round-well microwell plates from Corning with identical surface properties to T-flasks (section 2.3.1) were also used for cell expansion. Three different well size plates were used: 6, 12, and 24-well plates. Each well had a surface area of 9.5 cm^2/well in a 6-well plate, 3.8 cm^2/well in a 12-well plate, and 1.9 cm^2/well in a 24-well plate, with working volumes of 3, 2, and 1 ml respectively unless indicated otherwise.

2.3.3 Microcarriers and Microcarrier Cultures

Three different microcarries were tested for cell expansion of hMSC. Ultra-low attachment coated polystyrene surface well plates by Corning were used for all microcarrier experiments to avoid cell attachment to the surface of the wells. This surface is a covalently bound hydrogel layer that is hydrophilic and neutrally charged. Proteins and other biomolecules attach to a surface through either hydrophobic or ionic interactions (Grinell, 1978), and so this hydrogel surface inhibits nonspecific immobilization via these forces, thus inhibiting subsequent cell attachment. Shake flasks, 125 ml, with a working volume of 20 ml, from Corning, were also used for larger cultures with 2D-microhex microcarriers.

2.3.3.1 Cytodex 1

Cytodex 1 (Pharmacia) are transparent non-porous microcarriers made of a spherical matrix of cross-linked dextran with positively charged N,N,N-trimethyl-2-hydroxy-aminopropyl groups for optimal cell growth. The charged groups are distributed throughout the microcarrier matrix. They have a density of 1.03 g/ml, average diameter of 180 μm providing a surface culture area of 6000 cm^2/g dry weight, a ratio of microcarrier per gram of $6.8x10^6$. The microcarriers were hydrated and swollen in Ca^{2+}, Mg^{2+} free DPBS and pre-conditioned for a minimum of 3 hours at room temperature. The supernatant was decanted and the microcarriers were washed in fresh DPBS and sterilized in an autoclave.

One gramme of microcarriers was recovered from the sterile solution, DPBS was removed and replaced with culture medium at 37˚C, at a concentration of 9.6 mg microcarriers/ml. Microcarrier cultures were set in 24-well ultra-low attachment

plates, at cell densities of $5x10^3$ and $1x10^4$ cells/cm^2, or 13 and 26 cells/microcarrier respectively with a final microcarrier density of 3 g/L. All the cells and microcarriers were seeded with an initial working volume of 0.5 ml/well to aid cell attachment, and culture medium was added after 24 hours in culture up to a final working volume of 2 ml/well. The plates were incubated in a 37˚C humidified incubator with 5% (v/v) CO_2 either in static conditions for the first 6 hours with periodical shaking at 250 rpm for 5 min every 2 hours, or under continuous agitation of 250 rpm on an orbital shaker (KS 130 control, IKA) placed inside the incubator six hours after inoculation.

2.3.3.2 Cytodex 3

Cytodex 3 (Pharmacia) consists of a matrix of cross-liked dextran coated with a layer of denatured Type I collagen in an approximate amount of 60 μg/cm^2 which results in maximum cell yields (Gebb et al., 1983). These microcarriers have a density of 1.04 g/ml, average diameter of 175 μm providing a surface culture area of 4600 cm^2/g dry weight, a ration of microcarrier per gram of $4.0x10^6$. The microcarriers were sterilized in the same manner as with Cytodex 1 microcarriers (section 2.3.3.1).

One gramme of microcarriers was recovered from the sterile solution, DPBS was removed and replace with culture medium at 37˚C, at a concentration of 9.6 mg microcarriers/ml. Microcarrier cultures were performed in 24-well ultra-low attachment plates, at cell densities of $5x10^3$ and $1x10^4$ cells/cm2, or 10 and 20 cells/microcarrier respectively with a final microcarrier density of 3 g/l. Cultures were performed as described in Section 2.3.3.1.

2.3.3.3 2D-Microhex

2D-Microhex (Nalgene Nunc International) are solid two dimensional microcarriers made of polystyrene, non-porous and non-absorbing particles with the same properties as the cell culture plastic-ware produced by Nunc. They are gamma irradiated, and do not need conditioning prior to use. The microcarriers are flat flakes of hexagonal shape, with dimensions of 125 μm in side length and 25 μm in thickness, a density of 1.05 g/cm^3 and cultivation area of 760 cm^2/g.

Microcarrier cultures with 2D-Microhex were inoculated at a cell density of $5x10^3$ cell/cm^2 and a microcarrier density of 10 cm^2/ml in a 125 ml shake flask (Corning) with a 20 ml working volume. The shake flask was placed in a humidified incubator at 37˚C, with 5% (v/v) CO_2 atmosphere under static conditions for one hour to allow for cells to attach to the microcarriers. The flask was then shaken manually for 2 minutes after one hour in static condition, and continually after three hours from inoculation at 100 rpm in a orbital shaker.

Microcarrier experiments were carried out in 24-well ultra-low attachment plates, seeded at $1x10^2$ and $5x10^3$ cells/cm^2 and a microcarrier surface density of 5 and 10 cm^2/ml. Initial working volumes ranged from 0.5 to 1.5 ml/well. After the cells were allowed sufficient time to attach to the surface of the microcarriers, additional culture medium was added to a final working volume of 1.5 ml/well. Plates were placed in an incubator, same conditions than above, in static culture conditions and shaken for 5 minutes at 250 rpm at inoculation and at different time intervals post inoculation ranging from once every one to ten hours afterwards. Continuous shaking conditions were started three to 16 hours after inoculation in an orbital shaker placed inside the incubator at stirring speed ranging from 200 to 280 rpm.

2.4 Cell Expansion

hMSC thawed from a frozen vial (Section 2.2) or a previous passage, were seeded into a culture vessel from a diluted cell suspension prepared with culture medium and hMSC to a determined volumetric cell concentration (cells/ml) in order to achieve a desired surface inoculation cell density (cell/cm^2). When replicates were seeded in parallel, each vessel or well was inoculated from the same diluted cell suspension to reduce variation. Cell cultures seeded in T-flasks or microwell plates, were placed in a 5% (v/v) CO_2 humidified incubator at 37˚C unless otherwise specified. Complete exchange of the culture medium was performed at regular intervals, ranging from every 2 hours to every 3 days.

Once the hMSC had covered approximately 80% of the culture surface (or had reached mid-exponential phase of growth), the cell monolayer was detached with an enzymatic treatment. First the spent medium was decanted from the flask or

well, and replaced with an equal amount of DPBS without Ca^{2+} and Mg^{2+}, to remove traces of serum. The buffer was removed by aspiration, and 0.04 ml/cm^2 trypsin/EDTA was added to the cell monolayer to break cadherin mediated cell-cell adhesion by cleavage of peptide bonds at lysine and arginine residues and to sequester divalent cations that interfere with trypsin activity (Olsen et al., 2004, Freshney, 1994). Trypsin activity was aided by placing the culture vessels in an incubator under the same conditions as the ones used for cell cultures, for no longer than 10 minutes to avoid any damage to the cells. As soon as the cells were detached from the surface, which was determined by microscopic observation, trypsin activity was inhibited by addition of culture medium, in quantities from 0.04 to 0.08 ml/cm^2. To ensure optimal recovery of the hMSC from the culture surface, the cell suspension was pipetted up and down to wash cells from culture surface, prior to removal of the cell suspension from the culture vessel. Samples were taken from the concentrated cell suspension for cell density measurements, which was determined by Trypan Blue exclusion (Section 2.6.1) or by Guava analysis (Section 2.6.2).

2.5 Replacement of FBS with Protein Hydrolysates from Culture Medium

FBS was replaced by protein hydrolysates from the growth medium to test if this new media formulation without animal derived components could sustain hMSC growth. Four different protein hydrolysates were tested, HyPep 4601, HyPep 1511, HyPep 1510, and Hy-Soy (all from Kerry Bio-Science, Tralee, Ireland).

Culture medium was formulated with 1g/L glucose DMEM (BioWhittaker), 2mM L-glutamine (BioWhittaker), 100 U/ml penicillin and streptomycin (BioWhittaker) and 4 g/L (w/w) protein hydrolysate. After formulation, the medium was filtered through a 0.2 μm filter (Nalgene). hMSC diluted into each of the four animal-free medium formulations were seeded into 24-well plates with $5x10^3$ cells/cm^2. The cultures were kept for 13 days with medium exchanges every three days. Wells from each of the growth medium conditions were harvested at different time point intervals to determine cell growth kinetics based upon viable cell counts (Section 2.6.).

2.6 Quantification of Cell Viability and Cell Density

Two different assay techniques were used to determine cell viability and cell density in hMSC cultures; Trypan Blue exclusion and Guava Viacount (Guava Technologies, Hayward, California, USA). Trypan Blue exclusion is a widely used method for enumerating living and dead cells in culture. Guava Technologies have recently developed a new method to evaluate cell viability and density based on DNA fluorescent stains that can be detected with a Guava Easycyte flow cytometer (Guava Technologies).

In general samples from parallel replicate experiments were used for cell density determination, but when this was not possible, replicate samples from the same condition were analysed with either of the these two techniques.

2.6.1 Trypan Blue Exclusion and Haemocytometer for Cell Density and Viability Quantification

Trypan Blue is a vital dye. The reactivity of Trypan Blue is based on the fact that the chromophore is negatively charged and does not interact with the cell unless the membrane is damaged. Therefore, all the cells which exclude the dye are viable and the ones with permeable membranes that take up the dye are dead and appear dark blue under a microscope.

Cell suspensions of hMSC were mixed by gently pipetting up and down prior to sampling to ensure homogeneity of the suspension. Independent 0.2 to 0.5 ml samples were taken in 1.5 ml Eppendorf tubes. Trypan Blue was then added to each sample and a minimum of 3 minutes were allowed for the stain to penetrate the cells. Depending on the density of the cell suspension, the ratio in volume of cell suspension to dye used for haemocytometer measurements, ranged from 1:1 to 1:40. The stained cell suspension was then loaded into a haemocytometer. A haemocytometer is a specialized microscope slide with a thick base containing a grid in a counting chamber, and uses a special cover glass which is thick enough to stay flat under the pull of surface tension from the solution in the chamber. The haemocytometer chamber is divided into two sides with a grid of 9 squares each and a loading volume of 10 μl per side. The dye stained cell suspension was

loaded into the haemocytometer by pipetting 10 µl into each side of the chamber. Ten squares were counted per haemocytometer loaded, and cell density in cells/ml and percent viability were determined according to:

$$\text{Cell concentration (cell/ml)} = \frac{\text{no. of cells counted} \times \text{dilution factor} \times 10^4}{\text{no. of squares counted}} \qquad (2.1)$$

Cell concentration was expressed in surface cell density by the formula:

$$\text{Viable cell density (cell/cm}^2\text{)} = \frac{\text{Viable cell concentration (cell/ml)} \times \text{volume of cell suspension (ml)}}{\text{surface area (cm}^2\text{)}} \qquad (2.2)$$

Percentage viability was calculated according to:

$$\text{Viability (\%)} = \frac{\text{number of live cells}}{\text{total number of cells}}.100 \qquad (2.3)$$

2.6.2 Guava for Cell Density and Viability Quantification

Guava Viacount reagent was used in conjunction with a Guava EasyCyte 96-well flow-cytometer (both from Guava Technologies) to determine hMSC concentration and viability. Results were analysed using Guava's ExpressPlus software (CytosoftPCA, by Guava Technologies).

The Guava ViaCount assay consist of two DNA-binding dyes. One of the dyes is membrane permeable and stains all nucleated cells; fluorescent signal from the nuclear staining dye is detected by photomultiplier tube 2 (PM2). The other dye only penetrates cells with compromised membrane integrity (i.e. non-viable cells) and is detected by photomultiplier tube 1 (PM1). Forward light scatter (FSC) intensity is used to detect the size of a particle, and to distinguish between debris events with low FSC signal and cells with higher FSC signal.

Viable cell concentration and viability were measured by staining 200 µl of cell suspension with 3 µl of ViaCount dye followed by a 15 minute incubation period at room temperature in the dark. Each sample was loaded into a 96-well plate, and inserted in the autosampler platform of the Guava instrument. Samples were

mixed for 6 seconds prior to sampling with an internal rotating mixer and a minimum of 2000 events were collected for each sample.

2.6.3 Comparison of Haemocytometer and Guava Viable Cell Density Determination

Cell viability and cell density were determined using either Trypan Blue exclusion (Section 2.6.1) or the Guava method (Section 2.6.2). In order to evaluate the validity of the results obtained from either method and to enable a comparison of results from different experiments in this thesis, a comparison of viable cell counts from both assays was performed.

A total of 18 samples of hMSC of different cell concentrations were subjected to both assays to determine viable cell density. The results from the haemocytometer cell counts were plotted against the results from Guava Viacount as shown in Figure 2.2. Comparison between both results shows that viable cell count determination between both methods follow a linear relationship and that in general there is a good agreement between the two methods.

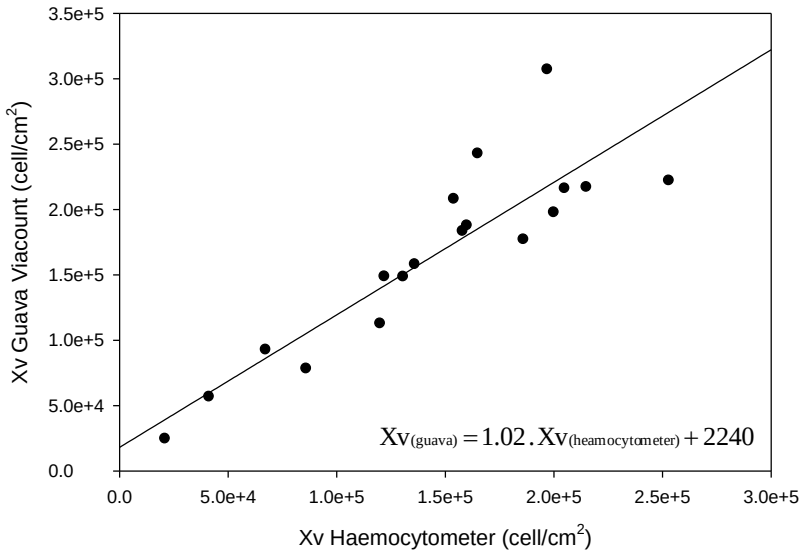

Figure 2.2 Comparison of the two different methods used to determine viable cell density. Haemocytometer counts as described in Section 2.6.1 and Guava counts as described in Sections 2.6.2.

2.6.4 Calculations Used for Cell Growth Characterisation

Based on viable cell density and viability measurements (Section 2.6) at specific time points during cell proliferation within one passage, cell growth rates and doubling times were calculated to enable quantitative comparison of culture performance and modelling of the cell expansion process.

2.6.4.1 Cell Growth Rate and Doubling Time

Cell growth rate is an intrinsic characteristic of hMSC for each donor and for each passage of the overall cell expansion process (Phinney et al., 1999; Bruder et al., 1997; Mareschi et al., 2006). It is used as an indicator of culture performance in response to different medium formulations and culture operating conditions. Solving a cell balance for a batch culture (Equation 2.4), yields the following equation to calculate cell growth rates (Equation 2.5):

$$\frac{dX}{dt} = \mu X \tag{2.4}$$

where X is the cell density at time t, and μ is the cell growth rate as described by:

$$\mu = \frac{\ln\left(X_f / X_0\right)}{\left(t_f - t_0\right)} \tag{2.5}$$

where X_f is the final cell density, X_0 is the initial cell density, t_f is the time at which the cell density reaches X_f and t_0 is the initial time. For cell growth rate calculations, the time that the culture is in lag or stationary phases is not taken into consideration, and t_0 and t_f are considered as the points in the culture when the cells enter and exit the exponential growth phase respectively as determined from the linear region of a plot of $\ln(X/X_0)$ against t.

Doubling time (T_d) is defined as the time taken for the cell population to double in number, or when X is equal to $2X_0$. By making this substitution in Equation 2.4, and solving for t, the equation for calculating doubling time is obtained:

$$Td = \frac{\ln(2)}{\mu} \tag{2.6}$$

For a limited number of cultures in T-flasks without replicates, where only initial and final cell densities are know, approximate growth rates are calculated based on these two data points. It is important to understand that when growth rates or doubling times are calculated in this manner, it represents an estimate of the real value. Other factors such as lag phase time length and duration of exponential growth will not be known and it can result in slower calculated growth rates and doubling times depending on the time at which the final measurement is taken.

2.6.4.2 Population Doubling Level

Population Doubling Level (PDL) indicates the number of times that the cells have doubled (divided) over the cell expansion process, as expressed by Equation 2.7. Changes in PDL can be calculated by solving Equation 2.7 for ΔPDL (Equation 2.8). The overall PDL of the culture can be determined by adding each ΔPDL if the history of the cells is known from P0 or from isolation. PDL is time independent, and it is a more accurate indicator of the age of the culture than a passage number.

$$X_f - X_0 = 2^{\Delta PDL} \tag{2.7}$$

which can be rearranged to give:

$$\Delta PDL = \frac{\ln\left(X_f / X_0\right)}{\ln(2)} \tag{2.8}$$

2.6.4.3 Metabolic Rates

Consumption rates for glucose and glutamine and production rates of lactate and glutamate give an indication of the culture behavior. These rates also help understand possible rate limiting components for growth in the culture medium, or toxic accumulation of byproducts that may inhibit growth. Metabolic rates were normalized on the basis of viable cell density, to give specific rates.

Metabolic rates were calculated with a mass balance on the metabolite over the period of the culture or of the sampling range as expressed by Equation 2.9:

$$\frac{dC_A}{dt} = qA \times X \tag{2.9}$$

where C_A is the metabolite concentration, qA is cell specific metabolite production/consumption rate (in mass per viable cell per unit time), and X is the cell density per unit volume.

2.7 Quantification of Metabolite Concentrations

Metabolites from 1 ml filtered samples of the spent medium collected at different time points during the culture of hMSC were measured using a Bioprofile 400 (Nova Biomedical, Waltham, MA, USA). This device provided readings for glucose, lactate, glutamine, glutamate and ammonium. In addition to metabolites, the Bioprofile 400 also provided values for pH, sodium, potassium, and osmolality.

2.8 Temperature On-Line Monitoring

Temperature variations during cell expansion of hMSC occur during medium exchanges or microscopic observations, when the cultures are taken out of the incubator into a biosafety cabinet or placed under the microscope. The two possible temperature step changes that the cultures are exposed to are: (i) a downward step change from 37˚C to room temperature and (ii) an upward step change from room temperature to 37˚C in a humidified incubator with air blowers that pump a controlled 5% (v/v) CO_2 atmosphere. Temperature changes in the culture medium due to these step change temperature variations were measured in 12-well plates.

All wells in a 12-well plate were filled with culture medium with a working volume of 2 ml per well, the same volume used for the culture of hMSC. Two glass fibre insulated type-T thermocouples (RS Components, Corby, UK) were immersed in the liquid of two wells in different locations in the plate (one at the corner well and another one in a central well), and another two thermocouples were placed 10 to 25cm above the plate to record the ambient temperature. The thermocouples were connected to a USB-based eight channel temperature

measurement module (USB-TC, Measurement Computing, Norton, Maryland, USA) that converted the signal from analog to digital and recorded the data into a computer. The USB-TC measurement module was allowed to equilibrate for a minimum of 30 minutes before calibration as per the manufacturer recommendations, and calibrated using *Insta*cal calibration software (Measurement Computing). The data was processed using TracerDAQ 2.0 (Measurement Computing).

A number of different operating scenarios were reproduced, and the subsequent temperature changes in the liquid of the wells as well as in the surrounding environment were measured.

1. Maximum temperature change from 37˚C to room temperature. The plate was equilibrated in the incubator until all temperature sensors recorded 37˚C. Then, the plate was removed from the incubator and left on the laboratory bench until the temperature of the liquid in the wells reached room temperature.
2. Maximum temperature change from room temperature to 37˚C. The plate was equilibrated on the bench top at room temperature to ensure that the liquid temperature was reading the same temperature as the sensors recording room temperature. Then it was placed in the incubator at 37˚C until the temperature sensors in the liquid of the wells reached 37˚C.
3. Fifteen minute step change from 37˚C towards room temperature. Fifteen minutes was determined to be the maximum time it takes for a trained operator to manually remove a 24-well plate from the incubator, perform a medium exchange in all wells of the plate, and place the plate back into the incubator. For this measurement, a pre-equilibrated plate was removed from the incubator and placed inside a biosafety cabinet removing the lid, to take into consideration the heat transfer effect of the blowers inside the laminar hood. After 15 minutes, the lid was placed back onto the 12-well plate, and the plate was placed back into the incubator.
4. Step change from room temperature to 37˚C with shaking. To accelerate heat transfer into the liquid of the wells orbital shaking of the plates was tested at shaking frequencies of 150 and 250 rpm.

2.9 pH Monitoring

The culture medium contains phenol red as a pH indicator, and is buffered to maintain a pH of 7.4. The pH of the culture medium changes during the cell expansion process and during manual manipulations with exposure to atmospheric CO_2 levels and it is dependent on temperature.

2.9.1 pH On-Line Monitoring

Changes in the pH of microwell cultures due to environmental variations (temperature and gas composition) were detected by pH-sensitive optical mini-sensors in conjunction with a pH-4 mini - Four Channel pH meter for fibre-optic pH mini-sensors (both from PreSens GmbH, Regensburg, Germany), based on pH sensitive, fluorescent dyes.

The pH-4 mini is a PC-controlled four channel pH meter device based on the DLR (dual luminophore reference) method. This referencing method uses the measurement of average decay times. The sensor (Figure 2.3) consists of a pH indicator with short decay time and an inert reference dye with long decay time. The average decay time is a measure of the ratio of the intensities of the two dyes and therefore for pH. This method allows therefore referenced measurements with the use of a single light source and detector and a single filter combination. The device is controlled through HView software, which also saves and displays the data collected.

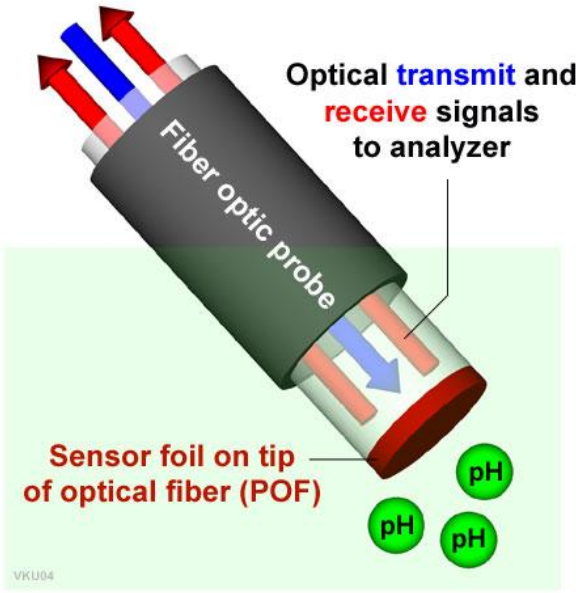

Figure 2.3 Schematic diagram of the pH sensor for the pH-4 mini. (Image sourced from www.presens.de).

The sensor foil on the tip sterilized by gamma irradiation are planar pH sensor spots made of polymer optical fibers (POF) containing immobilized indicator dyes. They can be detected in a non-invasive and non-destructive way from outside the wall of a transparent well, with a resolution of 0.005 in units of pH. These 2 mm in diameter circular spots were secured with silicon glue inside the wells of a 12-well plate in the centre of the well. The well plate was secured onto a raised platform with perforated holes to allow placement of the probe underneath the wellplate.. The fiber optic probe was connected to the spots from the outside of the well through the bottom of the platform. The optical sensors do not leach into the culture medium, but they are subject to photobleaching. Bleaching is proportional to the light dose with a decay rate of 0.01 pH for every 1000 measuring points, therefore it can be minimised by the decrease of LED current or larger measurement intervals.

A six point calibration of the sensor spots was performed before all measurements. The calibration has a sigmoid shape described by the Boltzman curve, Equation. 2.10:

$$\text{Phase} = \frac{\phi_{\min} - \phi_{\max}}{1 + e^{\left(\text{pH} - \text{pH}_0 / \text{dpH}\right)}} + \phi_{\max} \qquad (2.10)$$

Where $\phi_{\min}$ and $\phi_{\max}$ are minimum and maximum phase numbers, pH is the pH-value of the buffer solution, pH0 is the measured pH value, and dpH is the differential of the pH values.

Six pH calibration buffers (4.0, 5.0, 6.0, 7.0, 8.0, and 9.0) were used to obtain all the coefficients of the curve (Figure 2.4). PreSens provide a calibration programme DLR470.xls, in which by entering the phase values obtained from the measurement with each buffer solution at room temperature, values for $\phi_{\min}$, $\phi_{\max}$, pH_0, and dpH were obtained (Table 2.1). These values were entered in the set-up menu of HView software, which records and displays pH measurements.

Table 2.1 Example of calibration results from PreSens pH optical fibre sensor spots. Measurements performed as described in Section 2.9.1.

Calibration and Predicted		**Calibration Results**	
Buffer Soln	**Measured**		
4	52.9800	$\phi_{\min}$	54.917
5	51.7700	$\phi_{\max}$	18.663
6	45.7500	dpH	0.87
7	33.8100	pH_0	6.87
8	28.1900		
9	20.7600		

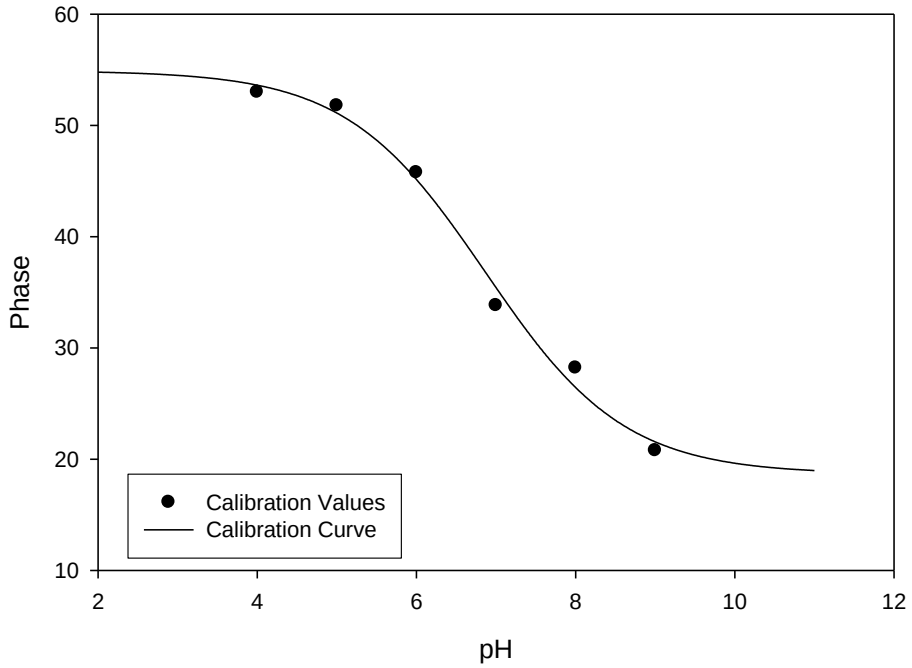

Figure 2.4 Example of a calibration curve for PreSens pH optical fiber sensor spots. Calibrations measurements performed as described in section 2.9. Calibration curve fitted according to Equation 2.10.

Experimental step up and environmental exposures to different temperature and CO_2 conditions were identical to the ones detailed in Section 2.7. All values obtained for pH were corrected for temperature with the measurements obtained from on-line temperature measurements collected in that section, following Equations 2.11 to 2.14.

$$\phi\text{min}(T) = \phi\text{min}(Tcal) - 0.05526 \times (T - Tcal) \quad (2.11)$$

$$\phi\text{max}(T) = \phi\text{max}(Tcal) - 0.04402 \times (T - Tcal) \quad (2.12)$$

$$pH_0(T) = pH_0(Tcal) - 0.01744 \times (T - Tcal) \quad (2.13)$$

$$dpH(T) = dpH(Tcal) - 0.00258 \times (T - Tcal) \quad (2.14)$$

where ϕmin(Tcal), ϕmax(Tcal), pH_0(Tcal), and dpH(Tcal) were the values obtained during calibration at a set temperature as shown in table 2.1, and ϕmin(T), ϕmax(T), pH_0(T), and dpH(T) were calculated for each measurement

taken at the temperature recorded at the same time. Both parameters, temperature and pH, were measured at identical time points in intervals of 15 seconds.

2.9.2 pH Off-Line Monitoring

A pH meter equipped with a temperature probe for temperature correction (SevenEasy pH, Mettler Toledo, Columbus, OH, USA) was used to measure pH off-line. A two point calibration at 4.01 and 7.01 pH was performed prior to each measurement. Measurements of media samples equilibrated inside the incubator at 37˚C and preset CO_2 concentrations of 0, 2, and 5% were taken within one minute of removal from these controlled conditions.

2.10 Cell Surface Marker Characterisation

Cell surface marker expression for CD90, CD105 (SH2) and CD166 was determined at different stages of growth. Mouse anti-human all surface marker antibodies were monoclonal mouse anti human FITC conjugated from AbD Serotec (Kidlington, UK). Mouse IgG1 FITC conjugated, also from AbD Serotec, was used as a negative control. Unstained cell suspensions stained with Viacount Reagent were also tested in parallel.

Cultures of hMSC were harvested during the mid exponential phase of culture as described in Section 2.4. The cells were trypsinized from the tissue culture surface, and samples were taken to determine cell density (Section 2.6). The rest of the cell suspension was centrifuged at 400 g for 5 minutes, and the supernatant removed. The cell pellet was washed twice with buffer (PBS containing 2 mM EDTA and 0.5% (w/v) BSA, pH 7.2) using centrifugation at 400 g for 5 minutes, to remove traces of media. Aliquots of $5x10^5$ to $5x10^6$ cells in 100 µl of buffer were incubated with 10 µl of the corresponding conjugated monoclonal antibody at 4˚C in the dark for 30 minutes. After incubation, samples were washed twice with buffer, and the cell pellets were resuspended in buffer to a 500 cell/µl suspension.

Surface marker expression was determined by flow cytometry using a Guava Easycyte 96 as described in Section 2.6.2. For each sample, 200 µl were loaded

into a well from a 96-well plate, and 3 μl of Viacount reagent was added to stain for nuclei. The plate was incubated in the dark for 10 minutes, and measurements acquiring 5000 events were performed. hMSC were gated in a plot of forward side scatter (FSC) versus PM3 (green fluorescence to detect FITC conjugated antibodies).

2.11 Cell Size Measurements

Cell size for hMSC at passage 1 (P1) and 5 (P5) was determined using two different devices, Zetasizer 3000 (Malvern Instruments Ltd, Malvern, UK) and Cedex.HiRes (Innovatis AG, Bielefeld, Germany).

2.11.1 Mastersizer

Cell suspensions harvested from hMSC cultures were sized by dynamic light scattering using a Zetasizer 3000 (Malvern Instruments Ltd). The principle of the measurement is based on the intensity of the scattered light of a laser when going through a sample of particles diluted in liquid (www.malvern.com). The intensity of the scattered light fluctuates at a rate that is dependent upon the size of the particles. Analysis of these intensity fluctuations can then be correlated to the average diameter of the particle.

The hMSC suspension samples were diluted in a 1:10 ratio with PBS and analyzed in duplicate. All measurements were taken from a reservoir at 25˚C, with a counting time of 60 s each, a low rotation speed of 400 rpm in the sample chamber to minimise cell damage, and were run at a 90˚ fixed angle. The measurements were analysed using the software supplied by the manufacturer.

2.11.2 Cedex Imaging

Cedex HiRes is an automated cell culture analyzer that uses the Trypan Blue exclusion method in conjunction with digital image recognition to determine cell density, viability, diameter and aggregate rate of the cell suspension. It uses a liquid handling system to load the cell suspension, and to stain it with Trypan Blue. The stained cell suspension is scanned and 300 images are analyzed per sample. Samples of harvested cell suspension from P1 and P5 were loaded into a

Cedex HiRes to measure average cell size and size distribution in the population. Each sample was of a minimum of 300 µl in volume.

2.12 Automation of Cell Expansion Process

A Tecan automated platform with liquid handling system was used for the expansion of hMSC throughout one passage (Figures 2.5 and 2.6).

Figure 2.5 Tecan Automated Platform for the expansion of hMSC. The robotic arm on the right-hand-side transports the well-plates from the incubator to the platform. The liquid-handling arm on the left-hand-side can perform medium exchanges as well as trypsinisation operations by aspirating spent medium and dispensing new media or cell suspensions into the wells or well-plates.

Figure 2.6 Automated system for the aseptic cell expansion culture of hMSC. The robotic platform that manipulates well-plate cultures is enclosed within a temperature and gas controlled biosafety cabinet. The system is equipped with a robotic incubator and a centrifuge, both of them with aseptic connections into the robotic platform.

2.13 Non-linear Regression Analysis

Growth curves of hMSC were characterised by a four-coefficient generalisation of the Gompertz equation as described later in Section 5.2. The experimental data were fitted using a non-linear regression algorithm provided with SigmaPlot (SigmaPlot for Windows, version 9.0). Values for the coefficients, standard errors, and correlation coefficients (r^2) for each fitted curve were generated by SigmaPlot.

CHAPTER THREE

hMSC Isolation and Cell Growth Characterisation

3 HMSC ISOLATION AND CELL GROWTH CHARACTERISATION

3.1 Introduction and Aims

As described in Section 1.1.2.1 hMSC are anchorage dependent, requiring a surface to adhere to for both survival and proliferation (Silva et al., 2003, Colter et al., 2000). They are also contact inhibited, meaning they only grow until a monolayer is formed and all cells are in contact with each other. At this point they will stop proliferating and apoptosis or senesce will be induced (Hayflick, 1965; DiGirolamo et al., 1999; Sekiya et al., 2001). From a biochemical engineering perspective, these characteristics make the cell expansion process more challenging than for suspension cultures, since large surface areas are needed to scale up the process (Barrilleaux et al., 2006). *In vitro* expansion of hMSC allows cell proliferation in an undifferentiated state while exhibiting characteristics typical of the Hayflick model of cellular senescence, having a limited lifespan which depends on the source of the cells, and it does not go beyond 38 population doublings while maintaining multipotency (Bruder et al., 1997).

In addition, various parameters intrinsic to the source of the cells also affect the proliferation potential of hMSC, and the quality of the cells at the end of the expansion process. Due to the variability of cell growth kinetics according to age, sex, and health of the bone marrow donor (D'Ippolito et al., 1999; Phinney et al., 1999), it is challenging to design a robust expansion protocol that would ensure provision of enough cells of the desired quality for clinical applications and which is able to account for the inherent variability of the cell source.

The aim of this chapter is to quantitatively study the characteristics of growth and differentiation of hMSC in relation to the isolation technique used to separate them from bone marrow. The specific objectives will be to characterise the influence of the culture vessel employed for the cell expansion process, the nature of the surface employed for attachment, and the extent to which cells can be expanded while retaining crucial stem cell like properties. Cell growth kinetics will also be modeled in order to enable a quantitative comparison of culture conditions and to provide a basis for a more detailed model of a multi-step,

automated cell expansion process as described later in Chapter 5. These studies thus serve to characterise the baseline profiles of hMSC growth under standard culture conditions, from which it will be possible to assess the success or failure of future optimisation experiments. The specific objectives of the work are:

- To examine different isolation techniques for the separation of hMSC from bone marrow and to assess the impact of such techniques in growth kinetics, as well as to evaluate the effect of cell banking on cell growth.
- To examine different culture surfaces for the cell expansion of hMSC
- To characterise growth kinetics over sequential passages with the objective of establishing a baseline cell expansion process for future optimisation in subsequent Chapters.

3.2 hMSC Isolation from Bone Marrow and Cell Banking

The first step toward the selection and characterisation of hMSC was to isolate the cells from bone marrow samples, and to create a bank of cells from different donors for subsequent experiments. Frozen bone marrow samples, acquired as described in Section 2.1, were used for all isolations. They contained a mixture of bone marrow fluid, blood, adipose tissue, and small pieces of bone in some cases. Creating a cell bank from a given source at a specific passage allows not just for the availability of cells for experimentation at a later time, but also for consistency of results within a given source of cells from the same origin and at the same stage of growth by removing any intrinsic variability that is observed in cells obtained from different donors and cells at different population doublings (Section 3.2.2).

A relatively limited number of techniques have previously been used for the isolation of hMSC from bone marrow extracts, such as Ficoll™ density gradient centrifugation, Direct isolation, fluorescence-activated cell sorting, and Immunomagnetic selection as indicated in Section 1.2.1. The most commonly used technique is Ficoll™ isolation, which uses a polysaccharide and sodium diatrizoate solution for density gradient centrifugation of mononucleated cells from bone marrow. This method is not highly selective, initially recovering all

mononucleated cells from bone marrow. However, the hMSC isolation is completed during the first passage on the basis that the hMSC are the only cells that attach to a surface-treated plastic culture vessel. Direct isolation, by seeding bone marrow alone or diluted with culture medium into a culture vessel, also achieves acceptable recovery levels of hMSC present in the original biopsy, while minimizing the stress exerted to cells during the sequential centrifugation steps required for a density gradient isolation. Selection of hMSC by Direct isolation is of special interest for this project since it allows potential implementation of the isolation step in an automated platform. From each of these two methods, Ficoll™ and Direct isolation, it was able to recover hMSC and to create cell banks for subsequent usage. Both methods were compared to establish differences in cell recovery and subsequent growth.

The effect of controlled freeze/thaw during cell banking and subsequent resuscitation of the cells was also assessed (Section 3.2.2). These are important control experiments that enable comparison of growth kinetics of hMSC that had been frozen with DMSO versus those that had not undergone such treatment. Such studies are also necessary with regard to the validation of this step in what is envisaged to be a cGMP compliant cell expansion process.

3.2.1 Ficoll™ Isolation versus Direct Isolation

Eighteen frozen bone marrow bags from different donors (stored as described in Section 2.1.) were used for these studies to compare isolation techniques and to recover hMSC for subsequent experimentation. The bags contained bone marrow samples in addition to heparin and DMSO to prevent clotting and cell membrane breakage when thawed as indicated in Section 2.1. They had been stored in liquid nitrogen for various length of time ranging from four to ten years. The volume of each bag varied between 120 and 74 ml.

All eighteen bone marrow bags were subjected to Direct isolation as per the protocol indicated in Section 2.1.2, and of those, five were also processed by Ficoll™ density gradient isolation as per the protocol indicated in Section 2.1.1. Eight of the eighteen bags failed to undergo isolation after plated in T-flasks due

to gel formation within thirty minutes to three hours after seeding or due to contamination. The cause of a gel formation was not further investigated, although there is a possibility that either the amount of heparin added following the initial donor biopsy was not sufficient to prevent clotting in those samples, or that the samples had been stored in liquid nitrogen for too long. No association with a specific isolation technique was identified as the source of clotting.

The initial number of viable cells present in the bone marrow bags tested, ranged from $7.5x10^6$ to $2.9x10^6$ cells/ml with an average of $4.9x10^6$ cells/ml (n=4). These numbers account for a mixed population of cells prior to isolation. The percentage of hMSC from this initial diverse cell population could vary and it was unknown for each specific sample, but it has been reported to be in the range around 1 in $1x10^7$ to 10^8 cells (Reyes et al., 2001; Silva et al., 2003). The initial viable cell densities were therefore not indicative of the possible success of hMSC isolation. This could only be assessed after a number of days in culture following the plating of the cells in T-flasks.

The effect of isolation conditions on hMSC recovery and growth kinetics was studied by subjecting cells from a common bone marrow sample to different isolation techniques. Ficoll™ isolations were performed as described in Section 2.1.1, in which mononucleated cells are recovered from an interface formed after centrifugation of PBS and bone marrow over a layer of Ficoll™. This technique exposes the cells to a minimum or two centrifugation steps prior to seeding into a tissue flask. Direct isolations were performed by seeding unprocessed bone marrow with different ratios of bone marrow to culture media into T-150 culture vessels. The effect of centrifugation on cell recovery was studied by centrifuging an aliquot of bone marrow diluted with PBS (1:1 v/v), removing the supernatant, re-suspending the pellet into media and seeding into a culture vessel.

For this comparison of isolation techniques four aliquots were prepared from the thawed content of a bone marrow bag. One aliquot was used to seed a T-150 flask with 10 ml of bone marrow and 20 ml of culture media (ratio of 1:3 v/v bone marrow to culture media). A second aliquot was used to seed 25 ml of bone marrow into a T-150 flask without any physical separation or media additions

(1:0 v/v bone marrow to culture media). A third 10 ml aliquot was mixed with 10 ml of PBS and centrifuged at 650 g, 21˚C for 15 minutes to mimic the centrifugation conditions during the washing step of the mononucleated fraction of cells recovered from the interface of a Ficoll™ separation. The remaining pellet of cells was re-suspended in 30 ml of media and seeded into a T-150 flask. The fourth 10 ml aliquot was subjected to a Ficoll™ separation and seeded with 30 ml of culture media into a T-150 flask. The flasks were monitored by daily microscopic observations, and the media was exchanged on day 1, and every three to four days from then on until harvest.

Microscopic observations on day one revealed a more uniform cell population in the flask seeded with mononucleated cells recovered from Ficoll™ isolation, than for any of the other conditions. However, after the first two medium exchanges on days one through four, this method appeared to yield cells with a similar cell morphology and percentage cell surface coverage to those found with the direct seeding with unprocessed bone marrow and culture media. After ten days in culture, Direct isolation with unprocessed bone marrow visually had a higher confluency of hMSC cells than any other condition. All flasks were harvested after 19 days in culture, at which point the cells isolated with Ficoll™ and Direct inoculation of unprocessed bone marrow with culture media had reached confluency. At the time of harvest the other two conditions, straight inoculation of bone marrow without media addition and centrifuged sample with PBS, did not exhibit any cells with hMSC morphology. This result indicates that culture media addition after thawing is essential for the survival of hMSC *in vitro* cultures, and that centrifugation can be detrimental to hMSC isolation and growth.

The cells from the two T-150 flasks containing hMSC were harvested after reaching confluency and seeded into T-150 flasks at an inoculation cell density of $5x10^3$ cell/cm^2 according to the cell expansion procedure indicated in Section 2.4. The medium was exchanged every three to four days, and the cells were recovered after seven days in culture. Cell density and viability were determined, indicating a 34% increase in hMSC growth and survival from the flask seeded with cells recovered by Direct isolation ($1.53x10^4$ viable cells/cm^2) than from the

flask seeded with cells recovered by Ficoll™ isolation ($1.00x10^4$ viable cells/cm^2). This effect could be an indication of accumulated stress damage to the cells after undergoing density gradient centrifugation, resulting in a decrease in cell growth rates for the first passage after isolation.

Variations of this experiment during the course of the project (data not shown) yielded the same trend as assessed by microscopic observation within four to seven days after initial seeding of cells recovered after isolation. Those cells that had undergone Ficoll™ isolation took longer to reach confluency in the first passage than the ones seeded directly from bone marrow and supplemented with formulated culture media in ratios of 1:3 or 1:4 v/v bone marrow to culture media. Any other dilution ratio of bone marrow to media tested proved to be unsuccessful for the isolation of hMSC. The overall number of cells recovered from each isolation procedure depended on the initial volume of the bone marrow sample, the initial number of cells/ml on the sample, or the donor, and consequently these values were not used to compare performance of the isolation for any cell source when coming from a different donor.

3.2.2 Cell Banking and the Effect of Freeze/Thaw on Isolated hMSC

Six cell banks were generated following the cell banking procedure indicated in Section 2.2. Each bank was generated from a different donor after a Ficoll™ or a Direct isolation, at passage numbers ranging from P0 (first recovered cells from initial seed into a culture vessel after Ficoll™ or Direct isolation) to P4 (cells expanded for four passages as per protocol in Section 2.4). Each bank generated provided from 5 to 34 one-millilitre vials containing $1x10^6$ cells/ml for subsequent experimentation. The number of vials created depended on the number of cells recovered from isolation as well as the volume of cell suspension removed at a given passage for subsequent experimentation, and therefore was not indicative of the yield of hMSC obtained from a specific donor. All banks created successfully provided a source of viable hMSC for further experimentation.

To understand if cell banking could cause any detrimental effect on cell growth kinetics when compared to cells that had not undergone a freeze/thaw step, hMSC that had reached P4 from subsequent passages after Ficoll™ isolation were banked, and the rest were carried forward for one more passage. From P4, nine vials were prepared and frozen with DMSO as described in Section 2.2. The rest of the cell suspension was used for a subsequent cell expansion in six-well plates, inoculated with $5x10^3$ cells/cm^2. The cells that were not frozen had reached confluency after five days in culture, to a final cell density of $2.37x10^4$ cells/cm^2. By comparison, one vial from this cell bank created from the same cell source was thawed, and the content of the vial was seeded in T-150 flasks with an equal initial cell density of $5x10^3$ cells/cm^2. It took 13 days for this culture to reach confluency instead of the 5 days required for the same cells when they had not undergone a freeze/thaw treatment. Also, the final cell density reached was lower for the cells expanded from the cell bank, reaching $1.30x10^4$ cells/cm^2 – a 50% reduction from the maximum cell density achieved with the cells obtained from cells that had not been frozen. The cell growth rate (calculated according to Equation 2.5) for this particular passage for cells that were not frozen was 0.31 day^{-1} in comparison to 0.07 day^{-1} for those cells coming out of a frozen vial. This represents a significant reduction of growth kinetics and provides insight into the operation of a hospital-based autologous cell expansion process. Not enough data was collected as to address any differences in the duration of the lag phase for each of these two conditions, therefore the reduction in the growth rate observed for the cell population recovered after thaw could be in part attributed to a longer lag phase. The difference in the apparent growth rate calculated with the final cell density at harvest is large enough as to indicate that also the rate of growth could have been hindered by the thawing process, and that an adaptation to the culture environment during a first passage of growth can be one of the reasons for the lower growth rate for the cells that had undergone freezing conditions. These results are summarised in Table 3.1.

Table 3.1. Effect of cell banking on hMSC growth characteristics for cultures expanded up until P4. hMSC isolated as described in Section 2.1.1 and then expanded as described in Section 2.4. Cell Bank indicates cells thawed from a frozen vial prior to seeding at P4, and Cell Train indicates cells that have been sequentially passaged without undergoing a freeze/thaw procedure prior to seeding at P4.

Cell Source at P4	Time to Reach Confluency (days)	Maximum Viable Cell Density (cell/cm^2)	Growth Rate (day^{-1})
Cell Bank	13	$1.30x10^4$	0.07
Cell Train	5	$2.37x10^4$	0.31

Both cultures expanded consisted of the same cell source at the same cell passage, same inoculation cell density, and medium exchanges performed every three to four days. Any effect on cell growth that could be attributed to the different dimensions of the culture vessels (6 well-plates versus T-150 flasks) was addressed, showing no impact in cell growth as detailed later in Section 3.3. The only difference between both cell cultures was a cell freezing step, that was shown to have a detrimental effect on cell growth for the first passage directly following vial thawing. Both growth kinetics, as well as maximum viable cell density achieved after seeding pre-frozen hMSC showed lower values than in those cells that had not undergone such treatment.

3.3 The Effect of Culture Surface Dimensions on hMSC growth

Characterisation of the cell expansion processes of hMSC can be carried out using different culture surfaces depending on the purpose of the experiment, the routine protocols of the laboratory, or the number of cells available at the time. As an example, to generate cell growth curves, it is necessary to collect cell density values at different time points during a passage. In order to obtain these time point cell densities, cells must be removed from the surface of a sacrificial vessel every day or every other day to determine the kinetics of growth. This protocol involves an initially large number of culture vessels to be sacrificed over the course of the passage, and consequently a large number of hMSC. For this reason, cell growth kinetic studies are more conveniently executed in well plates

than in T-flasks when cell numbers are a constraint, since the cell requirement to seed a smaller surface area on each well is minimum compared to the number of cells it would take to seed enough T-flasks to get the required data points throughout the time of the passage. In other cases, when a large number of cells are needed to perform a series of assays at a specific time point, or when the only purpose of a particular passage is to expand the cells for subsequent passages or to create a cell bank, T-flasks that provide a larger culture surface are more convenient.

In either case, even if all surfaces used are from the same manufacturer with the same surface treatment, there may be differences in cell growth from T-flasks to wells due to the difference in geometries and dimensions (Lundholt et al., 2003). In wells, the percentage of working volume in contact with the wall of the vessel is larger. Next to the wall there is a gradient of gas transfer from the head space due to the boundary formed by the plastic wall, and microscopic observations reveal that the cells tend to proliferate away from this location towards the centre of the well. For the results obtained from different cell expansion protocols to be comparable, it is important to first of all verify that the patterns of growth of hMSC in all vessels used are not affected by the dimensions or the geometry of the culture flasks or well plates.

To study cell growth kinetics for hMSC expanded in well-plates of different dimensions, a pool of cells from the same donor at the same stage of growth was seeded into 6, 12, and 24 well plates from Corning. Growth curves for each well plate were determined by sacrificing one well from each plate at different time points throughout the passage as described in Section 2.6.4.

The hMSC growth curves obtained from each of the three well plates tested (Figure 3.1), showed no significant difference in cell growth characteristics amongst any of the surface sizes. Similar growth rates ranging from 0.17 to 0.19 $days^{-1}$ were observed for all conditions as indicated in the leyend in Figure 3.1. Growth rates were calculated as per equation 2.5 detailed in Section 2.6.4.1. These results prove that hMSC spread evenly over the surface of the well and grow at similar rates, regardless of the surface area of the culture vessel.

Consequently, any of these three well plates will be acceptable to use as culture vessels to perform characterisation studies for the engineering parameters influencing hMSC cell expansion during an automated cell expansion process.

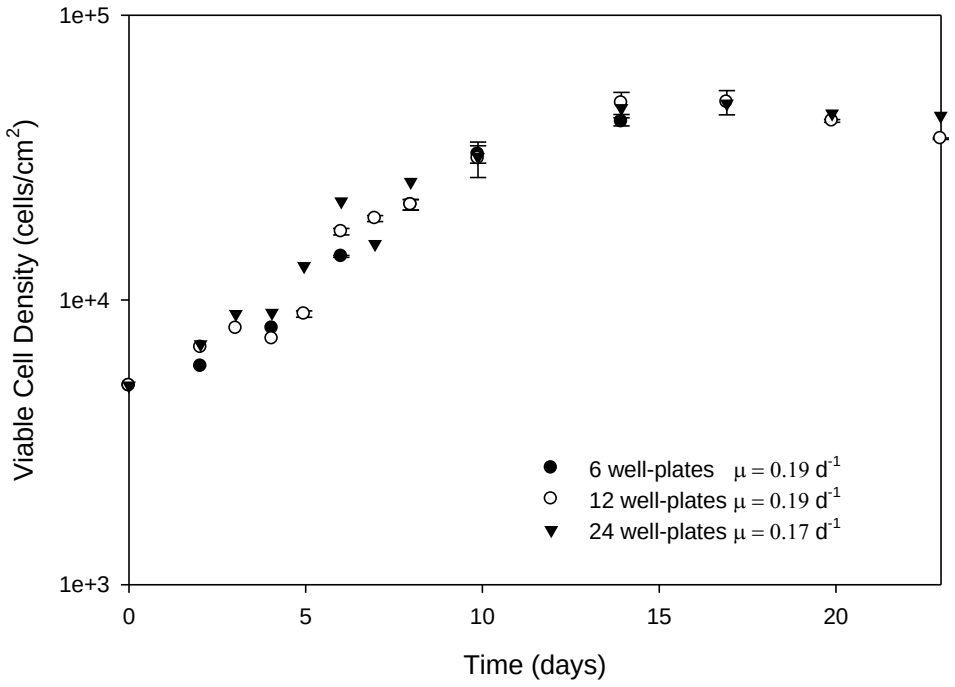

Figure 3.1 Comparison of hMSC growth kinetics in different well-plates over one passage. The effect of well size on hMSC cell growth kinetics in 6, 12, and 24 well Corning plates cultured for 22 days under identical set of conditions is shown. Error bars represent one standard deviation about the mean (n=3). hMSC isolated as described in Section 2.1.2 and then expanded as described in Section 2.4 from an initial cell density of $5x10^3$ cells/cm^2.

To study if there was any variation in cell growth characteristics when expanded in well-plates versus T-flasks, one pool of cells from the same donor immediately after isolation (P0) was seeded into T-flasks of different dimensions (T-25, T-75, and T-150) and 24 well plates all at an identical inoculation cell density of $5x10^3$ cell/cm^2. This cell train was expanded for five passages, during which cell growth curves were determined in either 24 well plates or T-flasks. Individual wells or T-flasks were sacrificed at different time points during each passage for surface marker analysis. Larger surface T-flasks of 150 cm^2 (T-150) were sacrificed during the first days of culture, smaller T-flasks of 75 cm^2 in surface (T-75) were used for time points during the mid-exponential phase of growth, and smaller T-flasks of 25 cm^2 in surface (T-25) were sacrificed for later time points within a

given passage. The medium was exchanged at the same time for all wells and T-flasks, and they were all cultured under the same conditions in a humidified incubator at 37^{o}C, with 5% v/v CO_2.

Comparison of hMSC growth in 24 well-plates and T-flasks of different dimensions is shown in Figure 3.2. Since two to four T-flasks were sacrificed during each passage of growth along with individual wells from 24 well-plates, a compilation of all the time points recorded along the five passages have been plotted against each other for those time points when a well and a T-flask were sacrificed at the same time. The data shows that cell densities are very similar in both wells and in T-flasks at any given time point. The linear fit of all the data shows a value for r^2 or 0.89 which is a reasonable fit considering the data is taken from over 5 cell passages. For some points, cell densities in T-flasks are slightly different than for well-plates, especially for those measuring higher cell densities or those at later stages of growth within a given passage. These discrepancies in cell densities, may be due to the different culture conditions that the cells have been exposed to during the passage. Although well-plates and T-flasks were kept in the same incubator at the same conditions, and medium exchanges were performed at the same time intervals, only the well-plates were exposed daily to environmental conditions for periods of 30 min approximately. This daily environmental exposure due to the harvest of individual wells from a plate, resulted in step changes in temperature from 37˚C to room temperature and gas compositions from 5% to 0.038% v/v CO_2 when the well plates were placed in the biosafety cabinet for manual operations. These changes can have an impact on cell growth, as shown later in Chapter 4. In contrast, T-flasks were only removed from the incubator only during medium exchanges every three to four days, up to the point of harvest providing them with more stable culture conditions over the period of incubation.

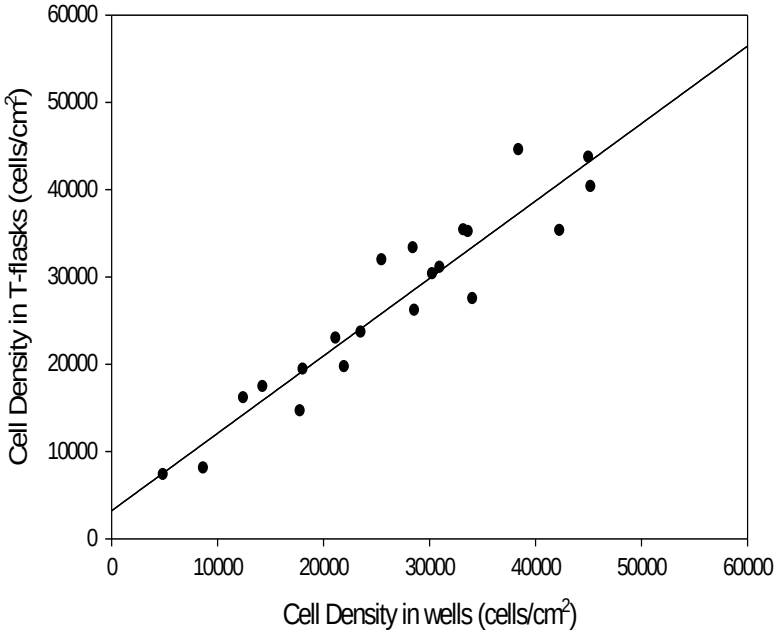

Figure 3.2 Comparison of hMSC growth in 24 well-plates and T-flasks. The effect of well size on hMSC cell growth on 24 Corning well plates and T-25, T-75, and T-150 Corning flasks at different time points over sequential cell expansion for five passages. hMSC isolated as described in Section 2.1.2 and then expanded as described in Section 2.4 from an initial cell density of $5x10^3$ cells/cm^2.

For all culture vessels tested, well-plates and T-flasks, hMSC essentially behaved in the same manner when exposed to the same environmental conditions during cell expansion. Consequently, all the results obtained for experiments performed on either T-flasks or well-plates can be interpreted without taking into consideration the culture vessel as a variable that could affect growth kinetics.

3.4 Effect of Well Location On hMSC Growth

Assuming the same working volume, medium formulation, feeding strategy, inoculation cell density and culture conditions, each well in a micro-well plate is considered to be an exact replicate of all the others. However, from an engineering perspective, there may be some significant and uncontrolled parameters that are intrinsically different from well to well according to the location of the well in the plate. Temperature gradients, and gas transfer is slightly different in the wells located at the edge and corners of the plate than the

ones at the centre due to the geometry of the plate (Burt et al.,1979; Oliver et al., 1981). It was also of interest to understand the well to well variability due to manual pipetting of the inoculum or any other operator routines in order to assess potential benefits of subsequent process automation.

It was therefore necessary to observe the differences if any, in growth kinetics of hMSC seeded in different well locations of the plate to understand if replicate wells used within one plate and would yield equivalent cell densities. Replicate wells seeded in different well-plates were also compared in order to evaluate possible operation errors due to sequential seeding from a common cell suspension.

To study the effect of well location and serial inoculation on replicate plates on hMSC growth, three 24 well-plates were seeded from a common pool of hMSC at P6. Eight wells were seeded on each plate with $5x10^3$ cell/cm^2 and two different wells from each plate were harvested per time point to evaluate cell densities on each well. During the time course of 23 days, a cell growth curve was generated from each of the three well-plates, and the individual data points were compared to understand if well location or seeding errors caused any discrepancy on the overall curve.

Figure 3.3 shows the growth curve generated from the three different well-plates. The individual data points originate from two wells at each time point. Wells harvested from each of the 24 well-plates are indicated in different colour and shape as indicated in the legend. For samples taken at a given time, two wells from the same plate were harvested, to compare the well to well variability. For each time point, one well was harvested from a corner or edge location and another one from a centre location from the same plate. A different plate was sampled every day to observe plate to plate variability, which could be accounted for by the lack of accuracy during serial inoculation. Even though the cell suspension was mixed and considered homogeneous, it was of interest to observe if serial pipetting during inoculation of several plates was a cause of variability between wells.

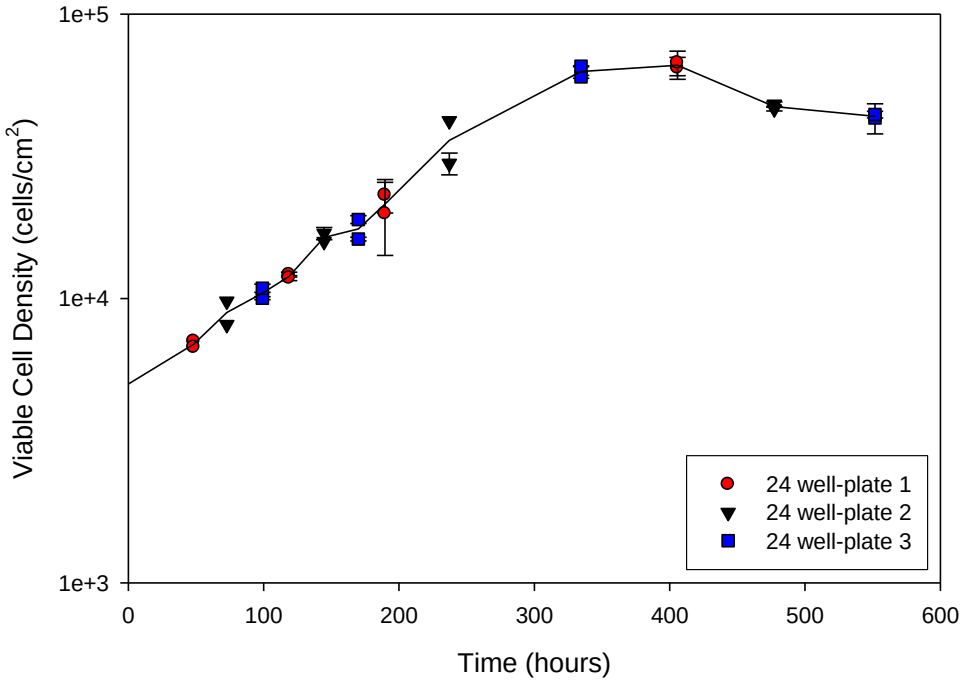

Figure 3.3 Well-to-well and plate-to-plate variability. Comparison of cell growth kinetics on different wells within plates and in different plates from identical geometries. Error bars represent one standard deviation about the mean (n=3). hMSC isolated as described in Section 2.1.2 and then expanded as described in Section 2.4 from an initial cell density $5x10^3$ cells/cm^2.

The results show that all time points collected fell within the cell growth curve generated for this particular cell population, regardless of the plate or the well from which a time point was generated. The difference in cell density observed in some points harvested from two wells in the same plate at the same time is no larger than the standard deviation due to the intrinsic error in haemocytometer counting technique (Section 2.6.1). The shape of the growth curve was not affected by well-plate variability either, and therefore no difference in cell behaviour was encountered between cells growing in replicate plates.

3.5 hMSC Growth Using Microcarriers

Microcarrier culture systems have been designed to increase the yield of anchorage-dependent cells, as they increase the culture surface available for growth while minimizing the volume of culture medium required per surface unit (Crespi et al., 1981; Pharmacia Fine Chemicals, 1979). The cells can then grow

attached to the surface of microcarries while these are placed in stirred-tank bioreactors under controlled environmental conditions. Control of culture parameters such as pH, temperature, and gas tension is much easier to achieve in microcarrier cultures expanded in bioreactors versus static cultures (van Hemert et al., 1969). Another advantage of stirred tank cultures is temperature and media homogeneity throughout the vessel, eliminating diffusion limitations of nutrients and gasses to the cell membrane. When it comes to process optimisation, different feeding strategies such as semi-batch or perfusion cultures, can be easily implemented in stirred tanks to improve growth kinetics. Such an approach would be very labour intensive and hard to execute in static cultures, unless aided with automated liquid handling systems. Bioreactor cultures are also attractive because of the reduction in the number of open manipulations which consequently lowers the risk of contaminations due to exposure to open systems during sequential passaging (Crespi et al., 1981). For all these reasons, hMSC ability to attach and grow in microcarriers was studied as a viable option for the cell expansion process. A wide range of commercially available microcarriers has already been used for the production of biological products using mammalian cells, but their use in tissue engineering has been explored to a limited extent. A small selection of commercially available microcarriers was chosen to explore their performance with hMSC cultures.

Three different types of microcarriers were used to expand hMSC: 2D Microhex, Cytodex 1 and Cytodex 3, whose characteristics are listed in Section 2.3.3. Cytodex microcarrier systems were selected for these studies for their reported ability to support growth in fibroblasts and/or mesenchymal stromal cells, and 2D Microhex for their surface material which is the same used to produce Nunc T-flasks. Different parameters were studied in order to aid cell attachment and expansion of hMSC on each type of microcarrier system, such as inoculation cell density, microcarrier density, working volume, stirring speed, and culture vessel geometry.

The ability of hMSC to attach and proliferate in 2D Microhex were studied in 125 ml shake flasks and 24 well ultra-low attachment plates. Microhex carriers are hexagonal polystyrene two-dimensional flakes of low density that can be kept in

suspension. They have been proven to support attachment and proliferation of CHO-K1 and VERO cells (Kenda-Ropson et al., 2002; Lenglois et al., 2004). Following the manufacturer's directions, the gamma-irradiated Microhex flakes were aseptically seeded into 24 well-plates and 125 ml shake flasks at cell densities of 5 and 10 cm^2/ml taking the surface density provided by the microcarriers as 760 cm^2/g. Cell densities of $1x10^2$ and $5x10^3$ cells/cm^2 were tested for cultures seeded in 24 well-plates, and $5x10^3$ cells/cm^2 for cultures seeded in shake flasks. The working volume for 125 shake flask was 20 ml/flask. For 24 well-plates initial working volumes of 1 ml and 0.5 ml per well were tested to aid initial attachment. The working volume was increased to 1.5 ml after microscopic observation confirmed cells were attached to the microcarrier surface within the first 8 hours. The cultures were placed in a shaker in a humidified incubator under static conditions for the first three hours, with periods of 5 min agitation every hour or two hours. After the first three to sixteen hours in culture the stirring speed was kept at 200 rpm for shake flasks and 240, 250, and 280 rpm for 24 well-plates.

Samples of 0.5 ml each were removed aseptically and placed on a slide for microscopic observation at different time points. This revealed that the lowest inoculation cell density of $1x10^2$ cell/cm^2 failed to encourage cell attachment onto the microcarriers, and so consequently no further analysis was conducted. Higher cell densities of $5x10^3$ cell/cm^2 did show some visible attachment to microcarriers. The optimum attachment judged by the highest number of carriers with cells attached to them per sample was observed in 24 well-plate cultures when the initial working volume was minimised to 0.5 ml, the cell density adjusted to $5x10^3$ cells/cm^2 with a surface to volume density of 5 cm^2/ml, and 2 hr intervals of static conditions during the first 8 hr before incubating the plates at 250 rpm for the remaining of the culture. Although a higher number of microcarriers showed hMSC attached to them for this condition, the attachment primarily occurred on the edges of the hexagonal flakes and no expansion towards the flat surface was observed. After the first four days in culture no cell proliferation was observed, and a half-volume medium exchange was performed to encourage cell growth. The cultures were terminated after five to ten days in culture, showing a reduction on the number of cells attached to microcarriers and

no proliferation. The supernatant was centrifuged and analysed for viable cell density but the number of cells was too low to consider statistically representative. Due to the low percentage of cells attached to microcarriers after cultivation, no further quantification analysis could be done to determine cell densities. Attachment and proliferation of cells can be further enhanced with coatings such as collagen or fibronectin, and such an alternative could be pursued in the future. Other materials such as poly (lactic-co-glycolic acid) (PLGA), poly-(L)-lactic acid (PLLA) and hydroxyapatite are also promising candidates for the production of microcarriers as reviewed by Malda et al., 2006 and could yield better results in the future. However, there are already commercially available microcarriers that have shown better results than 2D Microhex for cells of similar characteristics than hMSC such as porcine MSC or fibroblast. From these studies with 2D Microhex, no hMSC proliferation was observed under the set of conditions studied and consequently other microcarrier systems were tested.

Cytodex 1 and Cytodex 3 microcarriers are transparent spherical beads composed of a dextran matrix and developed for high yield culture of anchorage-dependent cells (Pharmacia, 1989). Cell attachment and proliferation of porcine MSC has recently proven successful on Cytodex 1 over the course of 28 days (Frauenschuh et al., 2007), and so they are a viable and attractive alternative to static monolayer surfaces.

Both Cytodex 1 and Cytodex 3 microcarriers were tested for the attachment and proliferation of hMSC. The physical and chemical characteristics of these microcarriers as well as preparation and manipulation techniques are detailed in Section 2.3.3.1 and Section 2.3.3.2 respectively. These microcarrier experiments were carried out in 24 well ultra-low attachment plates, seeded at $5x10^3$ and $1x10^4$ cells/cm^2 with microcarrier surface density of 10 cm^2/ml in working volumes ranging from 0.5 to 2 ml/well. The initial volume of media added per well was 0.5 ml with the purpose of increasing the probability of contact and attachment between cells and beads. The working volume was increased to 1 ml on day 1, 1.5 ml on day 2 and 2 ml on day 2. Plates were placed on a shaker in a humidified incubator at 37°C in static conditions and agitated at 250 rpm at inoculation, and every two hours post inoculation for a period of 5 minutes each

during the first 3 to 16 hours in culture. Continuous shaking was resumed at 250 rpm to avoid microcarrier aggregation due to cell attachment to more than one sphere. After 16 hours on an orbital shaker, static conditions were resummed, and intermittent 5 minute agitation of the cultures every two hours were carried out for a period of 8 hours afterwards to allow for further attachment of the cells. Daily microscopic observations monitored cell attachment and growth of hMSC on both types of microcarriers. On days 1, 6, 11, and 21, one well per condition was sacrificed and stained with neutral red and photographs with a 10X magnification were taken to monitor hMSC attachment onto the microcarriers.

As shown in Figure 3.4 hMSC could attach to both types of microcarriers within one day in culture. All pictures shown correspond to Cytodex 1 and Cytodex 3 seeded at $1x10^4$ cells/cm^2, showing the most optimum condition tested for both types of microcarriers. Results show that a higher percentage of microcarriers with hMSC attached to them was observed with Cytodex 3 than with Cytodex 1 on day 1. No further hMSC proliferation was observed after day 1 on Cytodex 1 microcarriers, with few cells left on some beads by day 21. The morphology of the cells still attached at that time had changed as well from flattened to round shape.

Cytodex 3 microcarries have thus been shown to encourage cell attachment of hMSC on day 1, and proliferation was observed during subsequent days in culture. Cell attachment was not uniformly distributed among carriers, exhibiting some beads with a high surface coverage and others with no cells attached to them. From those microcarriers with high hMSC coverage, most of them formed aggregates of three to seven beads interconnected by cells that add attached to two or more microcarriers. Still with a high availability of free culture surface provided by empty microcarriers, hMSC failed to attach and expand on those passed day 6. By day 21, hMSC had proliferated onto the culture surface of the ultra-low attachment well whilst empty microcarriers still remained in the culture medium.

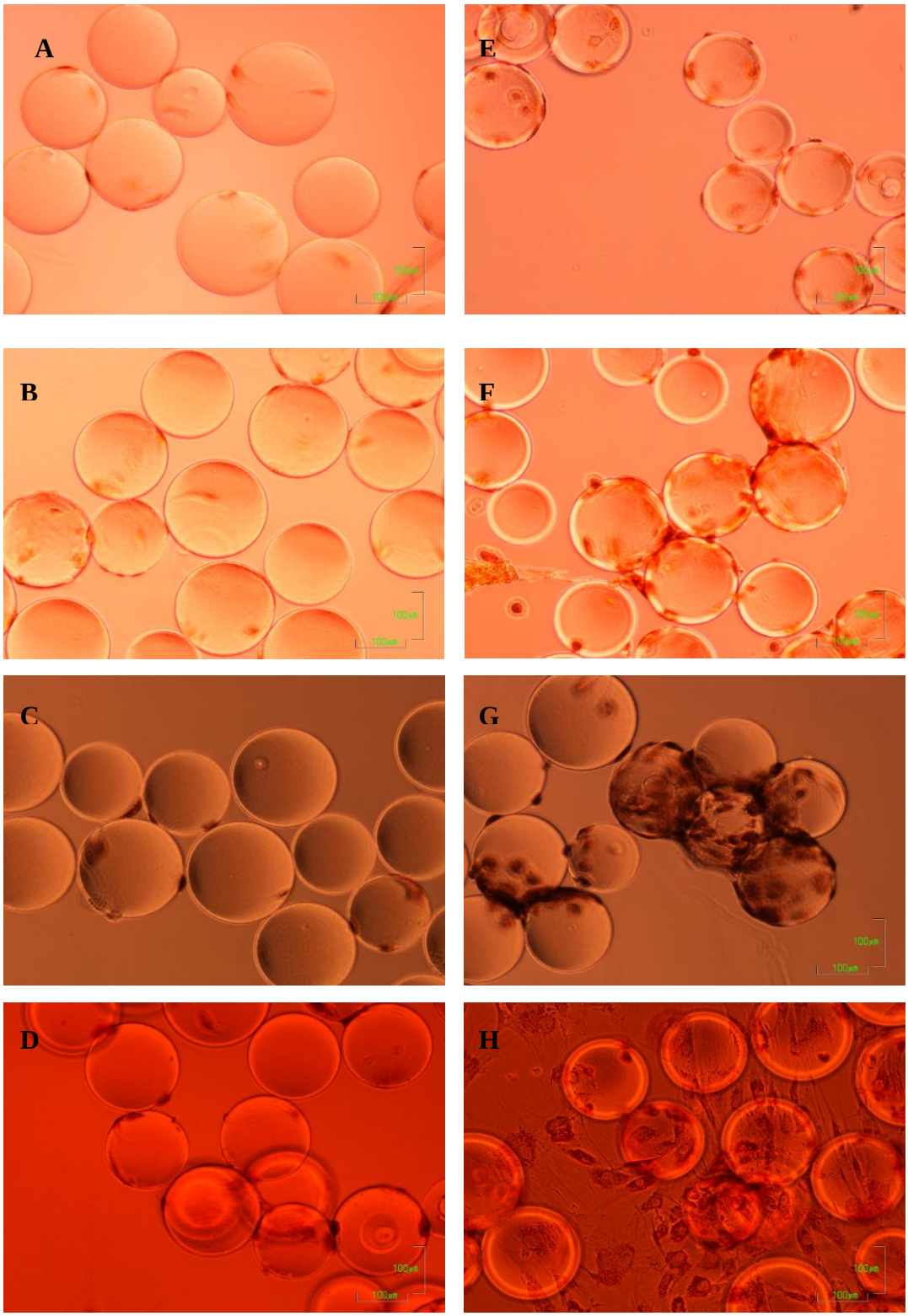

Figure 3.4. hMSC seeded onto Cytodex 1 (A, B, C, D) and Cytodex 3 (E, F, G, H) on days 1 (A, E), 6 (B, F), 11 (C, G), and 21 (D, H). hMSC isolated as described in Section 2.1.2 and then expanded on microcarriers as described in Section 2.4 from an initial cell density of $1x10^4$ cells/cm^2.

After a series of optimisation experiments in which inoculation cell density, microcarrier density, working volume, and agitation scheme were investigated (data not shown), the culture of hMSC on Cytodex 1 and Cytodex 3 did not show improved results over static monolayer cultures. Cytodex 3 microcarriers seeded with $1x10^4$ cells/cm^2 showed the best results in terms of initial cell attachment and proliferation, although they did not provide a uniform culture across all microcarriers. These findings are consistent with results obtained by Frauenschuh et al (2007) by which they achieved acceptable adherence of porcine MSC on Cytodex carriers when seeded at $1x10^4$ cells/cm^2 but low proliferation rates after 28 days in culture. So far, no many results on the expansion of hMSC on microcarriers have been published (Schop et al., 2008). The results presented in this chapter were satisfactory enough to believe that further optimisation experiments could result in a more uniform culture with faster proliferation rates but this was beyond the scope of this thesis.

3.6 Sequential Passaging of hMSC

The growth kinetics of hMSC are intrinsic to the source of the cells, and the overall growth rate depends on the donor from which the cells have been isolated (D'Ippolito et al., 1999; Phinney et al., 1999). Also, the doubling time or growth rate of hMSC is not constant over the cell expansion process (Kang et al, 2004). Several parameters can be optimised to speed up the rate of growth of hMSC, however it has been proven that under a constant set of conditions, the rate of growth decreases with increasing passage number, or with increasing population doubling level (Bruder et at., 1997). This effect has been attributed in part to the shortening of the telomeres and the lack of telomerase activity in hMSC (Banfi et al, 2002). For this reason, hMSC can only be expanded *in vitro* up to a limited number of passages, after which they senesce.

From a bioprocess standpoint, it is important to determine the proliferation potential of hMSC at every stage of the cell expansion process in order to schedule medium exchanges and harvest times, as well as to determine the quality of the cells harvested from every passage. To study the effect of sequential passages on cell growth and differentiation potential, two bags of bone

marrow from different donors were thawed, hMSC were isolated from each one of them through Direct isolation (Section 2.1.2) , and the isolated cells were expanded through five passages, P0 right after isolation to P4. For each passage two to three 24 well plates were seeded in conjunction with one T-150 flask. The well plates were used to generate cell growth curves by sacrificing one well per time point, and the T-150 flask was used to inoculate the next passage. All passages were inoculated with cells recovered from mid-exponential phase, since inoculation from cells recovered from stationary exhibit lower growth rates than those inoculated from cells collected during the mid-exponential phase. (Appendix III).

For each donor the data was plotted and fitted to a Gompertz four-parameter sigmoidal curve as shown in Equation 3.1 (Melero-Martin, 2004). From the parameters obtained by the modified Gompertz model derived as per Section 5.3, maximum cell densities and growth rates were calculated according to Equations 3.2 and 3.3. Growth rate calculations based only on empirical data require two time points to be chosen as initial and final cell densities that will coincide with the start and end of the exponential growth phase. The selection of these two points is difficult depending on the time intervals of the data recorded and on the shape of the curve, and it may result in less than accurate results as shown in Section 5.2. The mathematical method used, based on the accurate representation of the growth curve by a sigmoidal equation, was chosen to calculate growth rates in a more objective manner. As explained in detail in Section 5.3 this modified Gompertz model closely represent growth kinetics for sequential passages when enough data from an initial passage is collected, and it is useful to describe growth kinetics for later passages specially in cases when not many data points are available to fully characterise growth. Details about each parameter in the model are discussed further in Chapter 5.

$$X = X_0 + a \cdot \exp\left(-\exp\left(\frac{t_0 - t}{b}\right)\right) \tag{3.1}$$

$$X_{\max} = a + X_0 \tag{3.2}$$

$$\mu = \frac{\ln\left(X_{max} / X_0\right)}{e \cdot b} \tag{3.3}$$

Where X is cell density, X_0 is inoculation cell density, a is the increase in cell density all in cells/cm^2, t is time, t_0 is related to the duration of the lag phase, b is related to duration of the exponential phase (as indicated in Section 5.2), X_{max} is maximum cell density at stationary phase, μ is the growth rate and e is constant 2.71828.

Growth curves obtained for the hMSC from donor A are shown in Figures 3.5 to 3.10 (and also shown in Figure 5.15 and 5.16) and the ones obtained from donor B are shown in Figures 3.11 to 3.16. Figures 3.5 and 3.11 compare the raw growth kinetic data from passages P0 to P4 for donor A and donor B respectively. From these two graphs the decrease in growth rates and maximum cell density achieved with increasing passage number is clear.

Quantitative values of the kinetic parameters obtained from the modified Gompertz model developed in Section 5.3 for each donor and each passage are shown in Table 3.2. Figures 3.6 to 3.10 (donor A) and 3.12 to 3.16 (Donor B) show there is a good fit of the model with the raw cell viability data for each passage with r^2 values ranging from 0.92 to 0.99.

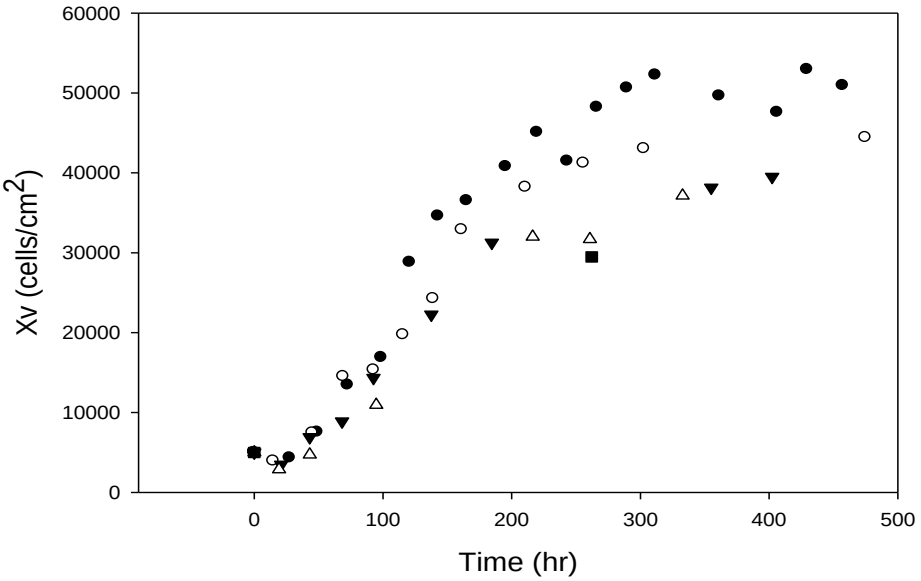

Figure 3.5 hMSC growth curves from donor A for passages P0 (solid circles), P1 (open circles), P2 (inverted solid triangles), P3 (empty triangles), and P4 (solid square). hMSC isolated as described in Section 2.1.2 and then expanded as described in Section 2.4 from an initial cell density of $5x10^3$ cells/cm^2.

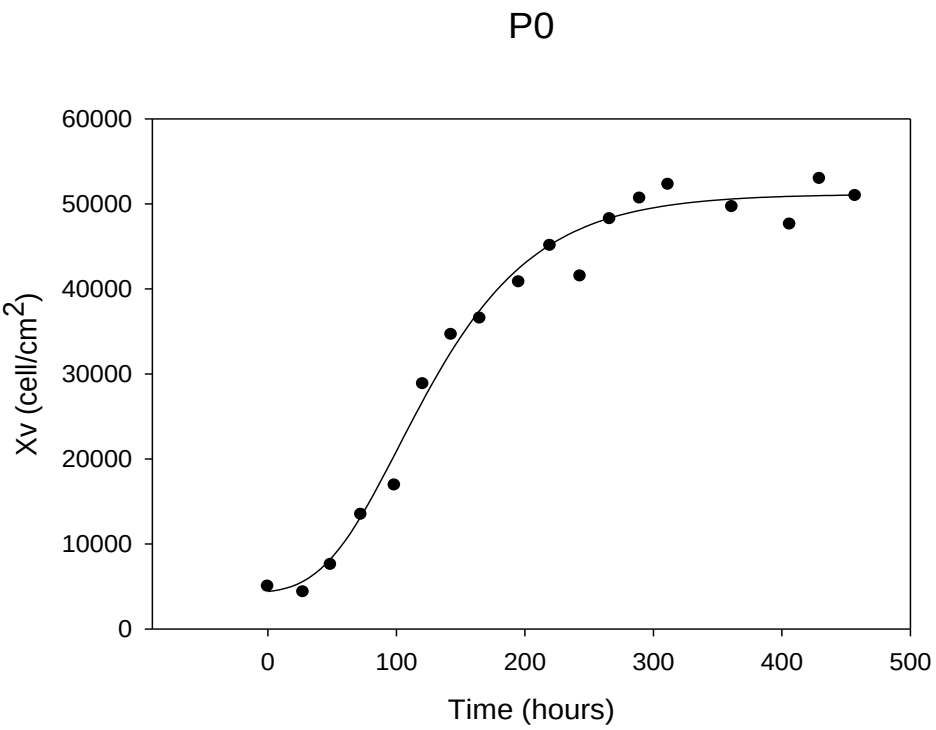

Figure 3.6 hMSC growth curve from donor A for passage P0. Experimental conditions as described in Figure 3.5. Solid line fitted according to Equation 3.1. ($R^2 = 0.99$).

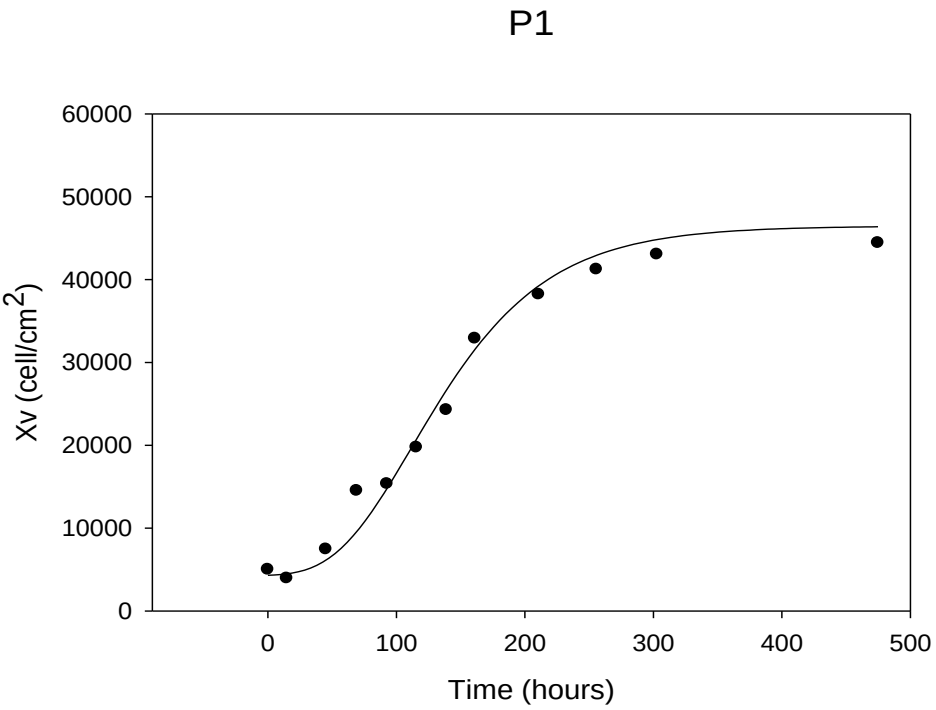

Figure 3.7 hMSC growth curve from donor A for passage P1. Experimental conditions as described in Figure 3.5. Solid line fitted according to Equation 3.1. ($R^2 = 0.99$).

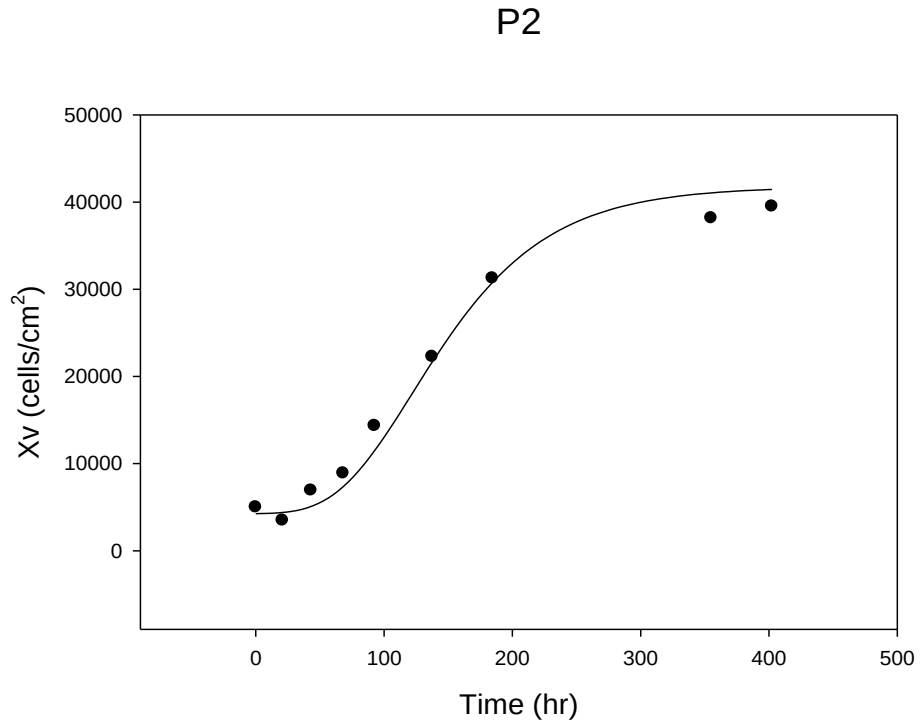

Figure 3.8 hMSC growth curve from donor A for passage P2. Experimental conditions as described in Figure 3.5. Solid line fitted according to Equation 3.1. ($R^2 = 0.99$).

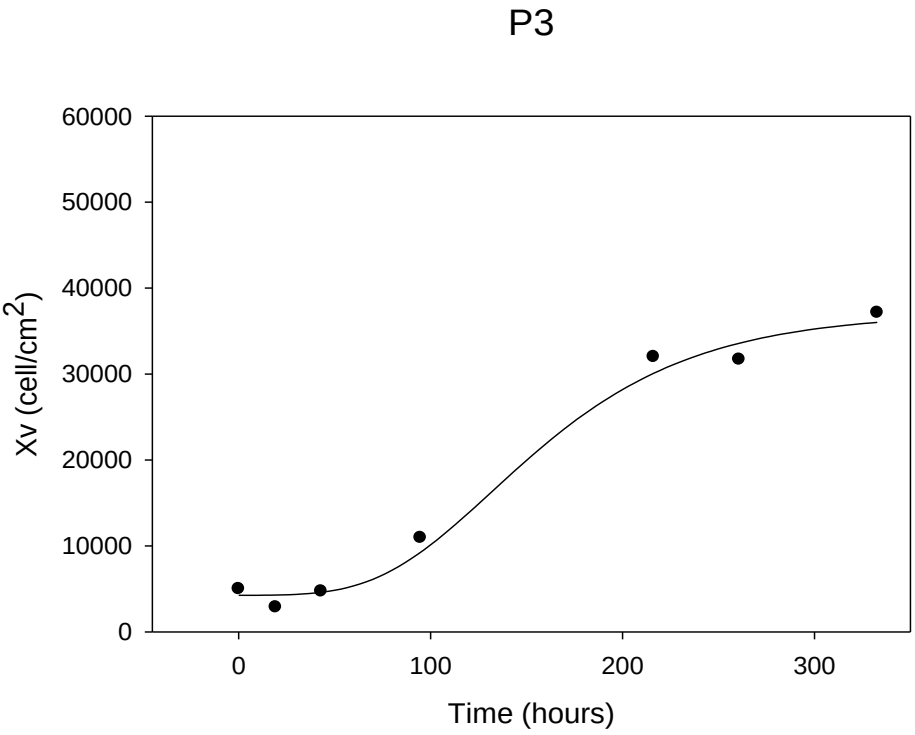

Figure 3.9 hMSC growth curve from donor A for passage P3. Experimental conditions as described in Figure 3.5. Solid line fitted according to Equation 3.1. ($R^2 = 0.99$).

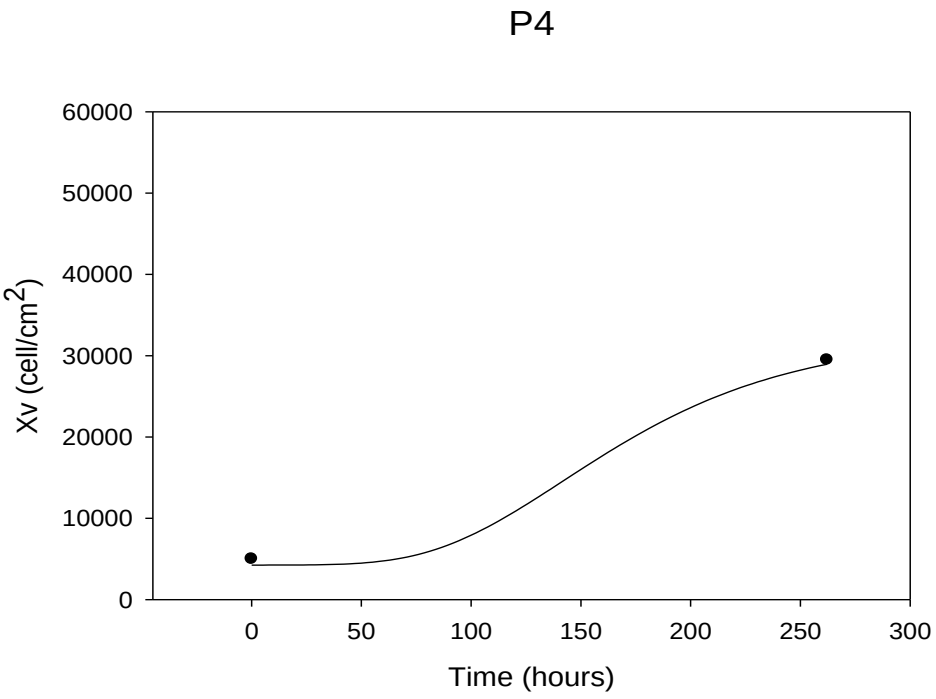

Figure 3.10 hMSC growth curve from donor A for passage P4. Experimental conditions as described in Figure 3.5. Solid line fitted according to Equation 3.1.

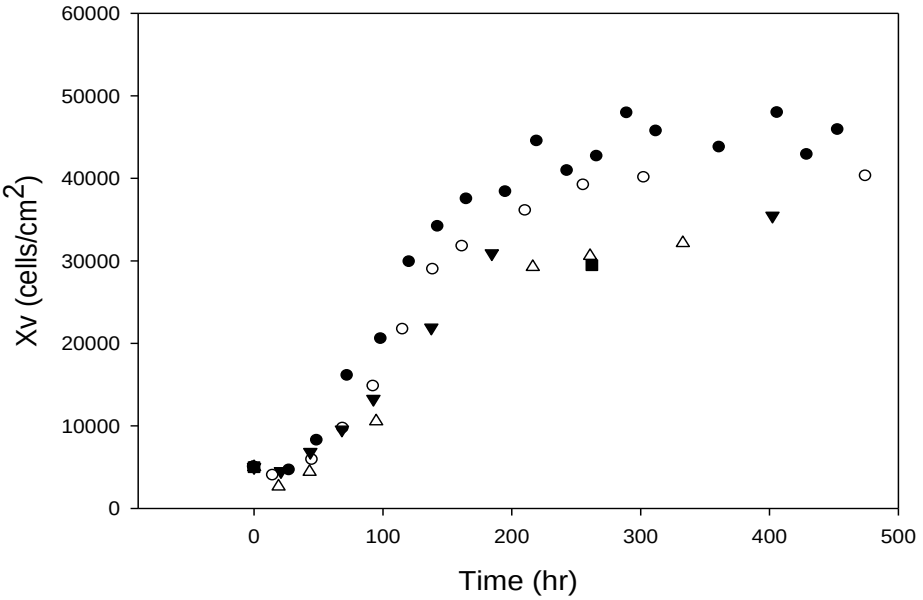

Figure 3.11 hMSC growth curves from donor B for passages P0 (solid circles), P1 (open circles), P2 (inverted solid triangles), P3 (open triangles), and P4 (filled square). hMSC isolated as described in Section 2.1.2 and then expanded as described in Section 2.4 from an initial cell density of $5x10^3$ cells/cm^2.

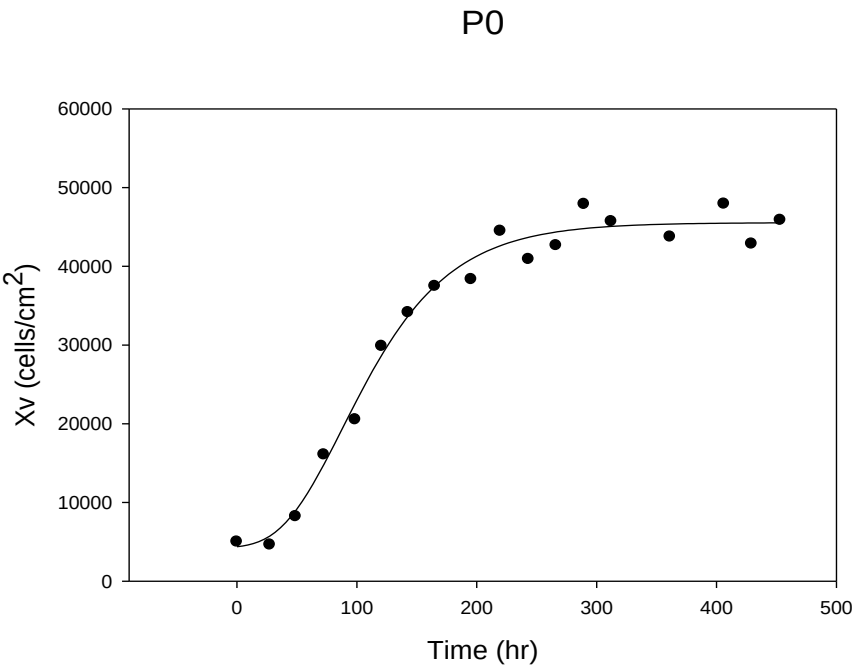

Figure 3.12. hMSC growth curve from donor B for passage P0. Experimental conditions as described in Figure 3.11. Solid line fitted according to Equation 3.1. ($R^2 = 0.98$).

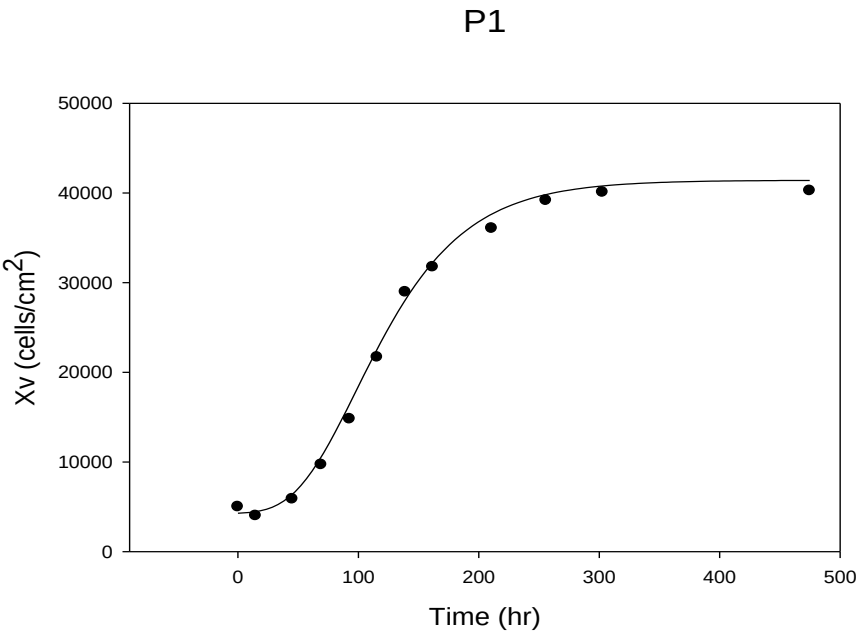

Figure 3.13. hMSC growth curve from donor B for passage P1. Experimental conditions as described in Figure 3.5. Solid line fitted according to Equation 3.1. ($R^2 = 0.92$).

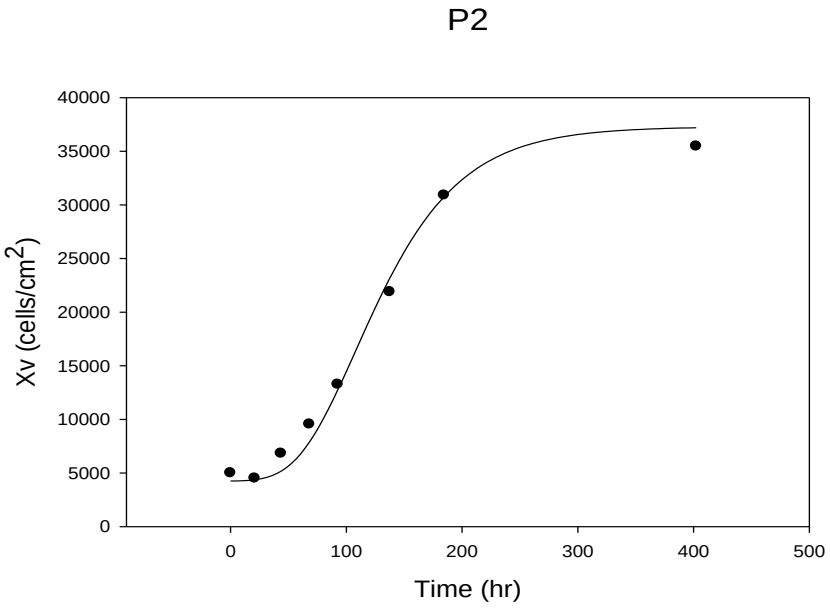

Figure 3.14. hMSC growth curve from donor B for passage P2. Experimental conditions as described in Figure 3.5. Solid line fitted according to Equation 3.1. ($R^2 = 0.99$).

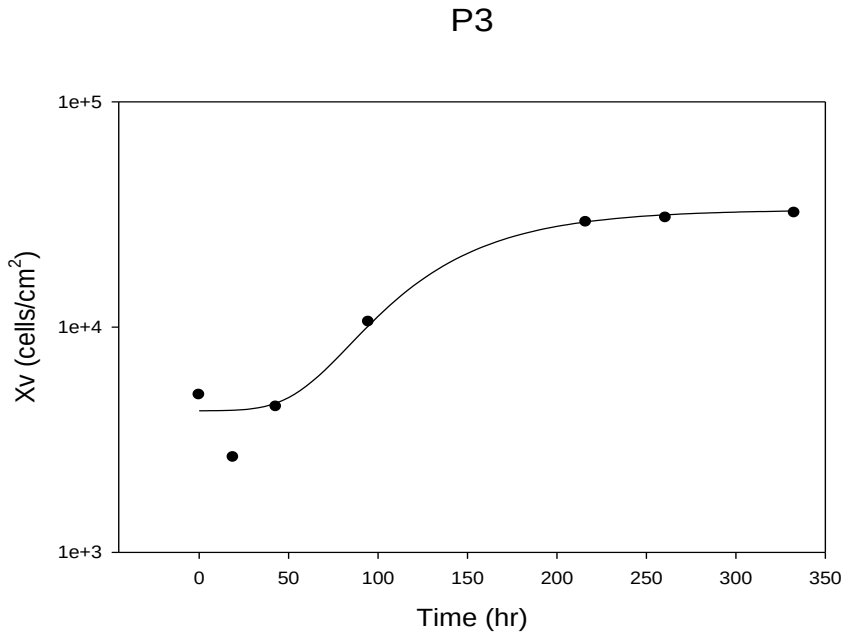

Figure 3.15. hMSC growth curve from donor B for passage P3. Experimental conditions as described in Figure 3.5. Solid line fitted according to Equation 3.1. ($R^2 = 0.99$).

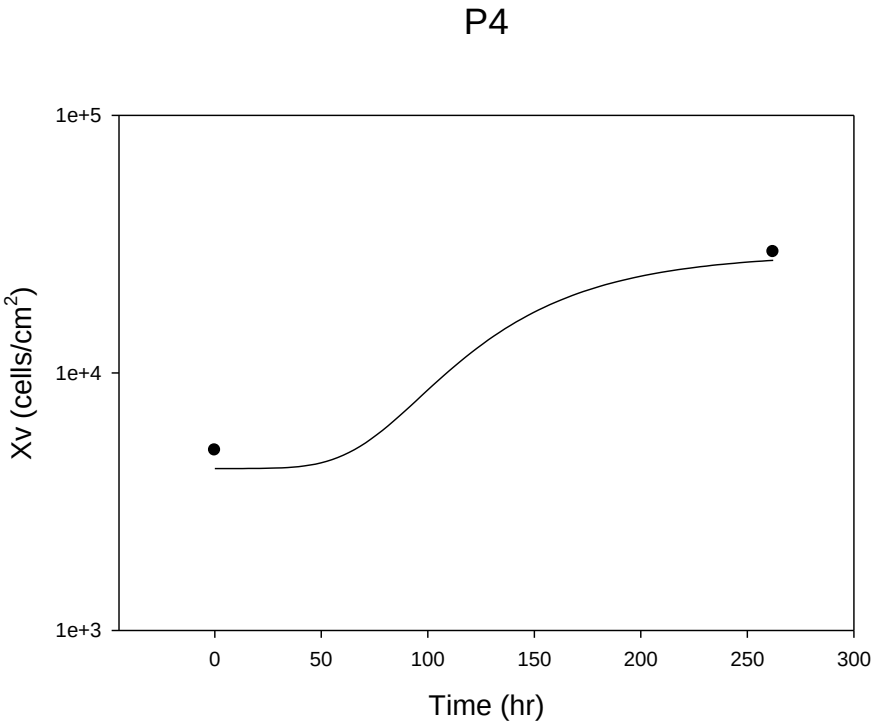

Figure 3.16. hMSC growth curve from donor B for passage P4. Experimental conditions as described in Figure 3.5. Solid line fitted according to Equation 3.1.

Table 3.2 Growth parameters and maximum cell densities for consecutive passages from P0 to P4 for hMSC isolated from two different donors, labelled as donor A and donor B. Kinetic parameter values obtained from fitting the modified four-parameter Gompertz model (Equations 3.1, and 5.5 to 5.8) to each set of data as illustrated in Figures 3.6 to 3.10 and 3.11 to 3.16. Growth rates (μ) calculated from Gompertz parameters and apparent growth rates (μa_{pp}) were calculated from empirical data for comparison purposes.

Donor A	X_0	*Xmax*	a	t_0	b	μ (hr^{-1})	μ_{app} (hr^{-1})
P0	$4.25x10^3$	$4.69x10^4$	$4.27\ x10^4$	102	59	$1.50x10^{-2}$	$1.29\ x10^{-2}$
P1	$4.25x10^3$	$4.22\ x10^4$	$3.80\ x10^4$	112	59	$1.43\ x10^{-2}$	$1.23\ x10^{-2}$
P2	$4.25x10^3$	$3.75\ x10^4$	$3.33\ x10^4$	122	59	$1.36\ x10^{-2}$	$1.04\ x10^{-2}$
P3	$4.25x10^3$	$3.28\ x10^4$	$2.86\ x10^4$	132	59	$1.27\ x10^{-2}$	$1.05\ x10^{-2}$
P4	$4.25x10^3$	$2.81\ x10^4$	$2.39\ x10^4$	142	59	$1.18\ x10^{-2}$	$0.66x10^{-2}$
Donor B	X_0	*Xmax*	a	t_0	b	μ (hr^{-1})	μ_{app} (hr^{-1})
P0	$4.25x10^3$	$4.13\ x10^4$	$3.71\ x10^4$	88	50	$1.66\ x10^{-2}$	$1.34\ x10^{-2}$
P1	$4.25x10^3$	$3.72\ x10^4$	$3.29\ x10^4$	98	50	$1.58\ x10^{-2}$	$1.28\ x10^{-2}$
P2	$4.25x10^3$	$3.30\ x10^4$	$2.88\ x10^4$	108	50	$1.49\ x10^{-2}$	$9.00x10^{-3}$
P3	$4.25x10^3$	$2.89\ x10^4$	$2.47\ x10^4$	118	50	$1.40\ x10^{-2}$	$1.15\ x10^{-2}$
P4	$4.25x10^3$	$2.48\ x10^4$	$2.05\ x10^4$	128	50	$1.28\ x10^{-2}$	$0.67x10^{-2}$

For both donors two major trends were observed over sequential passages of hMSC after isolation. The growth rate and the number of cells obtained at the end of each passage decrease with increasing passage number. Growth rates and maximum cell densities were also different from each donor studied. These differences are likely to be very important when determining the overall time required for a complete cell expansion process from isolation to delivery of cells to the clinic for patient therapy. The same trend was observed by Bruder et al. 1997, for twice weekly fed hMSC yielding a viable cell density of $3.12x10^4$ cells/cm^2 at P1 and only $1.35x10^4$ cells/cm^2 at P4. Both quantities compared closely to the values obtained and shown in Table 3.2. for hMSC. Apparent growth rates (μ_{app}) correlate closely with the values for growth rates (μ) calculated from the coefficients obtained from the modified Gompertz model developed in Chapter 5, section 5.3. The model uses the parameters obtained from the initial passage (P0) for which numerous data points are collected, to generate the parameters to be used for subsequent passages.

The data and results obtained show that such modifications to the model result in comparable results to the empirical data collected for all four passages. Also, some indication of the duration of the lag phase and the maximum cell density obtained at the stationary phase can be assessed with this model when not many time points are available for analysis. From the two donors studied, both the empirical data as well as the mathematical model agree with the trend indicating a decrease in maximum cell density with increasing passage number. Also, a trend indicating a decrease in growth rates as the passage number increases is confirmed. The degree up to which an increase in lag phase is contributing to this decrease in growth rates cannot be fully assessed for each passage, especially for later passages where not many points are present in the growth curves. Given the selection of parameters for the model, for which the parameter b and X_0 are fixed throughout the course of the cell expansion process for a given patient (Equations 5.7 and 5.8), the calculation of the duration of the lag phase could not be as accurate as the one calculated from empirical data if such data was available for all consecutive passages. For the later passages from donors A and B not enough data was available as to determine the duration of the lag phase. Future studies characterising this possible trend should be addressed. Shortening the sampling time intervals during sequential passages, as well as performing cell cycle analysis to determine the percentage of the population at different stages of division (G0, G1, S, or G2) will further enhance the understanding of hMSC expansion process as well as the possible extended capabilities of the modified Gompertz model developed in this thesis.

Other contributing factors to the difference in growth kinetics over time could be attributed to the possibility of a heterogeneous population isolated from bone marrow as discussed in Section 1.1.5. In the case of the existence of other population of cells other than hMSC with lower survival ability in culture, the decrease in growth rates and in maximum cell densities could be due to the disappearance of other populations from the culture over the cell expansion process. However, given the high viability of all samples tested, this explanation would not be able to account for the large decrease in cell recovery for later passages.

The implications of these growth rate variations over sequential passages, as well as the variability of growth characteristics from different donors are reflected in Table 3.3. The total cells recovered from each passage as well as the time that it takes for the cells to reach stationary phase was calculated assuming: (i) an initial number of cells of $7.5x10^5$ cells was available to inoculate one T-150 flask at P0 (ii) subsequent passages were performed with a split ratio of 1:2. Because cells are harvested and passaged during the mid-exponential phase of growth, the lower split ratio accounts for the lower cell density obtained when passaging the cultures before they reach stationary phase. The time employed by each passage was calculated from Equation 3.4, using the growth rates shown on Table 3.2.

Table 3.3 Total number of cells recovered from hMSC cell expansion process from two different donors between passage P0 to P4, and the time taken for each passage to reach stationary phase. Cumulative numbers in bold, indicate the final overall process time and the total amount of cells recovered from the process.

	Donor A		**Donor B**	
	Time (hr)	**X_{tot} (cells)**	**Time (hr)**	**X_{tot} (cells)**
P0	150	$7.04x10^6$	127	$6.20\ x10^6$
P1	149	$1.27x10^7$	127	$1.12\ x10^7$
P2	148	$2.25\ x10^7$	126	$1.98\ x10^7$
P3	148	$3.94\ x10^7$	126	$3.47\ x10^7$
P4	147	$6.75\ x10^7$	125	$5.95\ x10^7$
Total	**31 days**	**$6.75\ x10^7$**	**26 days**	**$5.95\ x10^7$**

The time required for the cells to reach final viable cell density for each passage was calculated by:

$$\Delta t = \frac{\ln\left(X_{\max} - X_0\right)}{\mu} \tag{3.4}$$

Where, $X_{\max}$ is the number of viable cells reaching stationary phase, X_0 is the number of viable cells inoculated in the flask and μ is the growth rate (h^{-1}).

For patient specific regenerative medicine applications where the timing and number of cells are critical for the success of the therapy, differences in processing time must be taken into consideration. The cell expansion process

would take 31 days for donor A and 26 days for donor B, which involves five more days of scheduled operations and a higher cost for the process.

3.7 Summary

Characterisation of the growth kinetics for hMSC has been performed for the standard culture conditions in T-flasks and also for well-plates and on microcarriers. Under constant operating parameters of temperature, aeration, humidity, culture medium, and incubation time, growth characteristics were shown to be similar for static cultures regardless of the geometry of the culture vessel (Figures 3.1 and 3.2). Microcarrier cultures were also tested as an attractive alternative to increase the yield of growth with reduced medium requirements and aseptic manipulations. From the three types of microcarriers tested, MicroHex, Cytodex 1, and Cytodex 3, only one of them, Cytodex 3 supported cell attachment and proliferation (Section 3.5). However, results for the conditions tested did not show any improvement of hMSC growth over static cultures and so microcarrier cultures were not investigated further.

Two different isolation techniques, density gradient centrifugation and Direct isolation, were implemented and compared (Section 3.2.1). Both techniques were successful for hMSC recovery, and cell banks were created from the cells obtained from each one of these isolation techniques. A comparison of the performance of the cells recovered from each different method concluded that Direct isolation exhibited higher recovery yields than density gradient centrifugations, with a 34% increase in cell recovery. Direct isolation is also a faster method with less centrifugation steps involved, which present itself as an advantage from an operations and automation point of view.

The effect of freeze/thaw was studied on cells that had undergone preparation steps to create a cell bank versus cells that were sequentially passaged without a freezing step. Cell banking is an important process that allows storage of a cell source for subsequent experimentation or future usage such as transport of cells to cGMP manufacturing facility, or to retain the cells during a halt in the cell expansion process. The effect of such procedure on cell growth were demonstrated to exhibit some detrimental effect on cell growth rate and

maximum cell density reached at the end of the first passage (Section 3.2.2). This effect may not be cumulative, however it has a negative impact on cells seeded right after thaw.

Finally, a study on the characterisation of hMSC over sequential passages confirmed a decrease in growth rates and maximum viable cell densities obtained as the passage number increases (Table 3.2). Quantitative analysis of the cell expansion process was aided by using a mathematical Gompertz model (Section 3.6) that accurately represents the growth kinetics of hMSC as further examined in Chapter 5. Results were confirmed by experimenting with two different sources of cells from two donors. The implications of the decrease in growth rate and cell recovery as the cell expansion progresses were assessed for the overall completion of the process (Table 3.3).

Having established hMSC culture conditions and a method to quantify cell growth kinetics, optimal culture conditions for the effective clinical scale production in an automated platform of vast numbers of hMSC will be evaluated in Chapter 4.

CHAPTER FOUR

Optimisation of Controlled Parameters for an Automated hMSC Expansion Process

4 OPTIMISATION OF CONTROLLED PARAMETERS FOR AN AUTOMATED HMSC EXPANSION PROCESS

4.1 Introduction and Aims

Previous research in the field of adult stem cells has tended to concentrate on understanding and controlling the differentiation potential of hMSC aided by chemical additives in the culture media. The main focus of recent studies have been that of finding therapeutic applications for these cells and their potential in tissue engineering applications. Much of this work was described in Section 1.1. To date, however, comparably little effort has been directed toward controlling physical parameters during the cell expansion process for hMSC and understanding the effect of these environmental factors on cell growth in an undifferentiated state. Recently, a number of groups have discovered the sensitivity of hMSC to some of the engineering parameters to which they are exposed in culture, such as oxygen (Moussavi-Harami, 2004), medium composition (Sotiropoulou, 2005), and inoculation cell density (Sekiya, 2002). This has directed attention to the importance of controlled environmental conditions during proliferation and differentiation of hMSC.

To ensure production of sufficient cells to satisfy market needs, bioprocess conditions and equipment for the expansion of hMSC need to be investigated and adopted, ensuring optimum growth in an undifferentiated state. The use of an automated platform will potentially facilitate higher output capabilities, whilst reducing variability due to operator manipulations (Terstegge et al., 2005, Joannides et al., 2006, Bernard et al., 2004). In addition, rigid control of determining parameters for growth will result in a robust cell expansion process for industrial applications in the emerging regenerative medicine sector. Study of the effect of physical conditions experienced by the cultures during automated manipulations will generate a set of Standard Operating Procedures for an appropriate range of conditions, aimed at ensuring cells are maintained in an undifferentiated and still multipotent state.

Despite recent efforts devoted to better understanding of the effect of different parameters on cell growth and differentiation of hMSC, there are some

differences amongst laboratories concerning process steps during the cell expansion process which may have an added effect on the results reported in literature in relation to cell growth kinetics and yields. Friendesntein et al., (1976) initially isolated and propagated hMSC, and essentially the same laboratory scale protocol has been used by all subsequent investigators (Colter et al., 2000; Pittenger *et al*, 1999). However, some parameters controlled during the cell expansion process vary from laboratory to laboratory and from operator to operator. These include inoculation cell density, when passages are executed as a split ratio of the harvested cultures (1:3 or 1:4), the frequency of medium exchanges (3 to 4 days), time of exposure to environmental conditions of the cultures while microscopic observations are taking place, etc. All these parameters are expected to have an impact on cell growth kinetics and therefore they must be controlled and understood in order to obtain reproducible results and to decouple the effect of process variations from any other parameter under study.

It is therefore the aim of this Chapter to define the optimal culture conditions for the effective clinical scale production in an automated platform of large numbers of hMSC, to serve for cellular therapy in transplantation, immunotherapy and regenerative medicine. The specific objectives of the work are:

- To assess the impact of inoculation seeding densities on doubling time for hMSC over sequential passages.
- To examine the effect of different media addition rates on hMSC growth kinetics, and to determine optimum values for such rates.
- To evaluate the effect of environmental excursions that the cells are exposed to during the expansion process on growth kinetics.

4.2 The effect of Inoculation Cell Density and Population Doubling on hMSC growth rates and yields

The most common protocol for expansion of hMSC states the use of inoculation cell densities of $5x10^3$ cells/cm^2 in T-flasks with medium exchanges every three to four days (Friendstein et al., 1976). This practice has been shown to result in variable doubling times depending on the cell source and the laboratory in which the work was performed (Castro-Malaspina et al., 1980; Phinney et al., 1999;

Lazarus et al., 1995). The wide variation between measured doubling times thought to be due to the donor age and health at the time of bone marrow extraction, culture media, and the number of doublings that the cells have undergone at the time of the study. These doubling times can be slower than most of the doubling times characteristic of immortalised mammalian cell lines for which the doubling times remain constant over passages (Westermark, 1974). As a result, the culture of hMSC requires longer times to complete a cell expansion process and an increase in the amount of resources needed such as culture media and plastic ware. A reduction in the doubling time for hMSC while maintaining them in an undifferentiated state could therefore have a significant process benefit. The number of cells per unit surface area at inoculation has also been proven to have an impact on the growth rates of hMSC. It has been reported that ICDs lower than $5x10^3$ cells/cm^2 result in an increase in doubling times (Sekiya, 2002).

To further investigate these phenomena, doubling times were determined for hMSC cultured in T-25 flasks as per the protocol indicated in Section 2.4. Calculations based on initial and final cell densities are indicated in Section 2.6.4.1. hMSC isolated from two different donors (labelled donor X and donor Y to protect the identity of each patient) and expanded up to different passage numbers were inoculated at cell densities ranging from $5x10^1$ to $1x10^4$ cells/cm^2. In addition, growth curves were obtained from a common pool of hMSC when seeded in 12 well plates at cell densities of $5x10^1$, $1x10^2$, $1x10^3$, $5x10^3$, and $1x10^4$ cells/cm^2 as per the protocol indicated in Section 2.4.

The results obtained indicate that not only do hMSC doubling times increase with increasing cell density, but that this behaviour is characterised by a linear relationship between inoculation cell density and doubling time as shown in Figure 4.1 (Data provided in Appendix I). The coefficients of the linear equation that characterises this trend are dependent on the source (Donor) of the cells and on the passage number for the same cell source. There is a considerable variation in the slope of the linear correlation from different donors for cells at the same passage with values of $0.81x10^{-2}$ and $2.69x10^{-2}$ for Donor X and Y respectively at Passage 2. There is, however, a larger difference in the slope between cells from

the same donor when seeded at different passage numbers, with a value of $7.61x10^{-2}$ at passage 9 versus $0.81x10^{-2}$ at passage 2 for donor X. Clearly the results show that hMSC growth rates are slower when seeded at a later passage for all inoculation cell densities, and that the linear correlation between inoculation cell density and doubling time still applies regardless of the age of the culture. Still remains to be determined if the decrease in proliferative potential of these cells over time is a result of the adaptation to environmental conditions in culture by which the cells remain at a G0 or quiescent stage for a longer period of time just as they would do *in vivo*, or if the duration of the cell division cycle becomes slower over passages. Self-selection of a population over time would be less likely to occur, since the result of such phenomenon would be an increase in growth rate by the faster growing cell population. All cultures retained hMSC morphology at the time of harvest, and results for the surface marker expression over the different passages to characterise identity of the cultures, will be described later in Chapter 5.

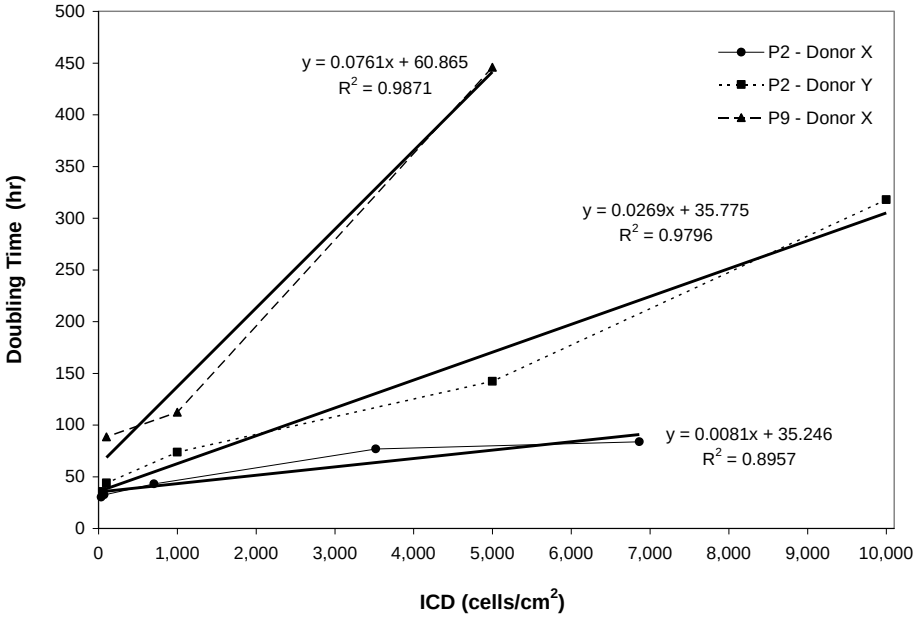

Figure 4.1 Effect of inoculation cell density (ICD), passage number, and donor on doubling time for the cell expansion process of hMSC seeded on T-25 flasks. Cells obtained from Donor X and Donor Y were expanded up to passage 9 following the protocol indicated in Section 2.4. At passage 2 for donor X, and 2 and 9 for donor Y, T-25 were seeded at ICD $5x10^1$, $1x10^2$, $1x10^3$, $5x10^3$, and $1x10^4$ cell/cm^2 and doubling times were calculated for each culture as described in Section 2.6.4.1. Solid lines fitted by linear regression.

The implications of this finding are that faster doubling times achieved at lower inoculation cell densities and lower passage numbers could reduce the total cell expansion process time considerably. This process optimisation would bring autologous stem cell therapy closer to the clinic as a cost effective treatment, whilst reducing the waiting time for patients that are in need of autologous regenerative medicine treatment. Calculations based on the time required to reach a final cell number of $1x10^8$ depending on the doubling time of the culture and assuming constant growth rates for the overall cell expansion process are shown on Table 4.1. The final cell number is based on a previously published case study for the number of cells required in an undifferentiated state to seed a tubular reactor for the construction of an artificial artery (Mason et al., 2006).

For the slowest growing culture observed for Donor Y when cells were seeded at $5x10^3$ cell/cm^2 at Passage 9, it would take 29 weeks to collect the required number of hMSC for therapy. As the doubling time decreases for cultures seeded at lower ICD and lower passage number, the overall cell expansion time shortens. The fastest doubling time obtained from Donor X when Passage 2 cells were seeded at low ICD of $5x10^1$ cell/cm^2, resulted in a decrease of the overall cell expansion time to just 4 weeks. These results show a reduction of 5 months in the overall delivery time of stem cell therapy to the clinic due to process optimisation as a result of a reduction in inoculation cell density and age of the cell source.

Table 4.1 Overall hMSC expansion process time required to achieve $1x10^8$ cells from a starting sample containing $1x10^5$ cells. Process times calculated based on the results obtained from two donors at different passages with and without optimised operating conditions based on modifications of inoculation cell density as shown in Figure 4.1.

hMSC Doubling Time (hr)	Cell Expansion Process Time (hr)	Cell Expansion Process Time (weeks)
445	202	29
100	59	8
75	48	7
50	38	5
30	29	4

The increase in doubling time as the age of the culture or passage time increases had been demonstrated in Section 3.6 and it has also been reported in the literature (Kang et al., 2004; Bruder et al, 1997). A decrease in doubling time with decreasing inoculation cell density had also been observed in hMSC by Melero-Martin et al. (2005) with chondroprogenitor cells, and Sekiya et al. with hMSC (2002). However, the linear relationship between these two parameters has not been previously demonstrated. Understanding that such a relationship exists, enables process modifications that can be made forward predicting the decrease in doubling times when inoculation cell densities are varied for a given culture of known characteristics.

This correlation suggests that hMSC growth rates at a specific passage may be sensitive to the physical distance between cells when all other cell culture parameters remain constant, such as frequency of medium exchange and incubation time and temperature. The study that corroborated this hypothesis was conducted in T-25 flasks with cell density measurements taken at inoculation and at harvest once the cells had reached 90% coverage of the culture surface. Cell growth characteristic such as lag phase or time period of the exponential growth phase could not be studied in T-25 flasks, and these parameters will aid the understanding on how inoculation cell density impacts cell behaviour in hMSC cultures *in vitro*. To further investigate this phenomenon, follow up experiments were conducted to understand cell growth behaviour on a daily basis in relation to the surface coverage at a given time in culture.

The growth curves from a common pool of hMSC, seeded at inoculation cell densities of $5x10^1$, $1x10^3$, and $5x10^3$ cells/cm^2 are shown on Figure 4.2. When investigating the effect of ICD on cell growth whilst observing growth characteristics of the culture at time intervals of two to three days over the course of the passage, it is clear that the growth rate changes over time. The trend shown in Figure 4.1 still applies, showing faster growth rates when fewer cells are covering the surface. However, growth rates are not constant over the period of the culture, slowing down as the cell density increases. This indicates that cell growth rates are dependent on the cell surface coverage at a given time, and that these growth rates decrease as the number of cells per cm^2 increases. This

modification in cell growth rates according to culture surface coverage did not seem to affect hMSC morphology. All cultures exhibited the characteristic spindle-shaped morphology at all stages of culture regardless of the number of doublings they had undergone by the end of the passage.

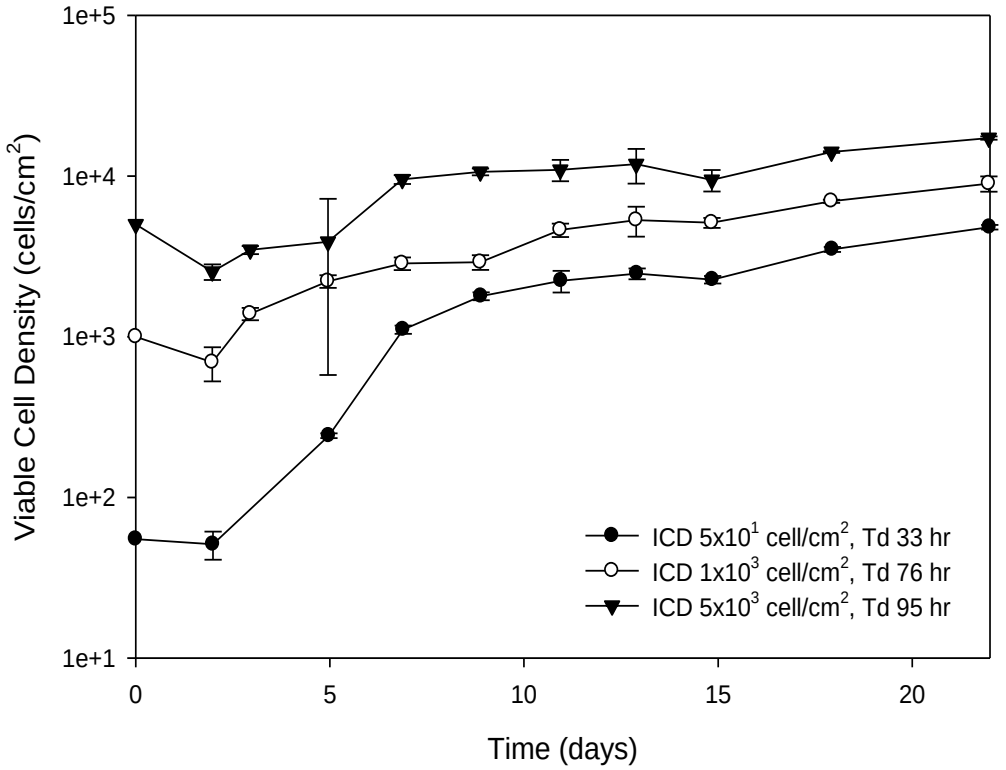

Figure 4.2 Effect of inoculation cell density (ICD) on hMSC growth kinetics. Passage 6 of hMSC was seeded at $5x10^1$, $1x10^3$, and $5x10^3$ cell/cm^2 in 24 well-plates as described in Section 2.4. Three wells from each condition were harvested and counted at 2 to 22 days. Doubling times calculated as indicated later in Section 5.2. Error bars represent one standard deviation about the mean (n=3). Maximum cell densities from empirical data reached were $3.53x10^4$, $1.75x10^4$, and $0.96x10^4$ cell/cm^2 for ICDs $5x10^3$, $1x10^3$, and $5x10^1$ cell/cm^2 respectively.

By looking at the shape of the curves in Figure 4.2 it is apparent that the culture seeded at the lowest ICD experiences an initial phase of rapid growth, but as time progresses the growth rate decreases before reaching stationary phase. Because of the difficulty in determining the beginning and end of the exponential growth phase for growth rate calculations, a 4 parameter sigmoidal Gompertz model was fitted to the data to obtain quantitative parameters for growth characteristics as

indicated later in Section 5.2. Results of growth kinetics obtained by the unmodified Gompertz equation as well as the parameters obtained are shown in table 4.2, where a comparison between doubling times (T_d) calculated from the Gompertz parameters versus the doubling times (T_d*) calculated from the best assessment of the duration of the exponential growth phase shows similar trends in the behaviour of the cultures. Overlap of the growth rate curves when a similar cell density is reached regardless of the initial cell density validates this as shown in Figure 4.3.

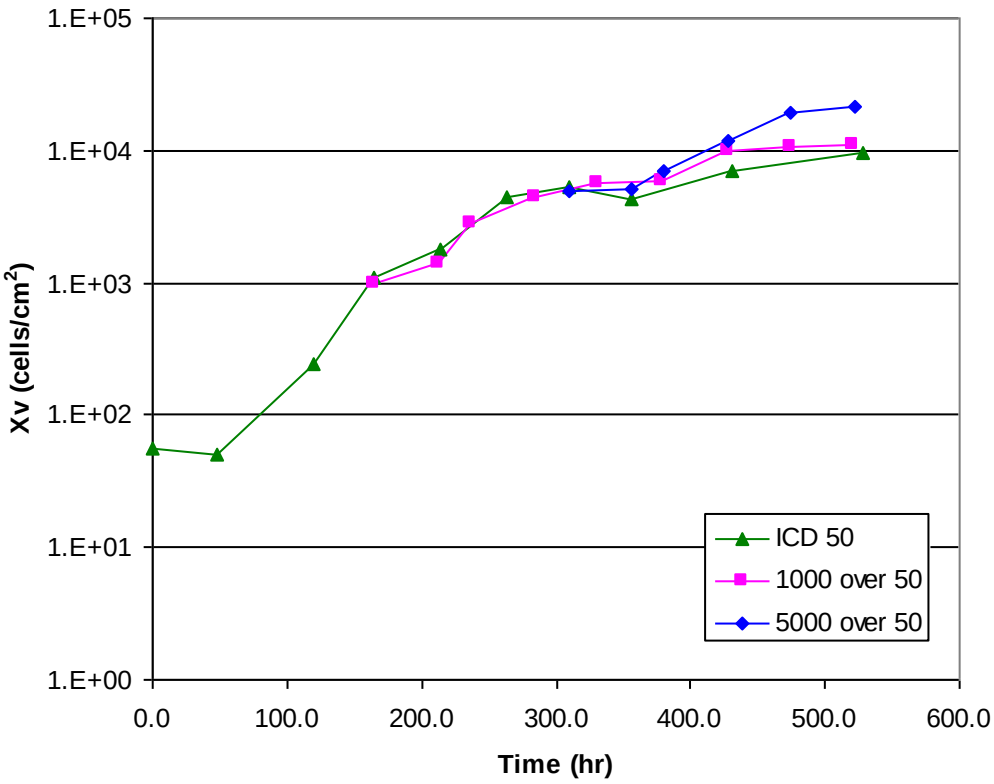

Figure 4.3 Overlay of hMSC growth curves seeded at $1x10^3$, and $5x10^3$ cell/cm^2 over a culture inoculated $5x10^1$ cell/cm^2. Data taken from Figure 4.2. The growth curve for ICD $5x10^1$ cell/cm^2 is shown starting at time 0 hr as it was performed experimentally. The growth curve for ICD $1x10^3$ cell/cm^2 was plotted starting at time 165 hr i.e. the time at which the cell density for the culture seeded at $5x10^1$ cell/cm^2 had reached $1x10^3$ cell/cm^2. Similarly, the growth curve for ICD $5x10^3$ cell/cm^2 was plotted starting at time 309 hr, the time at which the cell density for the culture seeded at $5x10^1$ cell/cm^2 had reached $5x10^3$ cell/cm^2.

Analysis of overlapping cell growth curves at common cell densities demonstrates that hMSC cell growth rate changes over time as the number of cells per surface area in the culture vessel increases. The faster growth rate observed when fewer cells are present per surface area is lost once the cell density reaches the same value as that one used to inoculate under the baseline or control condition of $5x10^3$ cell/cm^2. Furthermore, cultures seeded at low ICD of $5x10^1$ cell/cm^2 reached a lower cell density at the end of the culture than the baseline condition. From empirical data, only $0.96x10^4$ cell/cm^2 were recovered from the culture seeded at the lowest ICD whilst $3.53x10^4$ cell/cm^2 were recovered from the culture seeded at the baseline ICD at the time of harvest, with no clear indication of the stationary phase having been reached then. Because of the limited number of wells, not enough cells were available for cell density determination after twenty days in culture. Therefore based on the data available it is not possible to ensure that growth arrest had been reached by all populations at harvest, although the growth rate during the last days in culture had decreased severely..

Table 4.2. Effect of inoculation cell density (ICD) on hMSC growth kinetics. Passage 6 of hMSC was seeded at $5x10^1$, $1x10^3$, and $5x10^3$ cell/cm^2 in 24 well-plates as described in Section 2.4 . Kinetic parameter values obtained from fitting the modified four-parameter Gompertz model (Equation 3.1) in Figures 4.2. Growth rates (μ) and Doubling Time (T_d) calculated from Gompertz parameters, and Doubling Time (T_d*) was calculated from empirical data for comparison purposes

ICD	a	X_{max} (cells/cm^2)	X_0	b	t_0	μ (hr^{-1})	Td	Td*
50	$6.87x10^4$	$6.87\ x10^4$	$5.10x10^1$	126	209	0.0210	33	38
1000	$3.31\ x10^4$	$3.39\ x10^4$	$7.96x10^2$	151	202	0.0091	76	65
5000	$3.03\ x10^4$	$3.35\ x10^4$	$3.20x10^3$	119	139	0.0073	95	85

Sekiya et al. (2002) implied that the decrease in viable cell density at the end of the culture may be due to an increase in cell mass as the cell doubling number increases. The hypothesis is based on the assumption that although the cells utilise the same amount of resources they use them to build biomass within the cell and not to divide. If this was true and it was also accountable for the decrease of cell growth as the population doubles, size determination over time as a

measurement for an increase in cell mass will confirm this. For this purpose, harvested material for a culture at Passage 1 and Passage 5 but from the same cell source was analysed for cell size with a Malvern Mastersizer as indicated in Section 2.11.1.

(a) Particle size distribution for hMSC at Passage 1, measured in duplicate from the same cell suspension (red and green lines)

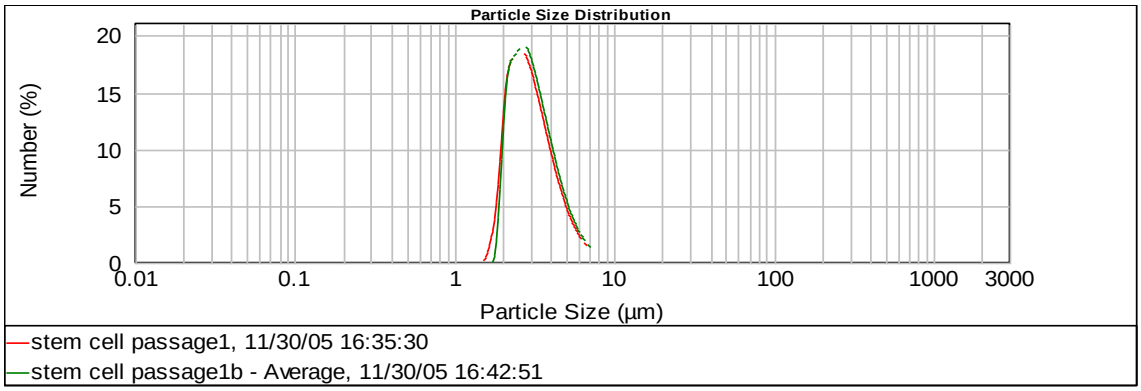

(b) Particle size distribution for hMSC at Passage 5

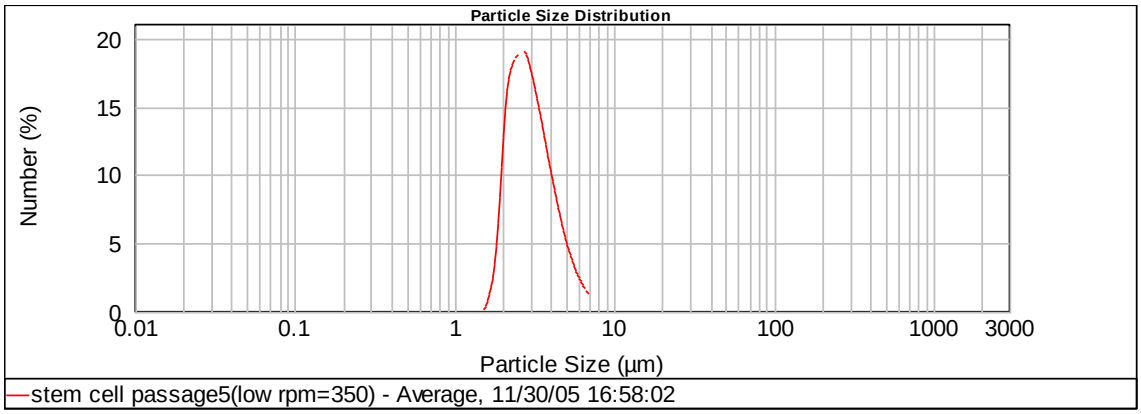

(Data provided by Ioannis Papantoniou)

Figure 4.4 Particle size determination for suspensions of hMSC in culture medium harvested at (a) passage 1 and (b) passage 5. Cells cultured as described in Section 2.4 and sized using a Malvern Mastersizer following the procedure in Section 2.11.1. Both cultures yield a D_{50} or 2.92 µm, indicating no size increase over population doubling increase.

Cell size analysis corroborated that as the population doubling increases, the size of the cells in culture remains constant. For hMSC measured at the end of the first and fifth passages the mean diameter observed was identical, as shown in Figure 4.4. Cell size determination through image analysis was also performed with a Cedex counter as per the protocol described in Section 2.11.2, and the results confirmed no difference in size (results not shown).

It is possible the increase in cell growth rate with decreasing ICD is a consequence of cell to cell physical distance or to the amount of media available per cell at a given time. Published data by Sekiya *et. al*. (2002) showing the same trend, failed to extend the period of the hMSC cultures seeded at low ICD until the stationary phase was reached. Consequently, although it is true that cells seeded at low densities of $5x10^1$ to $1x10^2$ cells/cm^2 double at a faster rate than those seeded at $5x10^3$ cells/cm^2, it is important to notice that they have to be maintained at such a low surface coverage before the growth rate slows down. This means that hMSC inoculated at $5x10^1$ cells/cm^2 would have to be harvested at cell densities below $1x10^3$ cells/cm^2 in order to accelerate the overall cell expansion time to reach the same number of cells at the end of the process. The implication for this process change is a considerable increase in raw materials such as culture media, trypsin, and plastic ware, in order to complete the cell expansion process, whilst reducing the overall processing time. The increase in open aseptic manipulations with the associated risk of contamination, cost of materials, and manual labour, does not justify the reduction of the overall cell expansion time achieved by this process parameter change.

4.3 Effect of feeding strategy on hMSC expansion

The effect of inoculation cell density during the cell expansion of hMSC in an undifferentiated state was investigated in Section 4.2. Faster growth rates than those obtained by the standard growth protocol - inoculation cell density of $5x10^3$ cells/cm^2 with medium exchange every three to four days - were shown for hMSC when cell surface coverage was maintained between $5x10^1$ and $1x10^3$ cells/cm^2. It is unlikely for the physical distance between cells to be an explanation for this decrease in doubling time for low cell surface coverage since

microscopic observation reveals that there is no contact between cells at densities of $5x10^3$ cells/cm^2. However, a possible reason for this effect is the accumulation of inhibitory factors secreted by the cells or the competition for growth factors or nutrients in the media as more cells per ml of media are present in the culture. Metabolic analysis of the spent media for all cultures did not reveal nutrient limitations – glucose and glutamine - or accumulation of toxic products – lactate and glutamate - for any of the conditions tested (data provided in Appendix II) but other media components such as growth factors, lipids, or amino acids were not analysed and could be responsible for this differences in growth rates. If this is the case, it would be possible to achieve the same high growth rates obtained when seeding hMSC at low ICD, by providing the same addition rate of media in a per cell basis for cultures seeded at $5x10^3$ cells/cm^2.

To test this hypothesis, media requirements for hMSC cultures seeded at low ICD of $1x10^2$ cells/cm^2 were calculated, based on media exchanges of every four days, to be $2.08x10^{-5}$ ml media/cell.hr. In order to match the same media availability to cultures seeded at a higher ICD of $4x10^3$ cells/cm^2 in 6 well plates, medium exchanges were performed every 2.5 hours for the initial 48 hours of the culture. After the initial 48 hours, medium exchange rates were decreased to one every 6 hours for the remaining 21 day of the culture for logistical reasons. As a positive control, hMSC were inoculated at $1x10^2$ cells/cm^2 with medium exchanges every four days. As a negative control, hMSC were inoculated at $4x10^3$ cells/cm^2 with medium exchanges every four days also. Three wells were sacrificed from each condition at every time point to generate growth curves, as shown in Figure 4.5.

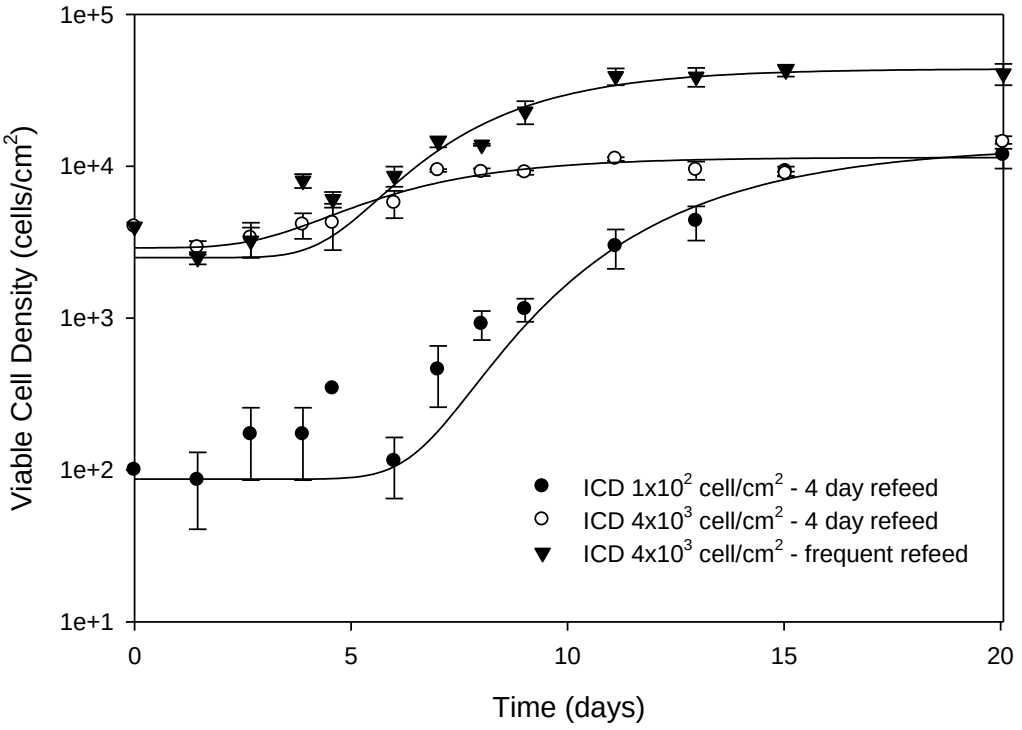

Figure 4.5 Effect of feeding strategy and inoculation cell density (ICD) on hMSC growth kinetics. hMSC from a common cell inoculum were seeded in 6 well-plates at $1x10^2$, and $4x10^3$ cells/cm^2 as described in Section 2.4. Feeding rates for ICD $4x10^3$ cell/cm^2 with frequent refeed matched the medium supplied in ml/cell.hr provided to the condition seeded at $1x10^2$ cell/cm^2 when refed every four days. Error bars represent one standard deviation about the mean (n=3). The data was fitted to a 4-parameter sigmoidal Gompertz model (solid lines) to determine quantitative growth kinetic parameters as indicated later in Section 5.2.

Analysis of the cell growth characteristics for each of the conditions tested (Table 4.3) corroborates the hypothesis that hMSC growth rate is dependent on medium addition rates and not on ICD as previously reported (Sekiya et al., 2002). The calculated growth rate of 0.53 days^{-1} achieved by hMSC seeded at low ICD of $1x10^2$ cells/cm^2 was closely reproduced at a rate of 0.42 days^{-1} for cells seeded at $4x10^3$ cells/cm^2 by normalizing the medium addition rate in a per cell per hour basis for the same cell source. The small discrepancy between the two values can be explained, as normalised media flow rates were calculated for the cell density of $1x10^2$ cells/cm^2 at inoculation time, and it was not recalculated over time to account for the increase of the number of cells in culture as the cells divided. For each cell doubling, the addition rate of media was not exactly equal in a per cell

per time basis for each condition. This resulted in a discrepancy of 0.1 $days^{-1}$ in growth rates for hMSC when seeded at $1x10^2$ versus $4x10^3$ $cells/cm^2$. However, the growth rates were considered close enough to prove that a higher frequency of medium exchanges resulted in an increase cell growth rates. Results showed an improvement in cell growth rate increasing from 0.16 $days^{-1}$ to 0.42 $days^{-1}$ when comparing the control culture seeded with ICD of $4x10^3$ $cell/cm^2$ with medium exchange frequency of four days with the optimised medium exchange strategy for the culture seeded at the same ICD of $4x10^3$ $cell/cm^2$.

To highlight the significance of this process optimisation parameter, quantitative values for growth rate obtained with a four-parameter sigmoidal Gompertz equation (Equation 5.1), and doubling time for each bioprocess condition tested are shown in Table 4.3 along with the time implications for delivery of undifferentiated hMSC to the clinic. A feeding strategy that would provide $2.08x10^{-5}$ ml media/cell.hr could easily be implemented in an automated robotic platform, yielding optimum hMSC growth rates of 0.5 day^{-1} in an undifferentiated state. The advantage of this process parameter implementation is that the overall cell expansion times will be reduced from 59 to 30 days (Table 4.3), while maintaining the same culture surface area over the completion of the cell growth within a passage. The use of an automated culture platform would also reduce the risk of contamination due to operator errors during open manipulations, as well as reducing the cost of manual labour.

Table 4.3 Effect of inoculation cell density (ICD) and feeding strategy on growth kinetics and overall cell expansion process time for hMSC. Process time indicates the number of days that would take for $1x10^5$ cells to be expanded to $1x10^8$ cells for each process. Calculations based on four parameter sigmoidal Gompertz model as indicated in Section 5.2 from data shown in Figure 4.5.

ICD (cells/cm^2)	Frequency of Medium Exchange	a	X_{max}	X_0	b	t_0	μ(d^{-1})	Td (hr)	Cell Expansion Process Time (days)
$4x10^3$	4 days	$8.50x10^{+3}$	$1.14x10^{+4}$	$2.91x10^{+3}$	2.4	5.6	0.16	102	59
$4x10^3$	6 hours	$4.13x10^{+4}$	$4.38x10^{+4}$	$2.50x10^{+3}$	2.5	7.8	0.42	40	34
$1x10^2$	4 days	$1.36x10^{+4}$	$1.37x10^{+4}$	$8.70x10^{+1}$	3.5	12.7	0.53	32	30

The only drawback associated with an increase in the frequency of medium exchanges is the associated increase in cost due to the larger amount of media requirements for the completion of the cell expansion process. The most expensive component in the media formulation used for the cell expansion is FBS. Due to the cost of this raw material as well as the undesired source (animal derived component) as explained in Section 1.3.2, an alternative supplementation to the media was tested. FBS was replaced by protein hydrolysates from the growth medium to determine if a non-animal derived complex component would sustain hMSC growth in a comparable way. Four different protein hydrolysates from Kerry Bio-Science were tested, HyPep 4601, HyPep 1511, HyPep 1510, and H-Soy as indicated in Section 2.5. Four different media formulations were prepared by adding one of the protein hydrolysates at a concentration of 4 g/L. A common pool of cells was used for growth comparison in parallel cultures with each one of these four media compositions as well as with the control media formulation with 10% FBS. The cultures were inoculated at $5x10^3$ cells/cm^2 in 24 well-plates, with medium exchanges every three days. Growth curves from each condition were generated as shown in Figure 4.6.

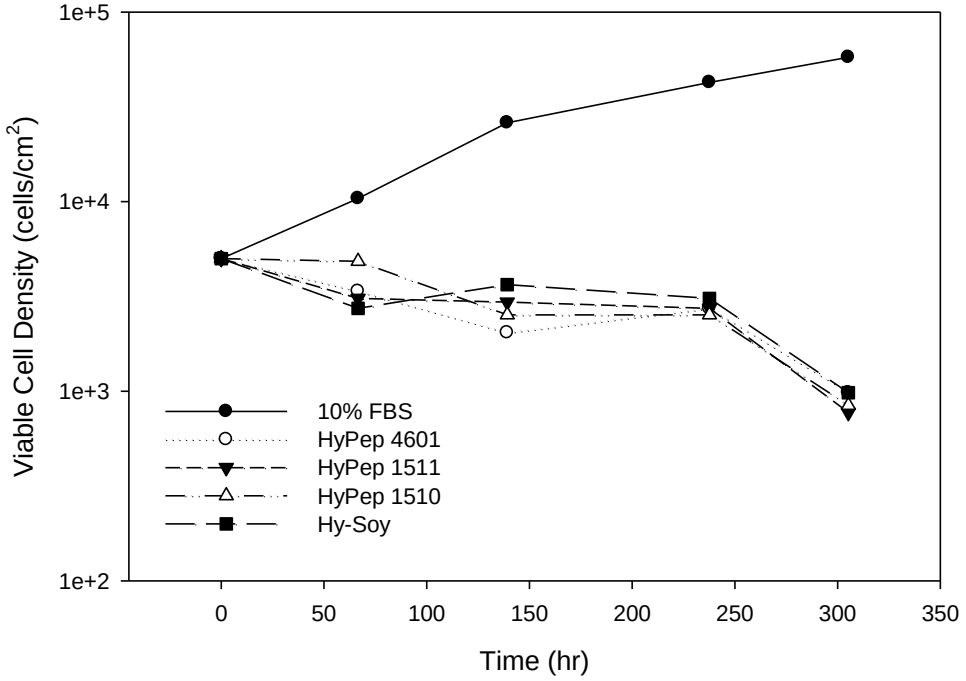

Figure 4.6. Effect of FBS replacement by Protein Hydrolysate on hMSC growth kinetics. hMSC from a common cell inoculum were seeded in 24 well-plates at $5x10^3$ cells/cm^2 with medium exchanges every three days. The control condition was cultured with the basal medium formulation containing 10% FBS. Four other formulations had FBS replaced with 4 g/L of each of the following protein hydrolysates: HyPep 4601, HyPep 1511, HyPep 1510, and Hy-Soy.

Growth curves generated from each one of the cultures with protein hydrolysate showed that neither of these commercially available components can support growth for hMSC. To corroborate this finding, the same cell source cultivated with 10% FBS did support growth, proving that no other parameter other than protein hydrolysates were responsible for the negative growth in these cultures. Results indicate that protein hydrolysates are not a viable replacement for FBS replacement for the lots of materials tested at 4 g/L concentration. No further efforts were dedicated to the replacement of FBS with non-animal derived or with chemically defined components, since such studies are outside the scope of this thesis.

4.4 Effect of Temperature and pH Deviations on hMSC expansion

As shown in Section 4.3, the feeding strategy for the culture of hMSC has a very significant impact on cell growth kinetics. As the frequency of medium exchanges increases, the growth rate of the culture increases significantly. The cause for this increase in growth rate due an increase in medium exchange rate is not fully understood, since there were no measurable chemical factors being depleted in the culture media when sampling the spent media for metabolites (Section 2.7). However, during each medium exchange there are not just chemical changes in the environment of the cells, but physical changes as well which maybe in part responsible for variations in growth rates.

During every full medium exchange the cultures are removed from the environmentally controlled incubators and placed in a non-environmentally controlled biosafety cabinet. Every time this happens, there is a step change in temperature from 37˚C to room temperature, and a step change in gas composition from 5% CO_2 to atmospheric concentration. It normally takes from 15 to 30 minutes to replace the media from all the wells in a 12 well-plate, and during that time the step change variations in the environment translate into changes in the pH and temperature in the culture media. It is therefore possible that exposure to these different, or fluctuating, environmental conditions had an effect on cell growth that it is independent on the media being replaced.

In order to test this hypothesis, the temperature and pH of the medium during the step changes experienced during a medium exchange were recorded. Control experiments were executed to decouple the effect of such pH and temperature variations on cell growth kinetics. The results of these studies are shown in Section 4.4.1 and 4.4.2.

4.4.1 Effect of Environmental Excursions on Temperature and pH of Culture Media

Cultures of hMSC are placed in humidified incubators at 37˚C, and a gas mixture containing 5% CO_2 to regulate the pH in the media. Every time a culture vessel is removed from the incubator the cultures are exposed to a step change in

temperature dropping from 37˚C to a room temperature of 20˚C to 22˚C, as well as an atmospheric gas composition. These step changes take place every time a culture vessel is removed from the incubator for a microscopic observation, to perform medium exchanges, or to harvest one or more wells from a well plate. However, the cells attached to the surface are protected by the layer of medium covering them, and they will only be exposed to the variation of temperature and pH that occur in the medium above them.

To study the variations of temperature in the media for 12 well-plates, thermocouples were submerged in the media of one well and also placed 10 inches over the plate to record the temperature profiles during temperature excursions as explained in Section 2.8. To record pH variations, small fluorescence-based pH sensor patches were placed at the bottom of the well as indicated in Section 2.9. The standard amount of time that a plate is placed outside the incubator during a medium exchange or a microscopic observation is approximately 15 minutes. This operation was mimicked by loading a 12 well-plate with 2 ml of culture media per well with thermocouples and pH sensors attached to the plate. The 12 well-plate was placed in a 37˚C incubator with 5% CO_2 until the readings equilibrated at the set-point conditions.

Once the media was equilibrated the plate was removed from the incubator and placed in a biosafety cabinet for 15 minutes, after which the plate was placed back in the incubator. Values for temperature and pH were recorded until both of the values equilibrated back to the initial values. Profiles generated from these temperature and CO_2 deviations are shown in Figure 4.7.

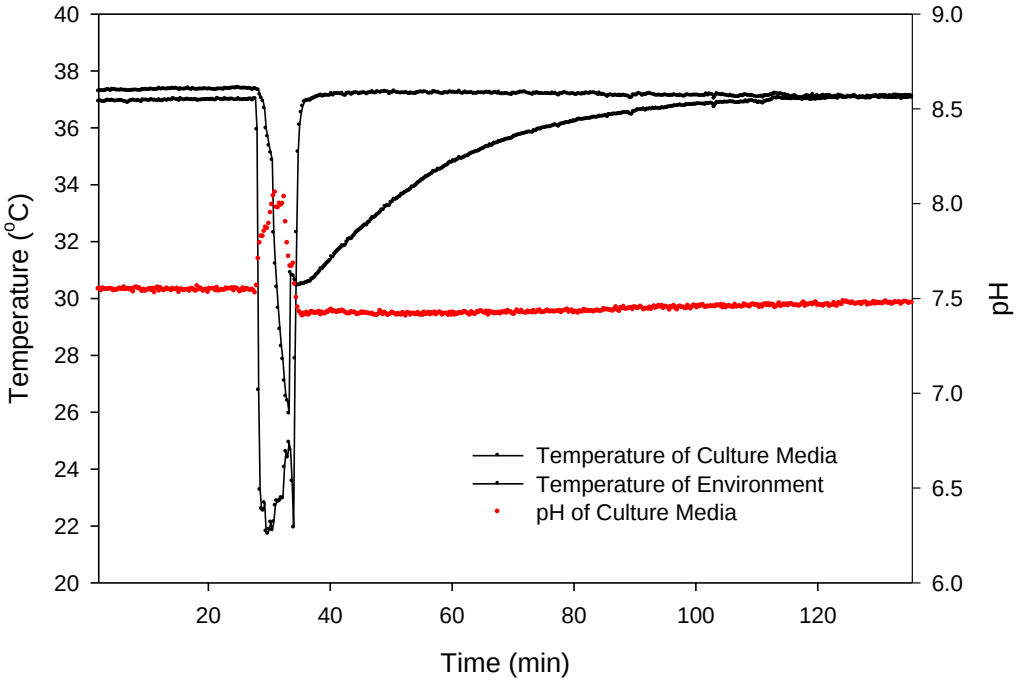

Figure 4.7 Effect of a 15 minute step change in environmental temperature and gas composition on culture media in a 12 well-plate. Temperature and pH variations in the culture media of one well from a 12 well-plate filled with 2 ml of culture media on each well were measured as described in Section 2.9.1. The plate was equilibrated in a humidified incubator with 5% CO_2 at 37˚C and removed into a biosafety cabinet for 15 minutes before placing back into the incubator.

From the profiles recorded during a 15 minute step change in environmental conditions, the medium pH is seen to increase from 7.5 up to 8.0 and the temperature in the media decreased down to 26˚C from the initial 37˚C. Once the plate was placed back into the incubator the pH went back to 7.5 almost immediately. However it took approximately one hour for the temperature of the media to regain the set-point temperature of 37˚C. This is not a significant amount of time if medium exchanges were to be performed every three to four days. However, in the case of frequent medium exchanges every 6 hours or less, which it has been proven to increase cell growth rates (Section 4.3), these environmental changes will represent 17% of the culture time taking place under 37˚C. Temperature stress has been shown to produce positive effects in murine MSC, up-regulating heat shock proteins and down-regulating pro-apoptotic proteins as well as decreasing proteasome activity (Stolzing et al, 2006).

Extracellular pH also plays an important role in cell growth in hMSC, showing a decrease in number of cells recovered when exposed to pH variations (Gaus et al., 2002).

The time taken for the plate to equilibrate within the biosafety cabinet, under non-environmentally controlled conditions was also established. This represents a more extreme deviation, for example when harvesting or staining some of the wells from a well-plate, or when taking photographs of the wells at an intermediate time-point during the culture. In this case it takes 50 minutes to reach room temperature and one hour and forty minutes for re-equilibration to the initial set points as shown in Figure 4.8. The pH was seen to re-equilibrated almost immediately according to the percentage of CO_2 in the environment going from 7.5 to 8.0.

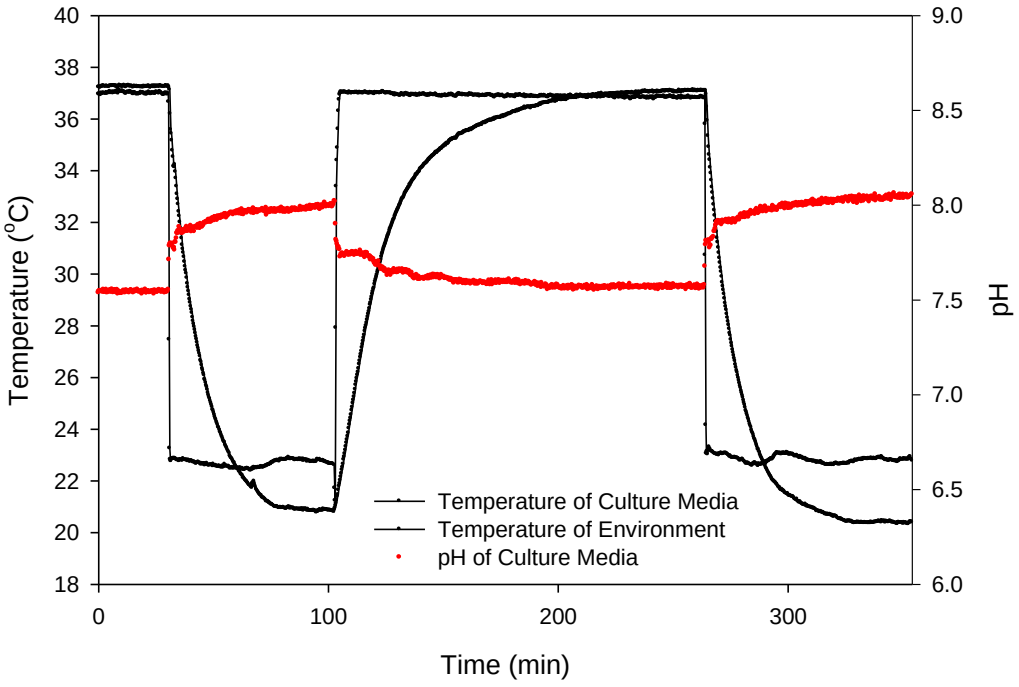

Figure 4.8 Effect of a maximum environmental temperature step change on culture media in a 12 well-plate. Temperature and pH variations in the culture media of one well from a 12 well-plate filled with 2 ml of culture media on each well were measured as described in Section 2.9.1. The plate was equilibrated in a humidified incubator with 5% CO_2 at 37˚C and removed into a biosafety cabinet until the temperature of the well reached room temperature. After equilibration at room temperature, the 12 well-plate was placed back into the incubator until it equilibrated again to the set values.

The recovery time for the temperature of the culture media to equilibrate back to 37˚C after manipulations in a biosafety cabinet can be minimised by increasing the heat transfer rate to the medium upon return to the incubator. This was evaluated by placing the 12 well-plate on an orbital shaker inside a controlled incubator and recording temperature and pH profiles while transferring the well-plate from equilibrium at room temperature and atmospheric conditions back to 37˚C and 5% CO_2 in the humidified incubator. Two different shaking speeds were tested, 140 and 250 rpm. The profiles are shown in Figures 4.9 and 4.10 respectively.

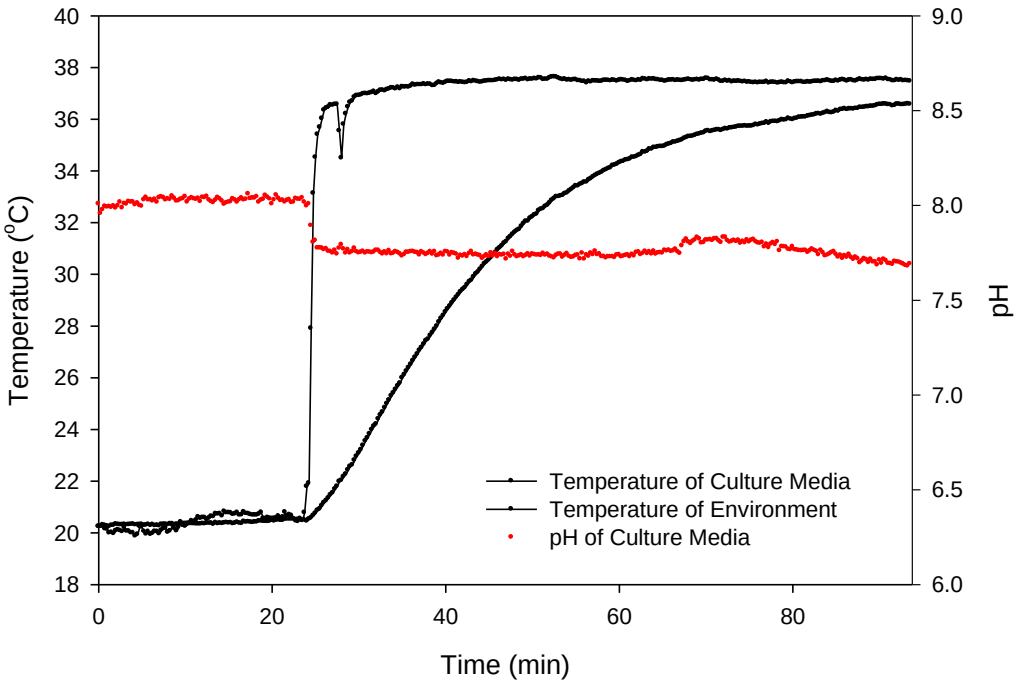

Figure 4.9 Effect of a temperature step change in culture media of a 12 well-plate with shaking during incubation. Temperature and pH variations in the culture media of one well from a 12 well-plate filled with 2 ml of culture media on each well were measured as described in Section 2.9.1. The plate was equilibrated in a biosafety cabinet and then placed into a shaker at 140 rpm in a humidified incubator with 5% CO_2 at 37˚C.

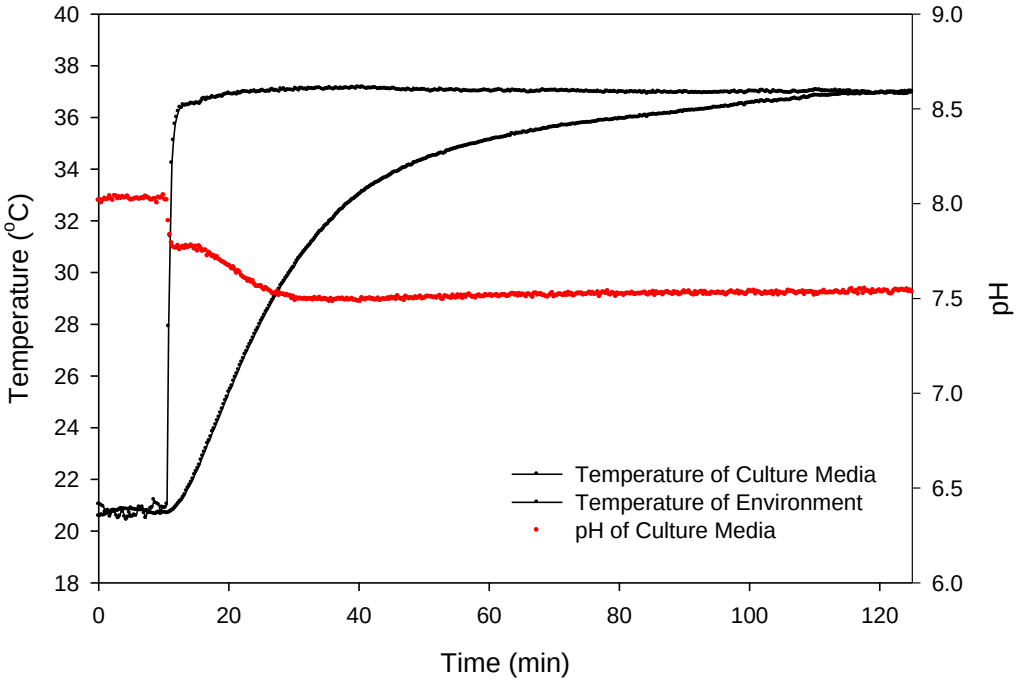

Figure 4.10 Effect of a maximum temperature step change in culture media of a 12 well-plate with shaking during incubation. Temperature and pH variations in the culture media of one well from a 12 well-plate filled with 2 ml of culture media on each well were measured as described in Section 2.9.1. The plate was equilibrated in a biosafety cabinet and placed into a shaker at 250 rpm in a humidified incubator with 5% CO_2 at 37˚C.

From the profiles obtained with shaking in the incubator at 140 and 250 rpm, an improvement in heat transfer rate for both conditions was observed in comparison with the normal static condition. It took 1 hour and 40 minutes for the temperature of the culture media to reach 37˚C in the incubator under static condition after being equilibrated at room temperature. However, it only took one hour when the plate was placed in a shaker inside the incubator. There was not a considerable difference in the overall time taken for temperature re-equilibration between 140 to 250 rpm, although the initial increase in temperature in the media was faster for 250 rpm than for 140 rpm as would be expected due to the increased gas-liquid surface area available for heat transfer at the higher shaking speed (Zhang., et al., 2008). Even with improved heat transfer in the system, the temperature variation of the culture media as a result of a step change in environmental conditions can be minimised but it cannot be eliminated. Consequently, the effect of these variations in the temperature and pH of the

culture media during hMSC cell expansion process have to be addressed, as described in Section 4.4.2.

4.4.2 Decoupling the Effect of Feeding Strategy from Environmental Variations During Medium Exchanges on hMSC Growth Kinetics

For the cell expansion process of hMSC under static conditions, more frequent medium exchanges result in faster growth rates as shown in Section 4.3. Two feeding strategies were implemented for the same cells source from Passage 1; medium exchanges every three days and every six hours. Considering the chemical and physical changes that occur in the cell environment during a medium exchange, it is important to understand which of these parameters is contributing to the measured increase in growth rates. In addition to the replacement of spent medium by formulated culture medium, during every medium exchange there is a variation in the pH and temperature of the cell environment that last for at least one hour, as shown in Section 4.4.1. The effect of pH, feeding strategy, and cumulative repetition of step changes on hMSC growth kinetics was thus attempted to be decoupled in the following experiments.

Two different feeding strategies were compared to the control baseline, which consists of medium exchanges every three days for a culture of hMSC seeded at $5x10^3$ cells/cm^2 in 24 well-plates. Growth kinetics were studied for hMSC cultures seeded at the same inoculation density from the same source of cells with higher frequencies of medium exchanges of 24 and 12 hours. As shown in Figure 4.11 a higher frequency of medium exchanges results in not just higher growth rates but also in a higher maximum viable cell density reached by the stationary phase. From the three feeding strategies studied, medium exchanges every 12 hours resulted in the fastest growth rates of 0.63 day^{-1} with a maximum cell density of $1.2x10^5$ cells/cm^2, followed by medium exchanges every 24 hours with growth rates of 0.51 day^{-1} and a maximum cell density of $1.0x10^5$ cells/cm^2 . Both of these represent an improvement over the control or baseline condition which gave a growth rate of 0.32 day^{-1} and a maximum cell density of $6.3x10^4$ cells/cm^2 . The quantitative results from each condition are listed in Table 4.4 for easier comparison.

To understand if the pH step changes that occur during a medium exchange had any impact on the improvement in process performance with more frequent feeding these pH changes were reproduced at a 12 hour frequency but the medium was replaced once every three days matching the baseline control feeding strategy. A CO_2 controlled humidified incubator at 37˚C was set at 0% CO_2 gas mixture balanced with O_2 and N_2 for this purpose. Pre-equilibrated medium for 24 hours at 0% CO_2 and 37˚C resulted in a pH of 8.6. Cultures of hMSC were seeded, plated, and cultured in identical fashion as the control baseline condition with medium exchanges every three days. However, every 12 hours, the plates were transferred to the 0% CO_2 incubator for 15 minutes, and then placed back into the 5% CO_2 incubator. One plate was seeded for each time point of data recorded, to ensure that no extra exposure to ambient temperature was taking place on the culture while harvesting individual wells during each time point. Interestingly, these series of pH variations every 12 hours alone did not result in comparable cell growth rates to the ones obtained when performing medium exchanges every 12 hours. By exposing the culture to higher pH conditions every 12 hours, a growth rate of 0.34 $days^{-1}$ was obtained, comparable to the growth rate of the control culture of 0.32 day^{-1} (Table 4.4). No decrease in the maximum number of viable cells at the end of the exponential phase was observed by exposure to these pH variations.

The possibility of higher pH having a detrimental effect on hMSC was studied by culturing hMSC in a humidified incubator at 37˚C with 2% CO_2 gas mixture balanced with O_2 and N_2. This gas composition resulted in a pH reading of 8.2 at 37˚C. The cultures were kept with a baseline condition feeding strategy of medium exchanges every three days. The same procedure was followed in an incubator with 0% CO_2 gas mixture, however no cells survived the first 24 hours at this high pH of 8.6 and the well-plates were discarded. For the culture of hMSC incubated at pH of 8.2 in the 2% CO_2 incubator, the slowest growth rates of 0.19 day^{-1} was observed over the period of the culture. However, a maximum cell density of $1.1x10^5$ $cells/cm^2$ was obtained at the end of the culture which is comparable to the maximum cell densities achieved by the faster frequency feeding strategies (Table 4.4). Higher pH in the medium resulted in a slower growth during the first days in culture which may be in part due to an adaptation

process of the cells to new environmental conditions. However looking at the cell growth curve in red in Figure 4.11 it does not appear as if the culture has reached stationary phase after the last time point was recorded. Because no more plates had been seeded the culture could not be continued any longer. Nevertheless, in spite the initial slower growth rate, the fact that high cell densities could be reached within the first passage suggest that hMSC can grow at higher pH and that it may be beneficial over a baseline condition once the cultures overcome an initial adaptation period.

Table 4.4. Effect of % CO_2, pH and feeding strategy on hMSC growth kinetics and maximum cell density reached for cell expansion in 24 well-plates. Experimental data taken from Figure 4.10. Growth rate and maximum cell density were calculated using a 4-parameter sigmoidal Gompertz equation as described later in Section 5. 2 for the growth curves generated for each condition. The control baseline is highlighted in bold.

% CO_2	**pH**	**Frequency of Medium Exchanges**	***a***	**X_{max} (cell/cm$_2$)**	***X_0***	***b***	***t_0***	**u (d^{-1})**	**Td (hr)**
5	7.5	12 hr	$1.15x10^{+5}$	$1.20\ x10^{+5}$	$4.78x10^{+3}$	45.4	137	0.63	26.5
5	7.5	24 hr	$9.78x10^{+4}$	$1.02\ x10^{+5}$	$3.87\ x10^{+3}$	56.9	135	0.51	32.8
5	**7.5**	**3 days**	**$6.11\ x10^{+4}$**	**$6.31\ x10^{+4}$**	**$2.08\ x10^{+3}$**	**95.0**	**140**	**0.32**	**52.4**
5 with 15 min exposure to 0 every 12 hr	7.5-8.6	3 days	$6.39\ x10^{+4}$	$6.75\ x10^{+4}$	$3.60\ x10^{+3}$	76	138	0.34	48.9
2	8.2	3 days	$1.10\ x10^{+5}$	$1.13\ x10^{+5}$	$3.60\ x10^{+3}$	164	269	0.19	89.6
0	8.6	3 days	0.00	0.00	$4.00\ x10^{+3}$	0.00	0.00	0.00	0.0

This data suggest that a combination of an increase in medium replacement as well as exposure to pH values higher than 7.5, results in an increase in hMSC growth rate as well as maximum cell numbers recovered from the culture. From these encouraging results, it is reasonable to believe that further optimisation of pH culture conditions in combination with frequent medium exchanges will provide even more satisfactory conditions of growth of hMSC in an undifferentiated state for sequential passages while reducing the amount of media and culture vessels required for the overall cell expansion process.

While these process optimisation parameters would be tedious to implement in cultures expanded manually, they can be easily implemented in automated robotic platforms. The feasibility of this concept is further investigated in Section 4.5.

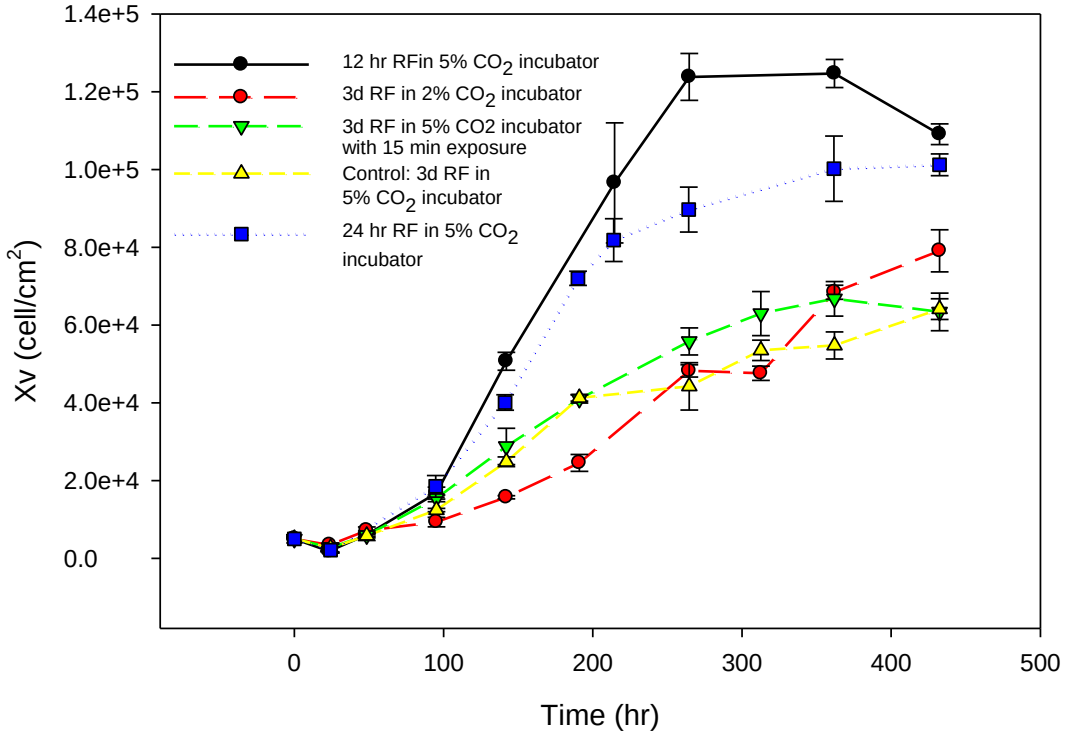

Figure 4.11. Effect of feeding strategy and percentage CO2 resulting in different pH, and transient environmental variations on hMSC growth kinetics. hMSC from a common cell inoculum were seeded in 24 well-plates at 5x103 cells/cm2 as described in Section 2.4. Three feeding strategies with frequencies of 3 days, 12 hours, and 24 hours were compared when incubated in 5% CO2 and 37˚C incubator. Three different pH conditions resulting for different exposures to CO2 were also compared for cultures undergoing medium exchanges every 3 days. Error bars represent one standard deviation about the mean (n=3). Quantitative parameters derived from these growth curves are presented in Table 4.4.

4.5 hMSC Cell Growth in an automated robotic platform

One of the main hurdles for the implementation of a robust process for cell expansion of large numbers of hMSC for use in regenerative medicine therapies, is the high number or manual operations required over the course of several passages and the consequent variation, high cost, and contamination risk that this

generates (Mason, 2006). There are also some process implementations, such as tight control of environmental conditions, that would be not possible to implement in open system cultures.

To demonstrate the advantages and feasibility of performing the cell expansion processes for hMSC under controlled environmental parameters, an automated system was used to culture hMSC with no manual manipulations involved. As indicated in Section 2.12, a Tecan robotic platform was enclosed in a biosafety cabinet with the capability to control temperature and gas composition. Two 12 well-plates were inoculated with hMSC at an inoculation cell density of $5x10^3$ cells/cm^2. The plates were placed in an automated incubator integrated with the biosafety cabinet, at 5% CO_2 and 37˚C. As shown in Figure 2.5, the incubator could be opened to the outside of the cabinet in order to load and unload the cultures, and it could also open to the inside of the biosafety cabinet where a robotic arm removed the well-plates and placed them in a platform inside a controlled environment. Once the plates were loaded into the incubator, no manual manipulations were required during the cell expansion process.

From the two plates placed in the incubator, one was scheduled to undergo medium exchanges every 4 hours, and the other one every 12 hours. The biosafety cabinet was not environmentally controlled for this experiment, and the front was kept open during this preliminary test. The medium exchange operations could be completed within 5 minutes for each plate, during which time the robotic arm could aspirate the spent medium from each well and replace it with culture medium before placing it back into the incubator. Due to the fact that the culture medium was kept inside the open biosafety cabinet during the three days that the experiment took place, a contamination of the medium prevented completion of the passage. The system is now set up to keep the culture medium refrigerated and to place it into a container for temperature adjustment and dispensing before a medium exchange. This piece of equipment was not ready at the time of this experiment. However, daily microscopic observations of the plates indicated higher cell surface coverage for the plate with medium exchanges every 4 hours compared to the plate with medium exchanges every 12 hours. This was a good indication that hMSC were proliferating and that the same effect

observed with manual manipulations (Section 4.3) could be obtained in an automated platform with the added advantage of reducing the need of an operator to perform the manual operations every 4 and 12 hours.

With appropriate implementation of an enclosed system within the biosafety cabinet that will hold culture media sterile and pre-warm to 37˚C before medium exchanges, culture of hMSC with no need of manual operations will be possible in this automated platform based on the preliminary experiment already performed. Further adjustment of environmental conditions within the platform will allow for a high throughput of experimental conditions and ensure the development and operation of a robust cell expansion process for hMSC cultures.

4.6 Summary

Process parameters for the cell expansion process of hMSC in automated microwells have been characterised. Also, optimum values for inoculation cell density, medium exchange strategies, and environmental control have been proven to reduce the overall time to reach $1x10^8$ hMSC, for their use in regenerative medicine therapies. Reduction in doubling times of hMSC was found to be mainly attributed to an increase in the frequency of medium exchanges, yielding doubling times of 32 hours when medium addition rates were normalized to $2.08x10^{-5}$ ml media/cell.hr. A modified version of the Gompertz equation was found to represent hMSC growth curves accurately, and it was used to determine growth rate, doubling time, maximum cell density, duration of lag phase and time to reach the stationary phase.

The effect of ICD on cell growth rates, duration of lag phase, and cell density achieved in the stationary phase showed a trend indicating highest growth rates for low ICDs of $1x10^2$ cell/cm^2 (figure 4.2) compared to the established cell expansion protocol that operates at an ICD of $5x10^3$ cells/cm^2. Further studies revealed that the source of this increase in cell growth rates is not dependent on an increase of cell-cell distance, but on an increase in medium exchange rates. Consequently, growth rates achieved at low ICD were reproduced for higher inoculation cell densities by matching feeding requirements in ml/cell.hr. This information was used to determine the duration of a cell expansion process that

requires $1x10^8$ of undifferentiated multipotent hMSC from an autologous source for their usage in regenerative medicine applications.

Environmental variations of pH and temperature during medium exchanges were recorded with the aid of temperature and pH sensors. These environmental variations persisted for over one hour after the operation was performed, and they were minimised when shaking the culture vessels at 140 and 250 rpm inside an incubator, although they could not be eliminated. The effect of these variations in growth kinetics of hMSC was evaluated, indicating that repeated exposures to pH step changes from 7.5 to 8.2 resulted in an increase in growth rates although they were not the only contributor to increased growth rates when similar frequency of step changes in conjunction with medium exchanges were performed in parallel.

Having proven that higher frequency of medium exchanges with repeated step change exposure to higher pH during the cell expansion of hMSC resulted in an increase in growth rates, an automated platform was used as a proof of concept for the implementation of such operations. The automated platform successfully performed medium exchange operations at higher frequencies of 4 and 12 hours, that otherwise would have required the use of two operators to accomplish. Further modifications of this automated platform will prove to be an effective way to ensure production of hMSC for autologous therapies with optimum growth in an undifferentiated state.

CHAPTER FIVE

Modelling and Prediction of hMSC Growth Kinetics and Performance of a Multistage Cell Expansion Process

5 MODELLING AND PREDICTION OF HMSC GROWTH KINETICS AND PERFORMANCE OF A MULTISTAGE CELL EXPANSION PROCESS

5.1 Introduction and Aims

The use of autologous hMSC for regenerative medicine therapies presents a suitable alternative for cell and gene therapy (Prockop, 1997) and regeneration of tissue (Oreffo et al., 2007; Caplan et al., 2001) for the treatment of degenerative diseases. One advantage of using autologous progenitor cells over any other source of cells is the lack of immunosuppressant requirements, since these cells are provided by the patients themselves. In the case of patients with immunological compromised systems the use of hMSC will provide a great alternative of care, not available to them otherwise. However, the disadvantage in terms of making this therapy available to satisfy market needs, is that the process of generating a final product varies from patient to patient due to the different cell growth characteristics from each donor.

The procedure involving patient specific autologous cell therapy requires a series of steps that must be carefully timed for the success of the treatment. First of all, the patient must be scheduled for the surgical collection of a bone marrow sample. Then the sample must be transferred to a laboratory where the hMSC are isolated from the bone marrow extract as indicated in Section 3.2. After cell isolation, hMSC must undergo a cell expansion process with the initial purpose to generate sufficient undifferentiated cells for treatment. Once the number of cells required have been reached, a differentiation step may be required if tissue regeneration is intended to occur *in vitro* or they can be returned to the hospital if tissue regeneration is intended to occur *in vivo*. Finally, the patient must be scheduled for implantation of the cellular material or regenerated tissue to coincide with arrival of the final product into the clinic. The timing of this process is critically dependant on the cell growth rate of the isolated cells which, as it has been shown in Chapters 3 and 4, depends on the donor and on the processing parameters. The process parameters can be fixed so as to implement optimum cell growth rate as shown in Section 4.3 to 4.5. However until data from the first passage is available, knowledge of the intrinsic growth characteristics

that depend on the source of the cells remains variable and unknown for each patient. This variability will result in an unknown delivery time for the therapy back to the patient, or an unrealistically broad timeframe.

For the success of this therapy, the surgical team, the patient, and the cells must be scheduled to coincide at a pre-arranged time. Any delay in the delivery of the cellular product into the clinic may jeopardize the success of the treatment and risk the health of the patient. It will also incur significant costs if the surgical team and facilities are assembled and the hMSC are not available.

For clinical applications the inability to predict the growth rate of isolated cells from a patient at each stage of the cell expansion provides a major obstacle towards the design of a time based automated bioprocess. In order to define processing times for the overall cell expansion of hMSC in an undifferentiated state, a simple mathematical model that can describe the kinetics of growth for each passage based on the parameters obtained from passage one after hMSC isolation from an individual patient would be extremely valuable. Such a model should be able to reliably forward predict processing times at each passage for each donor, taking into consideration the decrease in growth rates associated with the increase in cell doublings.

The aim of this chapter is to develop a mathematical model that could describe the kinetics of growth for each passage based on the parameters obtained from passage one after hMSC isolation from an individual patient. The intention of generating such tool is to forward predict the overall cell expansion process time for each individual patient. The validity of the model was tested with hMSC isolated from three different donors, and proven to be accurate in all cases. The specific objectives of the work are:

- To establish a mathematical model for hMSC growth kinetics.
- To generate quantitative values for model kinetic parameters based on an established mathematical model.
- By using cells from different sources show how model kinetic parameters vary with passage / donor.

- Finally demonstrate accurate forward prediction of the growth rate of cells from different donors over multiple passages as well as examining the surface marker expression of hMSC throughout the expansion process.

5.2 Development of Mathematical Model for Cell Growth Quantification

Diploid mammalian cells cultured without nutrient limitations undergo three distinct phases of growth: a lag phase, exponential growth, and stationary phase (Hayflick et al., 1961). One of the main parameters to characterise the growth of mammalian cell cultures *in vitro* is the growth rate. Growth rate is usually calculated from the slope of the exponential phase when plotted on a logarithmic scale. Unlike suspension cultures, anchorage dependent cells such as hMSC have growth curves that do not always exhibit three clear regions, attributed to lag, exponential, and stationary phases (Freshney, 1994). There are several reasons for this phenomenon, one of them being the difficulty in acquiring cell density readings. Cell suspension samples can easily be withdrawn from a shake flask or stirred-tank bioreactor without disruption of the rest of the culture in the vessel. However, the only way to determine cell densities for anchorage dependent cells is to sacrifice the culture vessel by enzymatic detachment of the cells from the surface. In order to collect sufficient time points to generate a growth curve, several culture vessels must be seeded in parallel to support sacrifice of the culture and collection of data at all the time points at which samples will be collected.

For the specific case of hMSC, the low number of cells available after their separation from bone marrow samples (1 in $1x10^7$ to 10^8 cells from a bone marrow sample is a hMSC (Reyes et al., 2001; Silva et al., 2003)), makes the generation of growth curves very challenging. The number of cells available to conduct an experiment with hMSC that have not undergone several doublings is very limited, and therefore makes it difficult to seed many parallel culture vessels, especially when several sets of analysis requiring a high number of cells are usually required. For example, surface marker characterisation by flow cytometry. This, accompanied by the long culture time for hMSC that can extend for up to 25 days, requires a large amount of cells seeded in parallel, allowing

sacrificial samples to be taken over such a long period of time. Consequently, it is not always possible to generate growth curves revealing cell density readings taken on a daily basis. Even when enough data points are analysed to generate a cell growth curve, the resulting data make it difficult to determine the points that mark the start and end of the exponential growth phase for growth rate and doubling time calculations. This can be seen, for example, in the growth curves generated in Figure 4.2, and subjective judgments are often required to calculate such parameters. The same problem occurs when trying to determine the duration of the lag phase and time to reach stationary phase.

To eliminate ambiguity and to help determine accurate growth rates, doubling times, and duration of the lag phase that characterise hMSC growth, it is of great interest to adopt a mathematical model that would accurately represent the shape of the growth curve. The Gompertz model has been used to accurately characterise cell growth kinetic parameters, such as growth rate and maximum cell density at stationary phase, while accounting for the duration of the lag phase, and the time needed to reach maximum cell densities.

The Gompertz model (Melero-Martin, 2004) not previously used with hMSC is described by the following equation:

$$X = X_0 + a \cdot \exp\left(-\exp\left(\frac{-(t - t_o)}{b}\right)\right) \qquad 5.1$$

Where X is the cell density, X_0 is inoculation cell density, a is the increase in cell density (all in cells/cm^2), t is time, t_0 is related to the duration of the lag phase, and b is related to the duration of the exponential phase.

The graphical representation of the model kinetic parameters generated by the Gompertz model is shown in Figure 5.1.

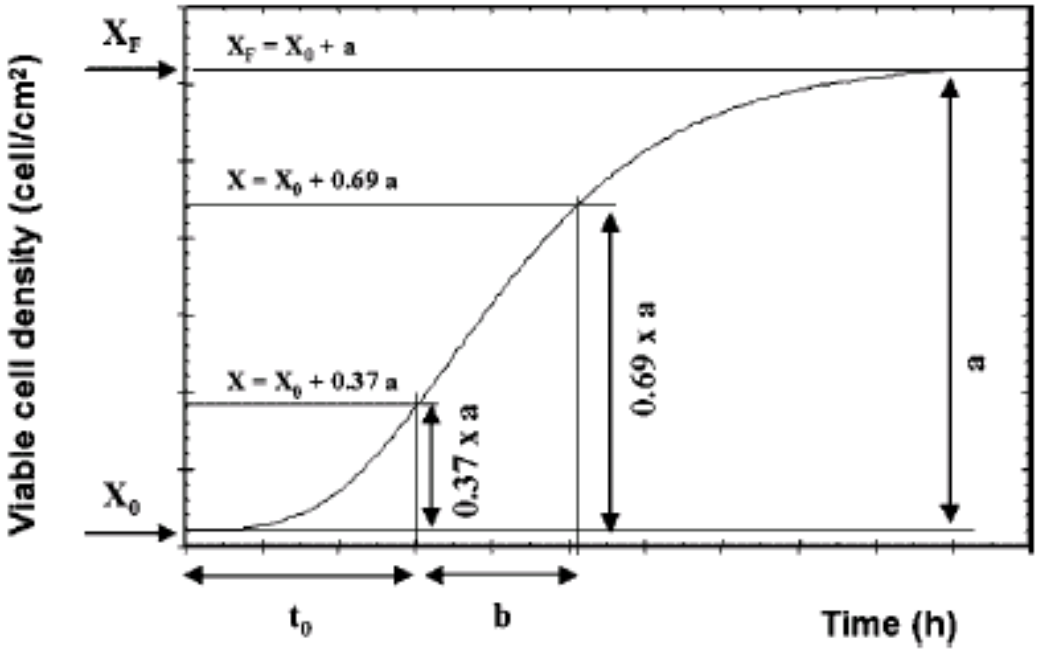

Figure 5.1 Schematic representation and approximate qualitative meaning of a four parameters generalisation of the Gompertz function [Equation 5.1] in relation to the growth curve of a hypothetical culture of cells. (figure reproduced from Melero-Martin et al., 2005)

From the parameters given by Equation 5.1, more accurate values for the model kinetic parameters than the approximations shown on Figure 5.1 can be calculated. Maximum growth rate can be obtained from the first derivative of Equation 5.1 at the point of inflection, and the lag time can be calculated as the intercept of the inflection line through the *t* axis (Zwietering et al., 1990). From this mathematical analysis, growth rate (μ) and lag time (λ) are calculated by Equations 5.2 and 5.3 where *e* is *exp*(1) and *X*max is the maximum viable cell density reached at the stationary phase of growth.

$$\mu = \frac{\ln\left(X_{\max} / X_0\right)}{e \cdot b} \qquad 5.2$$

$$\lambda = t_0 - b \qquad 5.3$$

To illustrate the advantage of using this mathematical model to determine cell growth characteristics a hMSC growth curve was generated with cells from Passage 1 in 24 well-plates. The experimental data is shown in Figure 5.2.

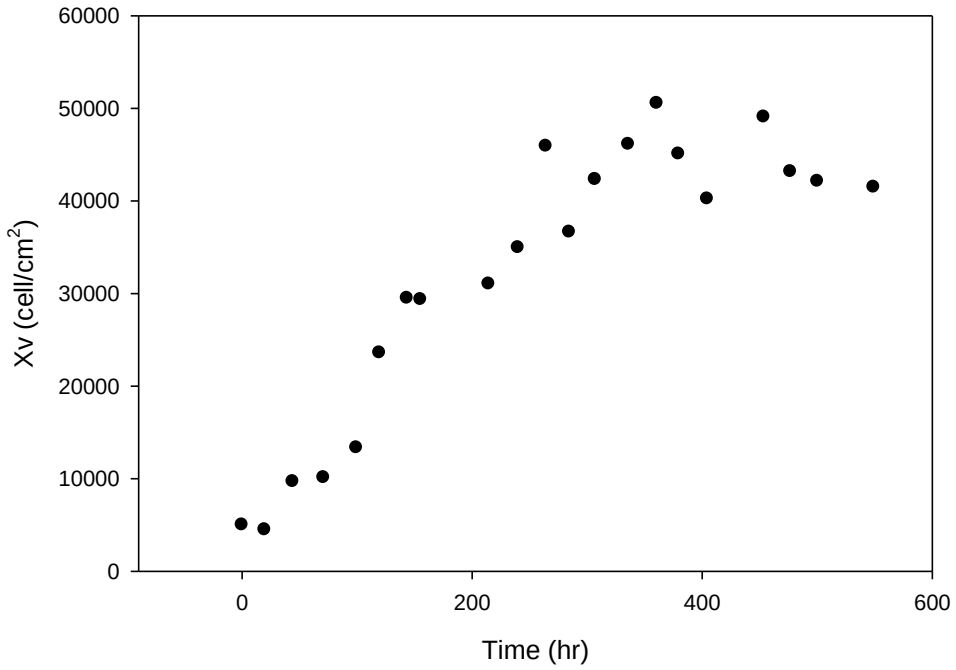

Figure 5.2 Typical cell growth curve generated from hMSC seeded at $5x10^3$ cells/cm^2 in 24 well-plates at Passage 1 with daily medium exchanges. Experiments performed as described in Section 2.4.

Calculating growth rates using Equation 2.5 requires the process operator or scientist to decide which point will mark the beginning of the exponential phase and which one will determine the end. If no growth curve had been generated, and only initial and final cell densities were available as it is the case with data obtained when passaging T-flasks i.e. much of the information currently available in the literature, the resulting growth rate from this culture would have been calculated as 0.15 day^{-1} or a doubling time of 114 hr. This calculation ignores the length of time when the cells remained in lag phase or stationary phase. However, having generated the cell growth curve, it is a subjective decision to pick the duration of the exponential phase. Table 5.1 indicates a series of possibilities in the selection of such data points and the growth rates and doubling times regenerated from each one of such selections.

Table 5.1. Calculation of cell growth rates and doubling times for the typical hMSC growth curve shown in Figure 5.2, based on different selections of initial and final time points of the exponential cell growth phase. The pair of points chosen as (a, b) indicate the initial (a) and final (b) points selected for each calculation. The numerical value for a and b indicate the order of the points on the cell growth curve, where 1 is the first time point of the curve at inoculation and 21 is the final point on the graph as the last time point collected for the growth curve.

Initial and Final Points Chosen to Define Exponential Growth Phase (a, b)	**Initial Point Values (X_0 (cells/cm^2) , t_0 (hr))**	**Final Point Values (X_f (cells/cm^2) , t_f (hr))**	**μ (day^{-1})**	**Td (hr)**
(2, 7)	(4491, 19.8)	(29474, 143)	0.365	45.5
(2,12)	(4491, 19.8)	(36632, 285)	0.190	87.4
(4,11)	(10105, 70.9)	(45895, 264)	0.187	88.6
(4,12)	(10105, 70.9)	(42315, 307)	0.145	114.3

As indicated in Table 5.1, different selection of the initial and final time points that determine the beginning and end of the exponential growth phase in a cell growth curve may result in different cell growth rate and doubling time values. The decision on what value best represents the growth kinetics of the culture lays on the subjective opinion of the bioprocess engineer, and it is dependent also on the number of time points collected during the generation of the cell growth curve and on the intrinsic variability of the data.

When fitting a 4-parmeter sigmoidal Gompertz model to the data shown on Figure 5.2, a more objective determination of growth characterisation parameters can be obtained. Figure 5.3 shows the same cell growth curve fitted to a Gompertz model. The parameters generated by the mathematical fit can then be utilised to calculate cell growth rates and doubling times.

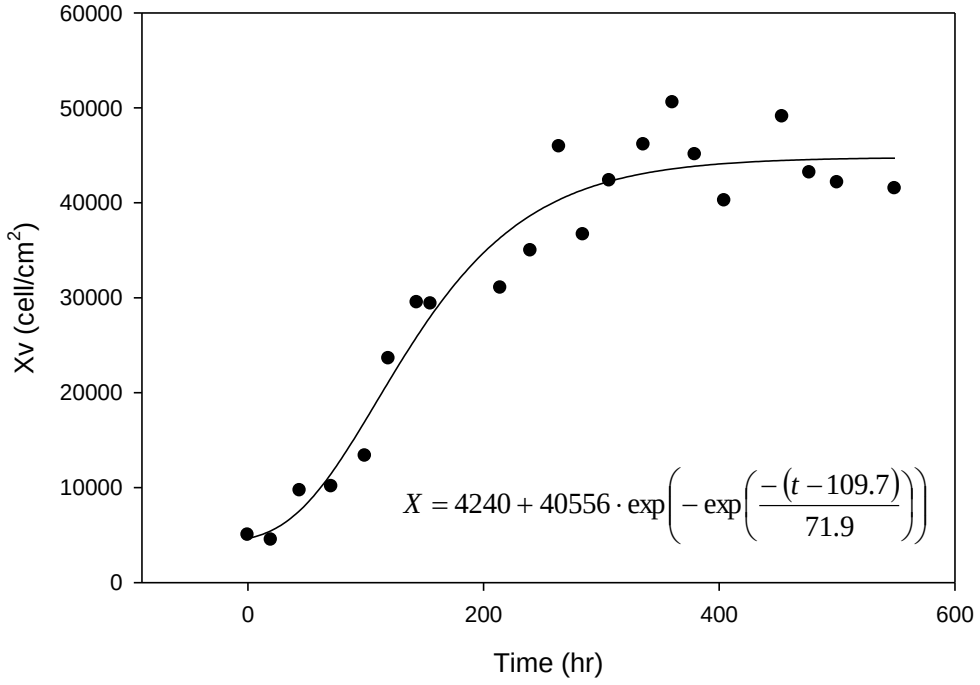

Figure 5.3. Typical cell growth curve (circles) generated from hMSC seeded at $5x10^3$ cells/cm^2 in 24 well-plates at Passage 1 with daily medium exchanges. Solid line represents best fit of the four-parameter Gompertz model. The resulting equation generated by the fit is shown in the inset. Experiments performed as described in Section 2.4. Model fitted to data as described in Section 2.13.

From the mathematical equation obtained from the fit shown in Figure 5.3, the four parameters generated by non-linear regression analysis executed in SigmaPlot 10.0 ($X_{0,}$ 4240, a 40556, t_0 109.7, and b 71.9) were used to calculate a cell growth rate of 0.28 day^{-1} or doubling time of 60 hours,. As can be seen by the fit (solid line) on Figure 5.3, this equation closely represents the growth behaviour of the culture and the quantitative data obtained from it did not require subjective manipulation of the data. This method has been used to calculate cell growth rates towards the work generated for this thesis as indicated in previous Chapters, except for the cases on which only initial and final cell densities were generated for a passage.

5.3 Development of a Modified Gompertz Model to Forward Predict hMSC Growth Kinetics

The intrinsic hMSC growth characteristics that are only dependent on the donor makes it hard to forward predict the duration of the cell expansion process required to achieve the required number of cells for a given therapeutic application (Phinney, 1999). In addition, there is a decrease in the speed at which the cells double as the passage number progresses. However the rate at which the cell growth rate decreases with increasing cell doublings has not previously been quantified.

To address the possibility of finding a pattern in the cell growth kinetic parameters as the age of the culture progresses during a cell expansion process, isolated hMSC from one donor were cultured over 5 sequential passages. A cell growth curve was generated for each individual passage, and Gompertz models were generated for each curve without any parameter constrain on $X_{0,}$ a, t_0, and b. From each passage, the Gompertz model provided a value for each of the four variable coefficients, $X_{0,}$ a, t_0, and b.

From the four coefficients obtained from each mathematical fit, an analysis of the variation of each of these four parameters obtained over subsequent passages enabled a correlation of how these values change over time. Analysis of the variation of these parameters over passage resulted in a modified Gompertz model that can be used to forward predict hMSC growth over sequential passages.

Cell growth curves generated from this patient's isolated hMSC with the Gompertz model for Passages 1, 3, and 5 are shown in Figures 5.4 through 5.6 to illustrate some of the data collected throughout the cell expansion process. Data from Passage 4 was collected but is not shown for purposes of clarity. The parameters generated from the Gompertz model each passage from 0 to 5 are listed in Table 5.2.

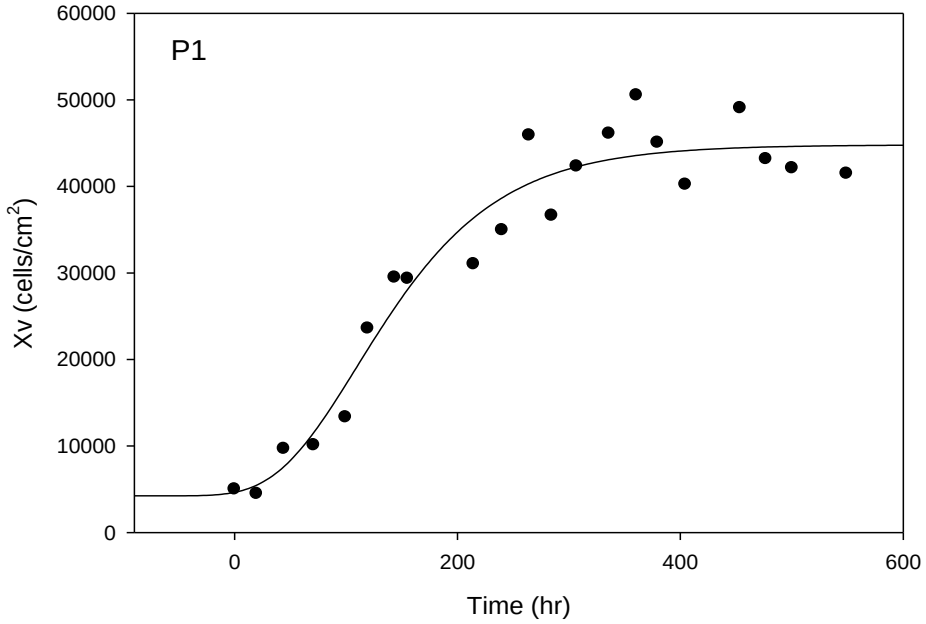

Figure 5.4 Cell growth curve (circles) for hMSC at Passage 1, seeded in 24 well-plates at an inoculation cell density of $5x10^3$ cells/cm^2 with daily medium exchanges. Solid line represents best fit of the four-parameter Gompertz model. Experiments performed as described in Section 2.4. Model fitted to data as described in Section 2.13.

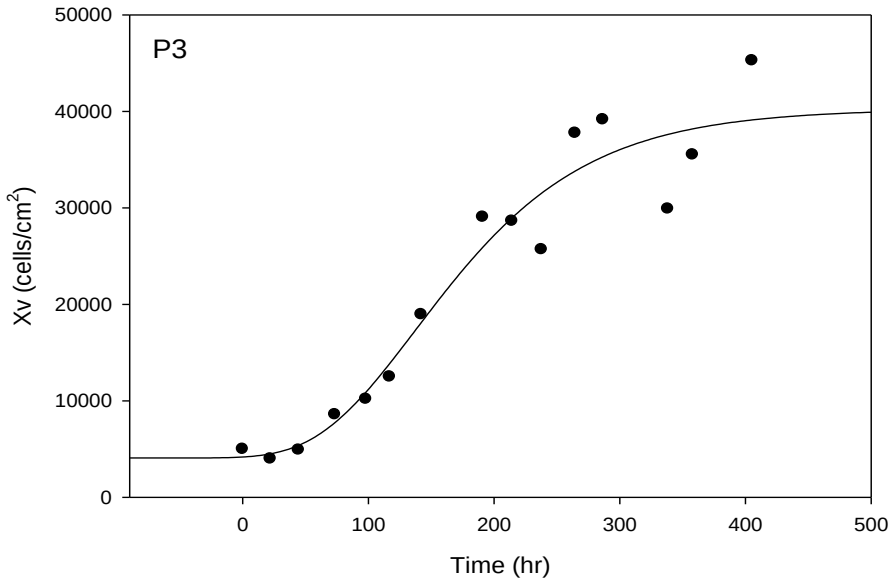

Figure 5.5 Cell growth curve (circles) for the same hMSC source as shown in Figure 5.4 at Passage 3, seeded in 24 well-plates at inoculation cell density of $5x10^3$ cells/cm^2 with daily medium exchanges. Solid line represents best fit of the four-parameter Gompertz model. Experiments performed as described in Section 2.4. Model fitted to data as described in Section 2.13

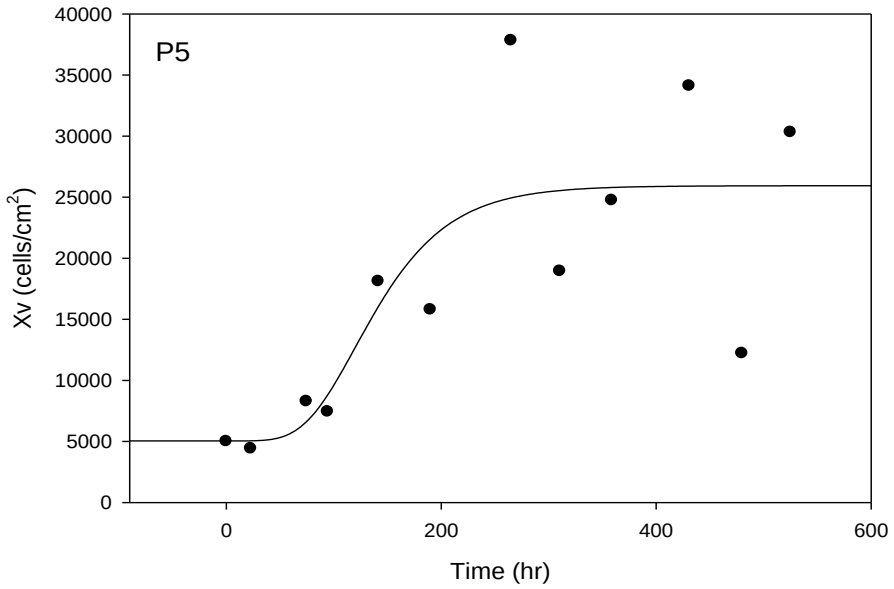

Figure 5.6 Cell growth curve for the same hMSC source than the ones shown in Figure 5.4 at passage five, seeded in 24 well-plates at inoculation cell density of $5x10^3$ cells/cm^2 with daily medium exchanges. Solid line represents best fit of the four-parameter Gompertz model. Experiments performed as described in Section 2.4. Model fitted to data as described in Section 2.13

As shown in Section 3.6, the cell growth decreases with every passage along with the number of cells reaching stationary phase. For this particular donor it is also noticeable that an increase in the variability of the data occurs between consecutive time points as the passage number increases and towards the final points of each growth curve. This may be due to seeding volume variations due to manual manipulations, and that being the case, this seeding density differences will be more noticeable as the culture progresses. Such variability would be greatly reduced by the use of automation, where a liquid handling system ensures accurate volumes of cell suspension dispensed into each individual well (Nealon et al., 2005).

Table 5.2. Calculated values of the kinetic parameters *a*, *b*, t_0, and X_0, from the Gompertz model(Equation 5.1) fitted to hMSC growth curves from a common donor expanded sequentially from Passage zero (P_0) to Passage 5 (P_5). Experimental data and model fits shown in Figures 5.4 to 5.6.

	P_0	**P_1**	**P_3**	**P_4**	**P_5**
a	42510	40556	36180	29073	20893
b	37.8	71.9	77.7	64.5	48
t_0	77.3	109.7	137.8	123.6	120
X_0	3845.8	4240.8	4074.8	4156	5043

Because passage number has been taken as a time parameter, or an indicator of the age of the culture, it was important first of all to understand if an increase in passage number could be correlated to intrinsic changes in the culture such as cumulative population doublings since these more accurately indicate culture age. From the values obtained for the Gompertz model for final cell density for *a* and X_0, as shown in Table 5.2, cumulative population doublings were calculated at the end of each passage following Equation 2.8. A good linear correlation between passage number and cumulative population doublings was found as shown in Figure 5.7. Another linear relationship could be found when comparing passage number with the maximum cell density attained on each passage, as shown in Figure 5.8.

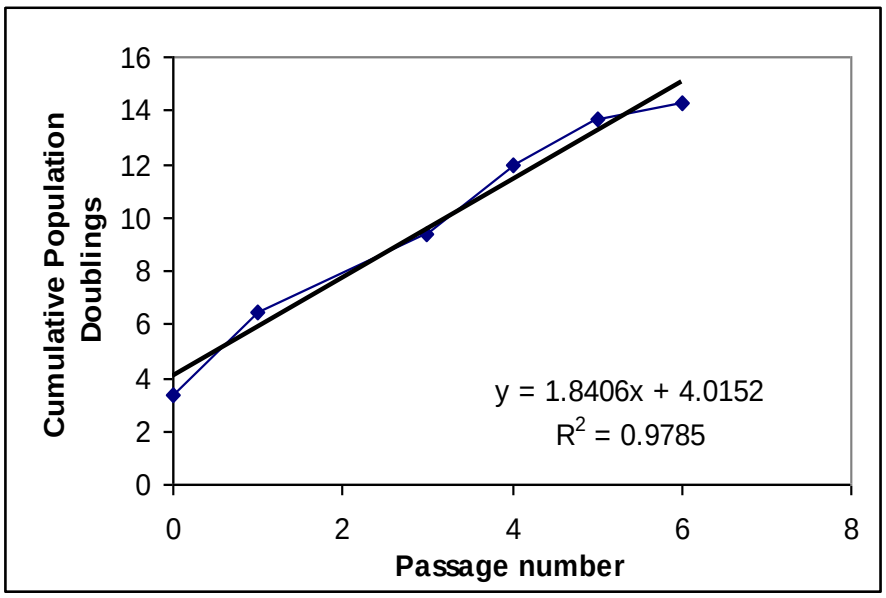

Figure 5.7 Relationship between passage number and experimentally determined cumulative population doubling (circles)for hMSC expanded through six passages. As the passage number increases the cumulative population doublings increase in a linear relation (solid line) expressed by the equation on the figure inset. Solid line fitted by linear regression.

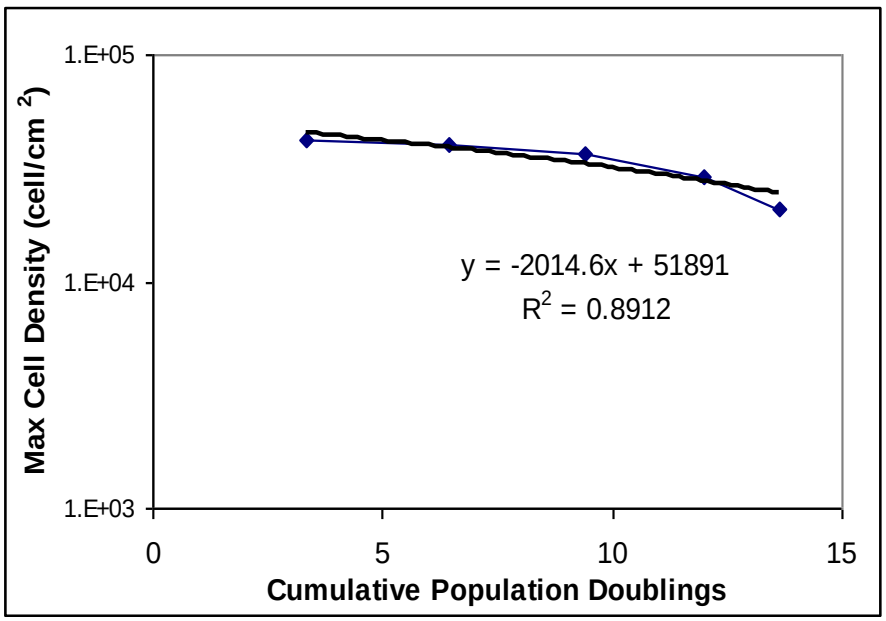

Figure 5.8 Relationship between Population Doublings and Maximum Cell Density. for hMSC expanded through six passages. As cumulative population doubling increases the maximum cell density at the stationary phase decreases in a linear relation expressed by the equation on the Figure.

Based on the two correlations shown in Figures 5.7 and 5.8, maximum cell density can then be correlated to cumulative population doublings at any point in the culture, which in turn can be correlated to passage number. From these correlations and from looking at Table 5.2, some observations can be made about the variation of the Gompertz model kinetic parameters over each passage or as the population doublings increase. First of all, parameter *a*, which represents the increase in cell density follows a trend that can be expressed as:

$$a = -2014\,(1.84 \times P_n + 4.01) + 51891 \qquad 5.4$$

Also, model kinetic parameters *b* and t_0 have similar values from P_1 to P_5, but vary significantly for P_0. For this particular donor, the values obtained for *b* averaged to 65.5 with a standard deviation of 12.8 from P_1 to P_5, with a value of 37.8 for P_0. As for the value for the coefficient t_0, the same trend is observed with an average of 122 with a standard deviation of 11.6 from passages P_1 to P_5 but a lower value of 77.3 for P_0.

The values for initial cell density X_0 did not vary greatly between passages and no clear trend was observed. This value tends to be lower than the targeted ICD for all cell growth curves generated. It may be due to a percentage of cells failing to attach to the culture vessel upon inoculation, and being removed during the removal of the spent medium while harvesting the vessel for cell number determination (Section 2.6).

Based on these observations, a modified mathematical model for the variation of the Gompertz model kinetic parameters over time was developed. The relationship found for *a* cannot be applied to other donors because the coefficients for Equation 5.4 were dependent on knowing the parameters for the mathematical equations of all sequential passages for that specific donor only. However, approximations that would reflect the same behaviour of these kinetic model parameters over time based on the known coefficients for P_0 only were selected. The selection of the equations that would describe the modification of these parameters over sequential passages for any given donor are based on the analysis of the coefficients obtained for sequential passages from the empirical data shown in this section. The mathematical expressions chosen as to

approximate future behaviour of the four Gompertz model kinetic parameters from known values at P_0 generated a modified Gompertz model that closely represents the unmodified Gompertz equation as shown in Figures 5.9 to 5.11.

Approximations for the variation of the four kinetic parameters for the Gompertz model only for passages above zero as a function of known parameters generated for this passage, were then established as:

$$a = a_{P_0} - \left(\frac{a_{P_0}}{10} \cdot p_n \right) \quad 5.5$$

$$t_0 = 10 \cdot P_n + t_{0P_0} \quad 5.6$$

$$b = b_{P_0} \quad 5.7$$

$$X_0 = X_{0P_0} \cdot 0.85 \quad 5.8$$

Where a_{Po} represents the Gompertz coefficient from passage zero, P_n is the passage number, t_{0Po} is the Gompertz coefficient t_0 at passage zero, b_{Po} is the Gompertz coefficient b at passage zero, and X_{0Po} is the inoculation cell density (ICD). Equation 5.5 was chosen as a close approximation for Equation 5.4, based only on terms of known values from passage zero with passage number as the only variable in the equation. Equation 5.6 and 5.7 were chosen knowing that these two parameters contribute to express the duration of the lag phase. Since *b* was the coefficient with less increase over the value recorded at passage zero, it was taken as constant for subsequent passages. The off-set that this approximation may cause for the duration of the lag phase was taking into consideration by increasing t_0 progressively as a function of the passage number. Equation 5.8 was chosen so as to account for a notional 15% loss of cells after inoculation for all passages from the initial inoculation cell density. It is important to highlight that due to the strong dependency of the model to the parameters obtained from data collected during passage zero, a full characterised growth curve must be determined for this passage in order to obtain representative parameters. The parameters returned from a Gompertz fit for

passage zero must be obtained from a set of data that includes numerous time point cell density determination collected for close time intervals.

Table 5.3. Modified values of the kinetic parameters *a*, *b*, t_0, and X_0, from the Gompertz model(Equation 5.1) to forward predict hMSC growth curves from a common donor expanded sequentially from Passage zero (P_0) inoculated with $5x10^3$ cells/cm^2 to Passage 5 (P_5). Parameters calculated from equations 5.5 to 5.8 from coefficients for Passage zero (P_0) shown in Table 5.2. Experimental data and model fits shown in Figures 5.4 to 5.6.

	P_0	**P_1**	**P_3**	**P_4**	**P_5**
a	42510	38259	36180	29073	20893
b	37.8	37.8	37.8	37.8	37.8
t_0	77.3	87.3	107.3	117.3	127.3
X_0	3845.8	4250	4250	4250	4250

This modified Gompertz model was first tested against the data that was used to generate the model, as shown in Figures 5.4 to 5.6. These approximations chosen for the four coefficients of the Gompertz equation (Table 5.3) resulted in new model predictions (shown as discontinued lines in Figures 5.9 to 5.11), closely representing the data as well as the Gompertz models generated from empirical data shown as a continuous line. It appears that it is possible to accurately correlate how model kinetic parameters will vary over subsequent stages of expansion.

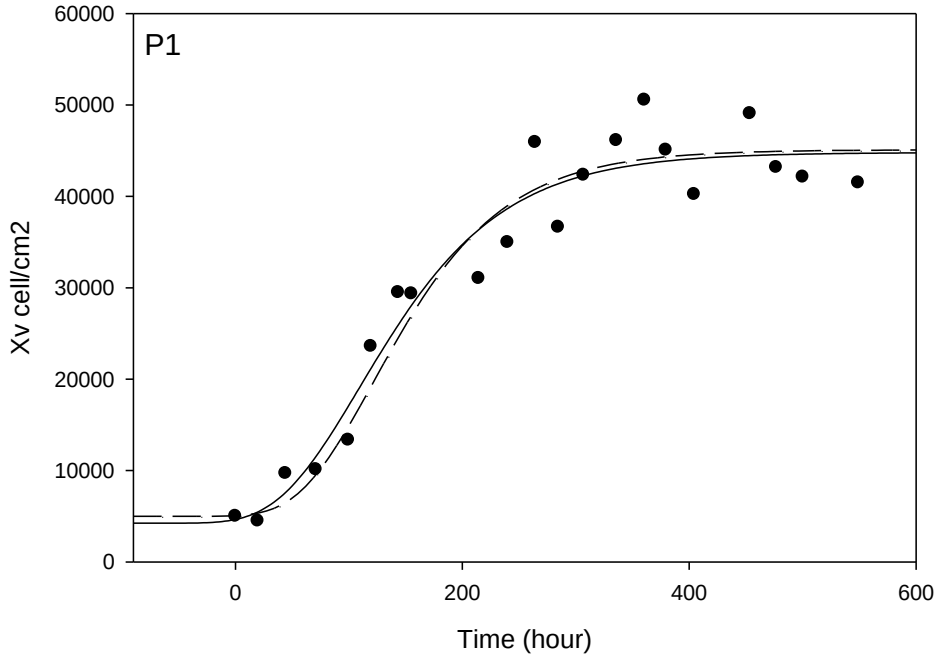

Figure 5.9 Cell growth curve (circles) for hMSC at Passage 1, seeded in 24 well-plates at an ICD of $5x10^3$ cells/cm^2 with daily medium exchanges. The data is fitted with a Gompertz model (solid line), as well as the modified Gompertz equation (dashed line) with parameters calculated through Equations 5.5-5.8.

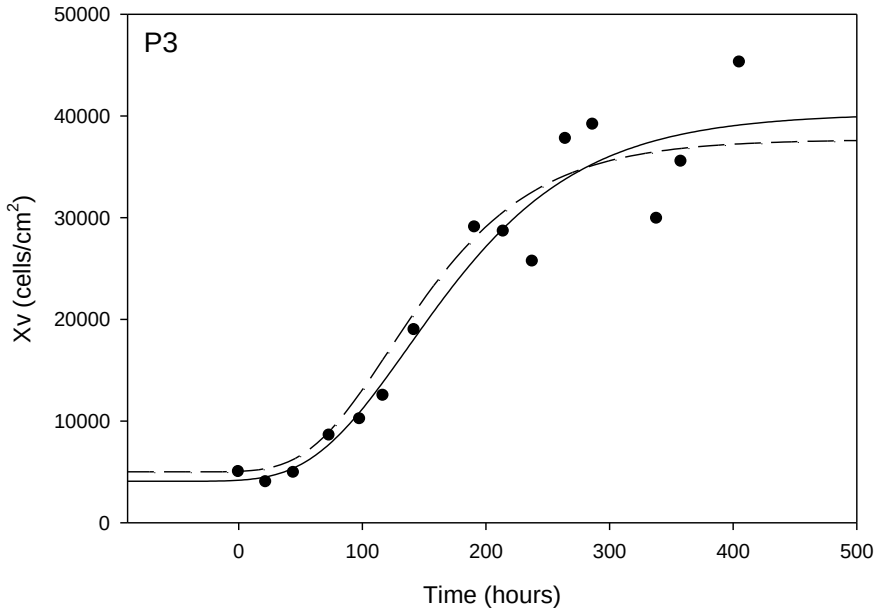

Figure 5.10 Cell growth curve for hMSC at passage three from the same cell source as the cells used at passage one for Figure 5.9. The data is fitted with a Gompertz model (solid line), as well as the modified Gompertz equation (dashed line) with parameters calculated through Equations 5.5-5.8.

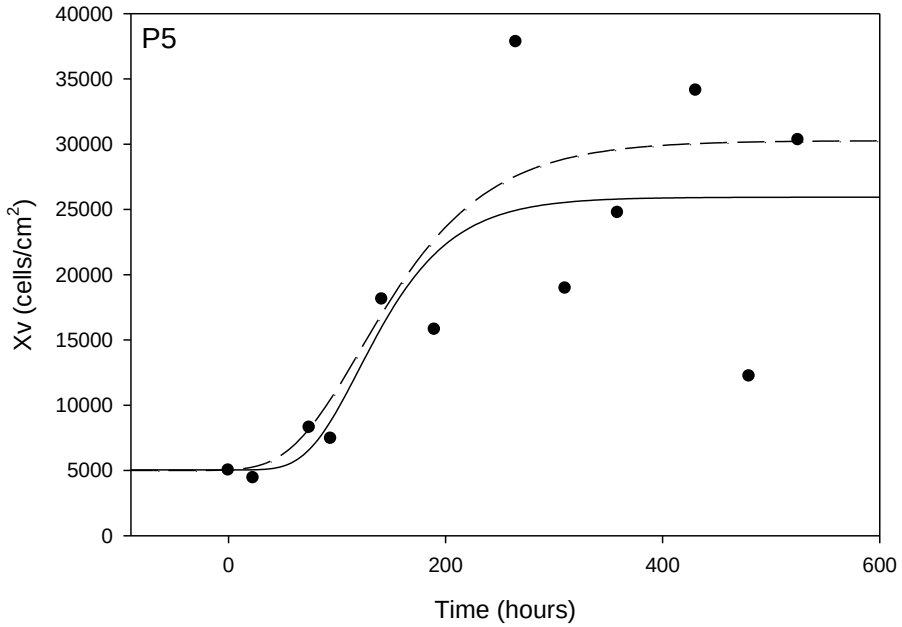

Figure 5.11 Cell growth curve for hMSC at passage five from the same cell source as the cells used at passage one for Figure 5.9. The data is fitted with a Gompertz model (solid line), as well as the modified Gompertz equation (dashed line) with parameters calculated through Equations 5.5-5.8.

5.4 Patient Specific Forward Prediction of hMSC Expansion Process Kinetics

A mathematical expression based on a Gompertz model was developed to describe hMSC growth behaviour for sequential passages in Section 5.4. This mathematical expression used correlations for each one of the four coefficients of the Gompertz equation as a function of the increase in passage number throughput the cell expansion process for hMSC. The model was compared over the data used to generate this approximated mathematical expression and it was proven to generate cell growth curves that closely matched the empirical data.

For this modified model to be proven successful it was necessary to forward predict cell growth behaviour of hMSC over sequential passages under a given set off environmental condition of processing parameters. Two further bone marrow samples (section 2.1) from different donors were used for this further experimentation. The goal is to isolate hMSC from a donor and generate a cell

growth curve during P_0. From this cell growth curve, the four Gompertz model kinetic parameters can be obtained. Based on this information, the modified equation developed in Section 5.3 should be able to forward predict the shape of the cell growth curves that could be generated during sequential passages from that same cell source. This information will allow for process bioprocess engineers to determine the duration of the cell expansion process, as well as the number or passages required to reach the target cell number. After this is calculated, future arrangements for the delivery of the final product can be scheduled along with the hospitalisation of the patient that awaits the implantation of these cells or for the tissue engineered organ generated from them. The flow diagram in Figure 5.12 demonstrates this procedure in detail.

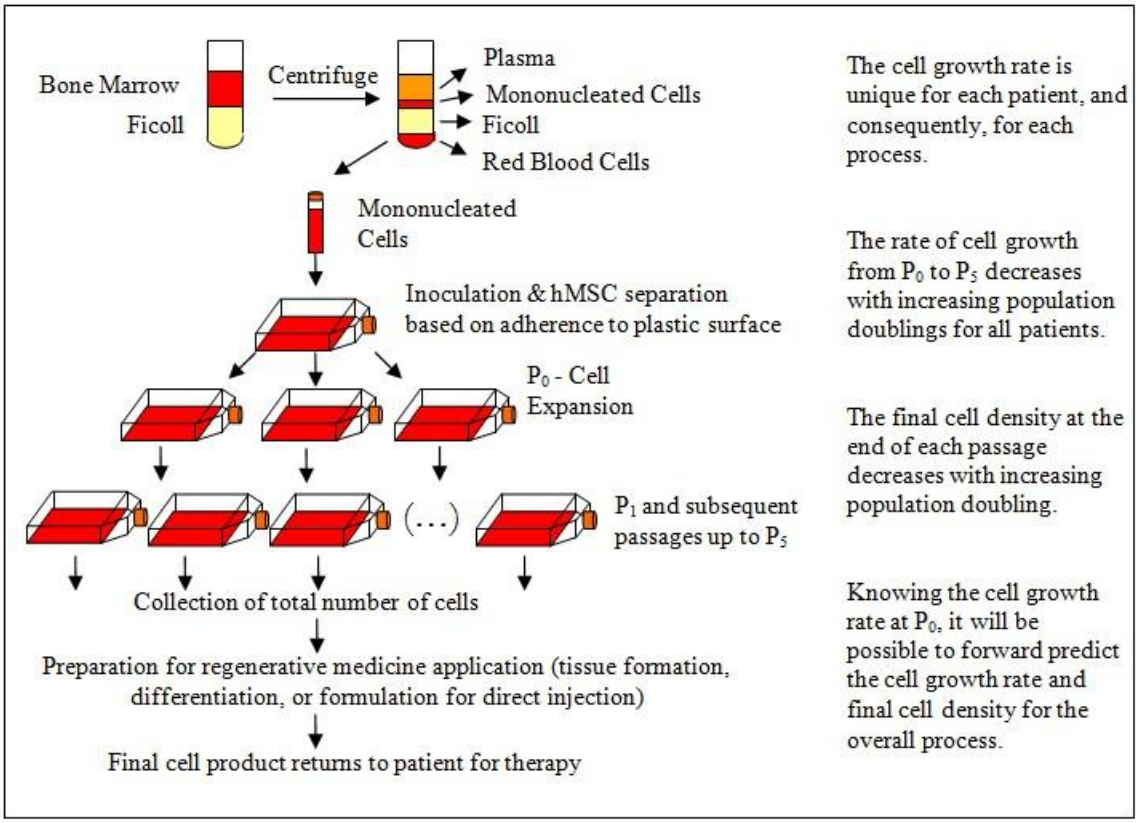

Figure **5.12.** Flow diagram for the cell expansion process of autologous hMSC isolated from bone marrow for regenerative medicine therapy. The main trends observed during sequential passaging of the culture are highlighted on the right hand side of the figure, along with the application of the model developed in Section 5.3 for this process.

The process diagram indicated in Figure 5.12 was followed with two different donors labelled as Donor C and Donor A (Data from donor A also shown in Section 3.6, figures 3.6 to 3.10). From each donor, cell growth curves were generated at P_0 and Gompertz models were applied to the data to generate the first four coefficients that determine the kinetics of growth for that passage the same way than detailed in Section 5.3. Once these first coefficients were obtained, the mathematical approximations stated in Equations 5.5 through 5.8 were used to generate Gompertz models for subsequent passages. The results from this exercise for the two donors are shown in Figures 5.13 and 5.15. To validate the results, cell growth curves were generated for sequential passages and the empirical data was added to the forward predicted cell growth curves. Those results are shown in Figures 5.14 and 5.16.

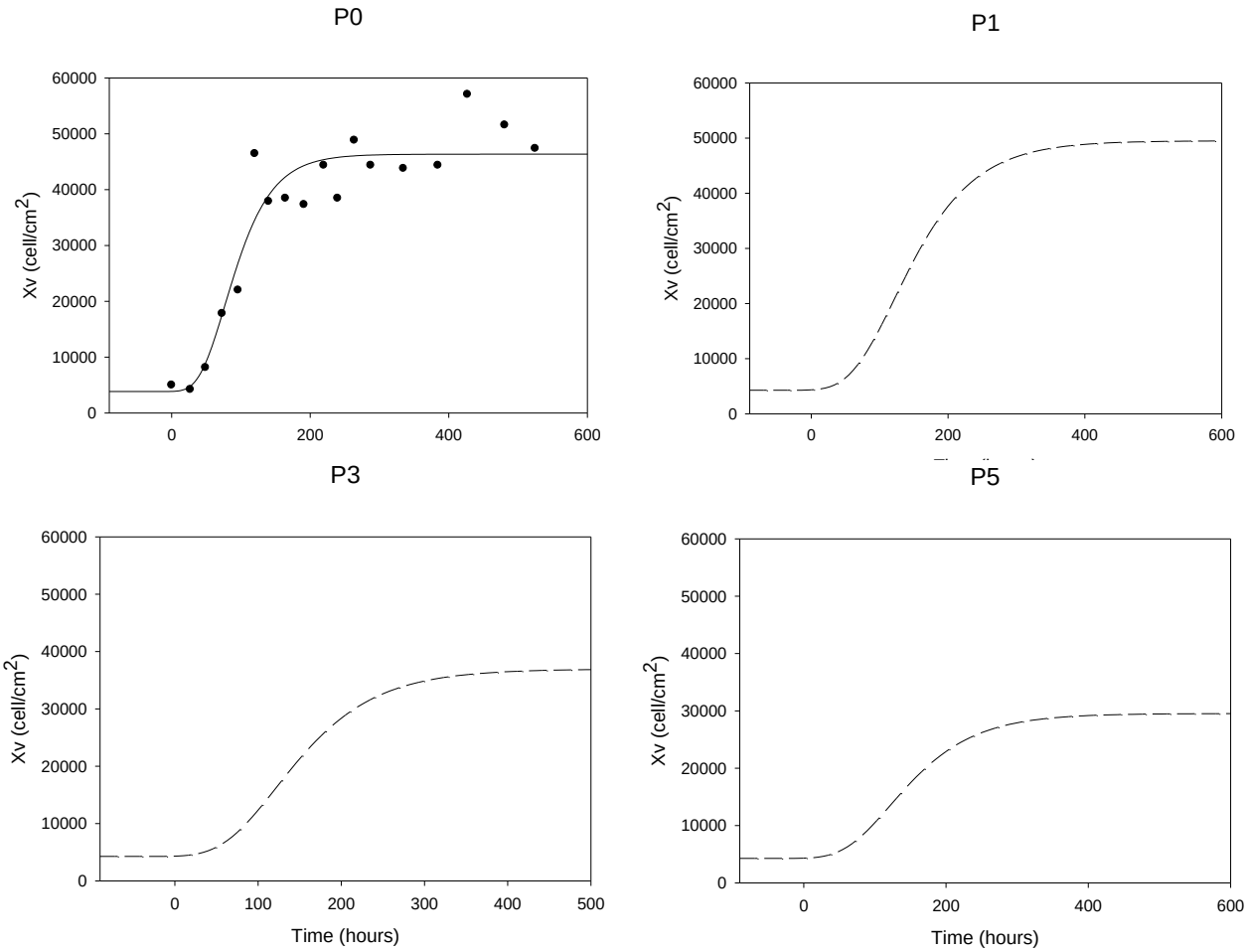

Figure 5.13. Forward prediction of hMSC growth kinetics during the cell expansion process in 24 well-plates for Patient C. Cell growth curves for P0, P1, P3, and P5 have been predicted based on the modified Gompertz model as indicated in Section 5.3. The cell growth curve generated for P0 shows the empirical data (circles) collected during the first passage of hMSC after isolation. This data is first fitted (solid line) with the Gompertz model (Equation 5.1) to determine patient specific hMSC growth kinetic parameters. The model coefficients obtained from this fit were then used to forward predict the growth curves for subsequent passages (dashed lines) following Equations 5.1 and 5.5 through 5.8.

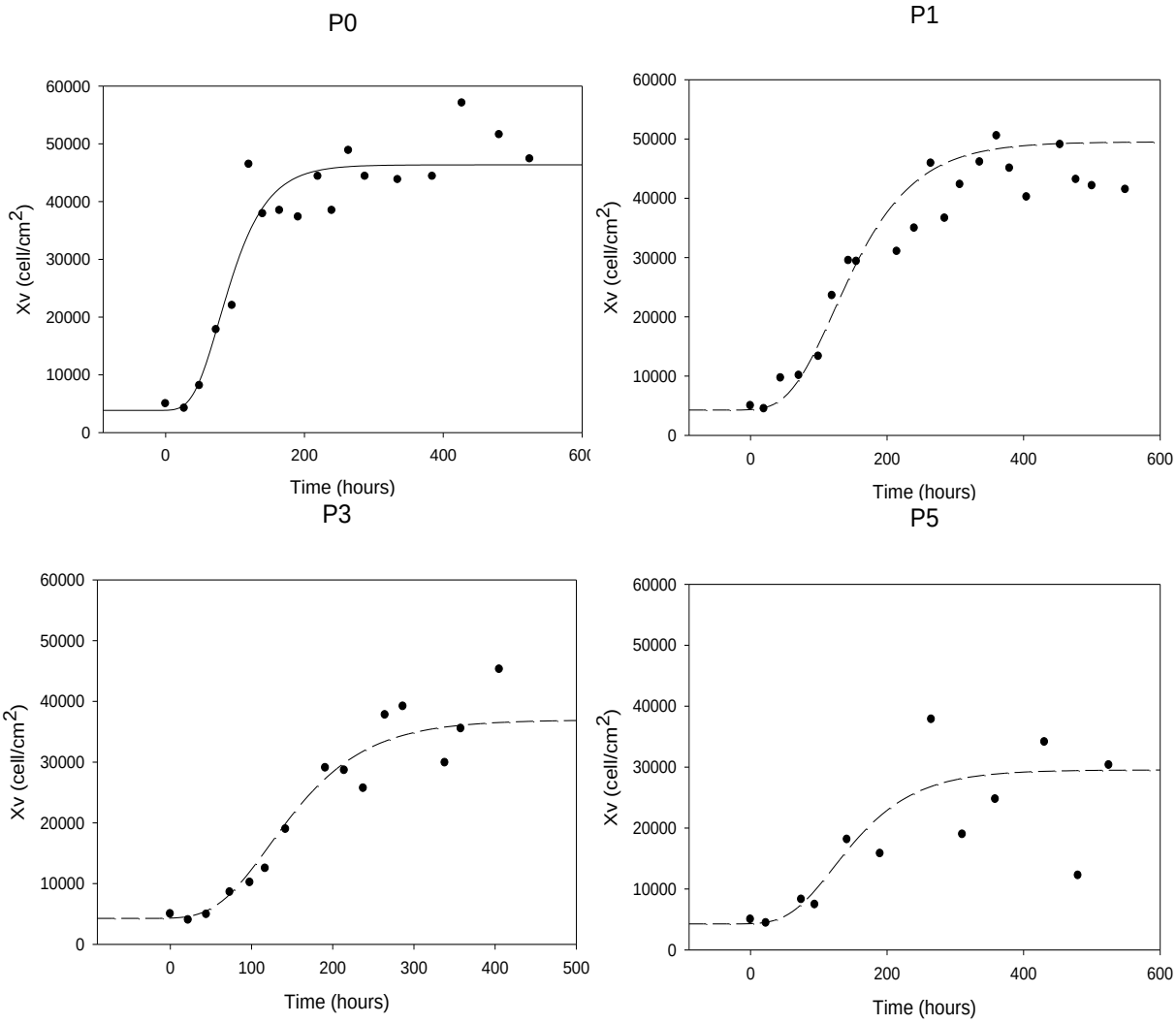

Figure 5.14 Agreement of forward predicted (dashed lines) cell growth kinetics with subsequently obtained experimental data (circles) for the prediction of hMSC growth kinetics during the cell expansion process in 24 well-plates for Patient C compared to empirical data obtained for subsequent passages of growth. The developed modified mathematical model is shown by discontinued lines. A Gompertz equation fitted through the data obtained during P0 is shown by a continuous line.

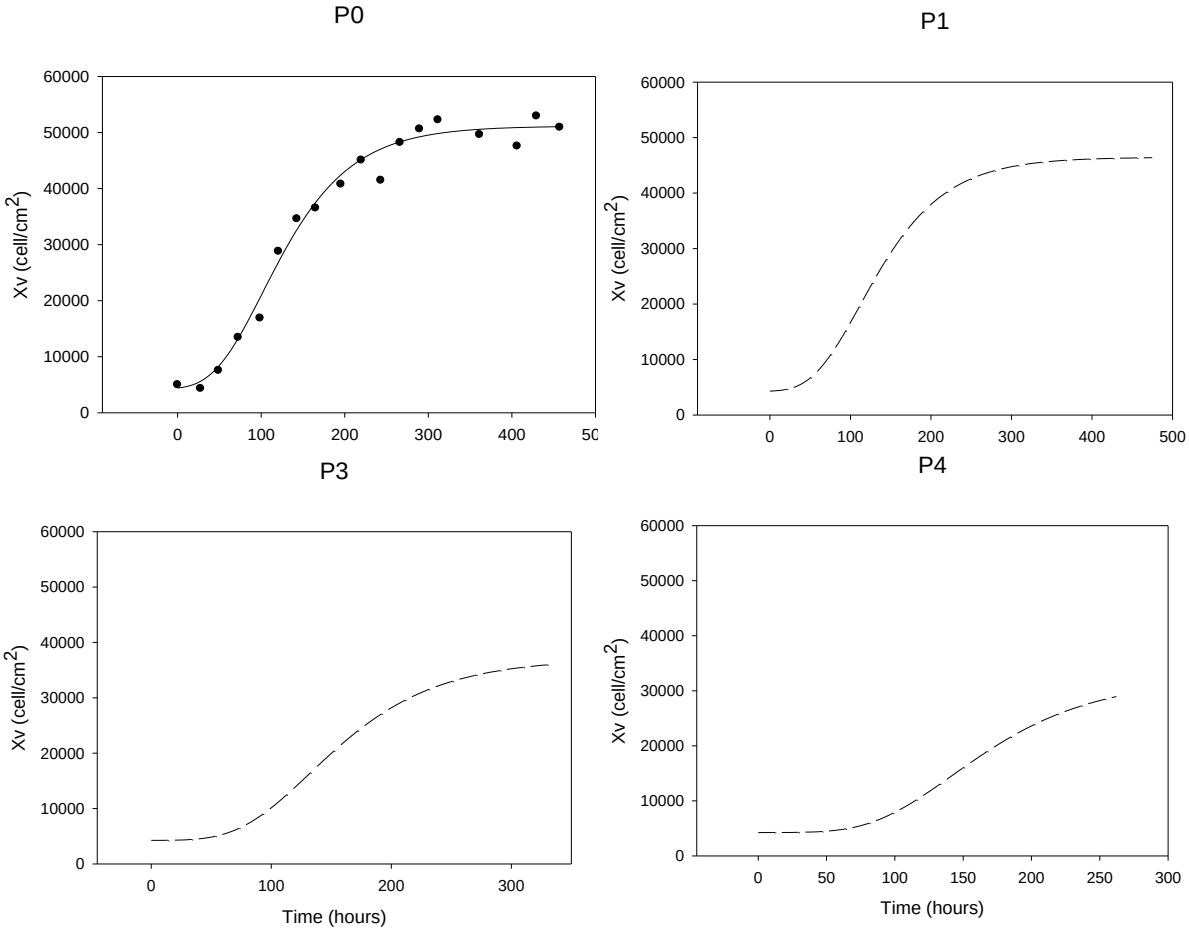

Figure 5.15 Forward prediction of hMSC growth kinetics during the cell expansion process in 24 well-plates for Patient A. Cell growth curves for P0, P1,P3 and P4 have been predicted based on the modified Gompertz model as indicated in Section 5.3. The cell growth curve generated for P0 shows the empirical data (circles) collected during the first passage of hMSC after isolation. This data is first fitted (solid line) with the Gompertz model (Equation 5.1) to determine patient specific hMSC growth kinetic parameters. The model coefficients obtained from this fit were then used to forward predict the growth curves for subsequent passages (dashed lines) following Equations 5.1 and 5.5 through 5.8.

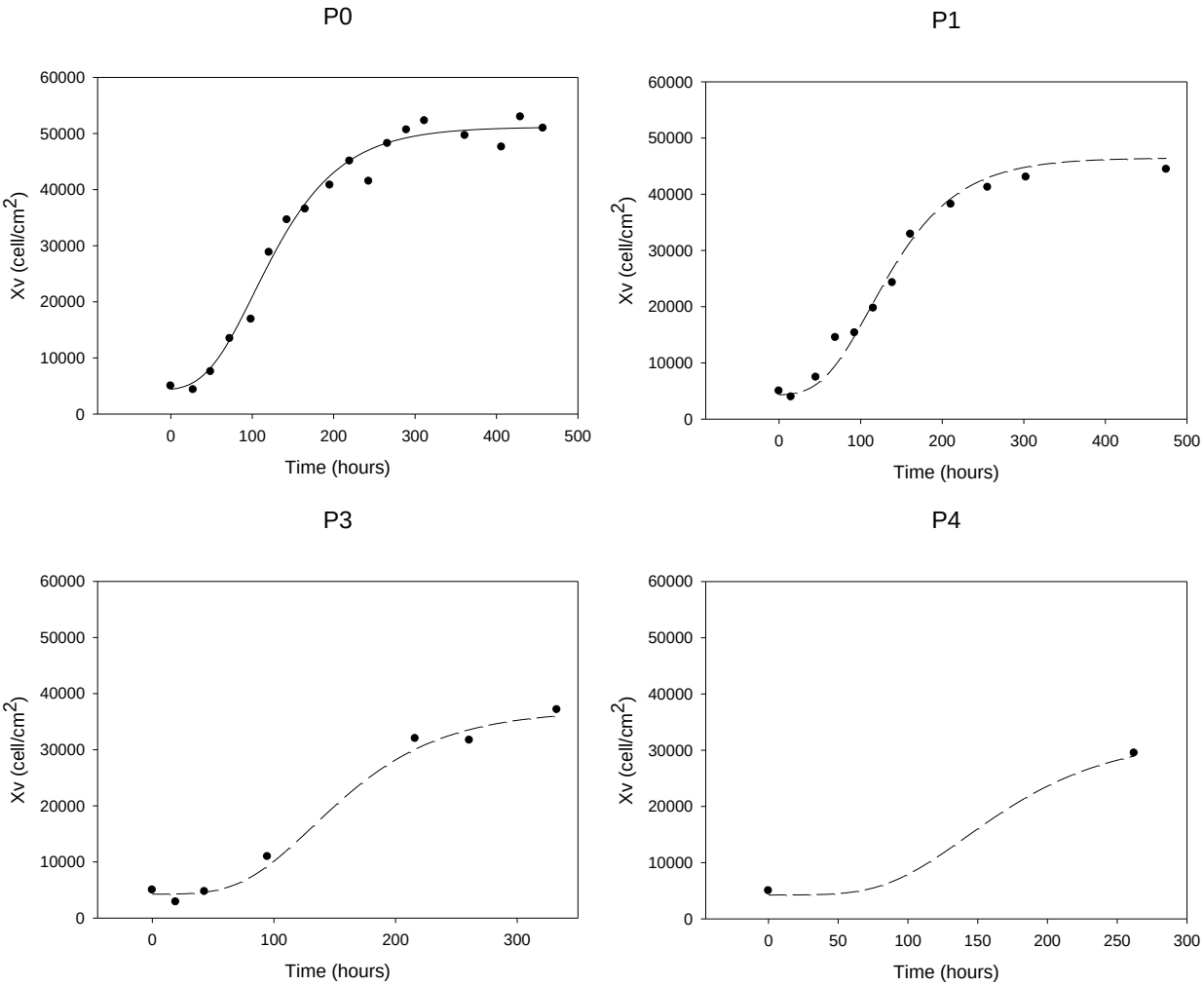

Figure 5.16 Agreement of forward predicted (dashed lines) cell growth kinetics with subsequently obtained experimental data (circles) for the prediction of hMSC growth kinetics during the cell expansion process in 24 well-plates for Patient A compared to empirical data obtained for subsequent passages of growth. The developed modified mathematical model is shown by discontinued lines. A Gompertz equation fitted through the data obtained during P0 is shown by a continuous line.

The validity of the modified Gompertz model (Equation 5.1 together with Equations 5.5 to 5.8) has thus been proven by the results shown in Figures 5.13 through 5.16, as an effective tool to forward predict the cell growth behaviour of hMSC during sequential passages. Accurate determination of the overall cell expansion process time, as well as the cell density obtained at the end of each passage can be predicted using this model after the patient specific hMSC kinetic parameters are determined in Passage 0.

Furthermore, processing decisions can be made early on based on the graphical representation of this model. So for example, if the growth rates obtained are slower than required for the prompt delivery of the cell therapy back to the clinic for a specific patient, process parameters can be altered so as to increase the growth rate of the culture taking advantage of the process optimisation parameters already known to affect growth such as increasing the frequency of medium exchanges (Section 4.3). Such changes can be easily programmed in an automated platform, where the frequency of medium exchanges can occur as often as required with no need for further staffing requirements.

5.5 Characterisation of hMSC During the Automated Cell Expansion Process

Phenotypic characterisation of hMSC can be determined by levels of expression of surface markers as well as by their functionality. However, despite expanding knowledge on the biology of these cells, there has not yet been found one single receptor expressed solely on undifferentiated hMSC that can be used as a marker for characterisation (Fickert et al., 2004). Several surface markers are expressed on hMSC but also on fibroblast and other differentiated progenitors which can be found in bone marrow. It is necessary then to select more than one surface marker, to ensure homogeneity of the culture as hMSC. The latest results reported on the expression levels of different surface markers indicate that expression of CD90, CD105 (SH2), and CD166 are positive indicators of the identity of the cells as hMSC. The selection of these surface markers to characterise hMSC has been selected based on the data reported by Fickert et al., in 2004, showing that a population derived from initially sorted CD90+ and CD166+ cells showed multipotency for chondrogenic, adipogenic, and osteogenic differentiation after cultivation. Surface marker CD105 is widely used in most publications as an established marker for hMSC (Honczarenkoa et al., 2006).

CD90 (Thy-1) is expressed in hematopoietic and mesenchymal cells (Lodie et al., 2002, Pittenger et al., 1999). CD105 (SH2) is expressed in endothelial cells, activated monocytes and stromal cells, but it will not be expressed in hematopoietic cells (Haynesworth et al., 1992, Barry et al., 1999). CD166 is a

Type 1 glycoprotein expressed on activated T cells, B cells and monocytes and appears to be the ligand for CD6. Human CD166 is used as a marker for hMSC as well, and it is thought to play a role for activation of T cells. Expression has been shown to be lost over passage but regained at low confluency levels (Yeh et al., 2005).

The level of expression of CD90, CD105, and CD166 on hMSC at passages zero and five for cells recovered before the end of the exponential growth phase are shown in Figures 5.17 and 5.18. Flow cytometry analysis with Guava Easycyte was performed for recovered cell pellets of no less than $5x10^5$ cells/cm^2 incubated with 10 μl of FITC-conjugated antibodies as indicated in Section 2.10. A mouse IgG1 FITC conjugated antibody was used as isotype control, to detect background staining.

The population of isolated cells at passage zero expresses all three markers characteristic of hMSC. However, expression of CD166 was almost lost by passage five, and a decrease of expression of CD105 started to appear at that passage as well, as shown in Figure 5.18. The decrease of expression of CD166 at passage five is the main reason why cell growth curves above five passages have not been modelled in Section 5.4 using the predictive mathematical model shown in Sections 5.3. Functionality assays to determine the differential potential of hMSC at this passage would have added information about the quality of the population, and it could have been the case that the decrease in expression of CD166 does not necessarily translates into the loss of differential potential for the cells, especially since the expression of this marker has been proven to be regained at low cell densities (Yeh et al., 2005). Having no other data to support such hypothesis for this particular culture of hMSC, the observed decrease of expression of CD166 was interpreted as an indication of undesirable changes in the cell population.

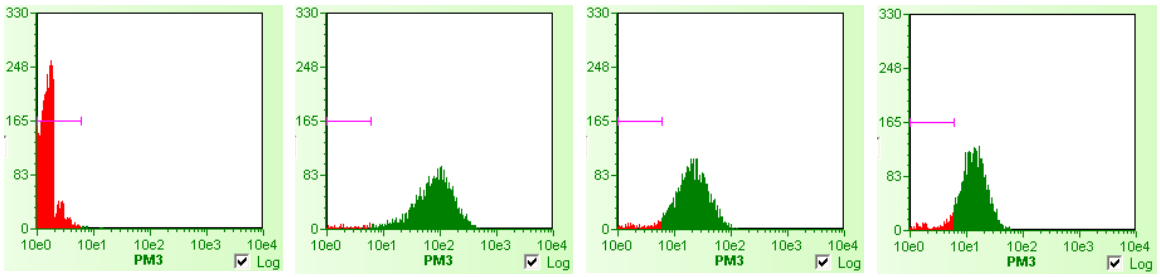

Isotype CD90 CD105 CD166

Figure 5.17 Surface marker expression of freshly isolated hMSC from bone marrow after the first passage in culture (P_0). FITC conjugated antibodies against CD90, CD105, and CD166 were used for flow cytometry analysis by Guava as indicated in Section 2.10.

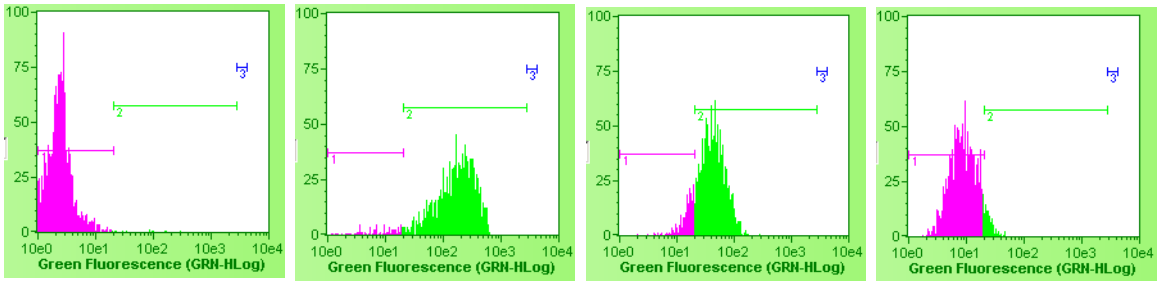

Isotype CD90 CD105 CD166

Figure 5.18 Surface marker expression of freshly isolated hMSC from bone marrow at passage five (P_5). FITC conjugated antibodies against CD90, CD105, and CD166 were used for flow cytometry analysis by Guava as indicated in Section 2.10.

5.6 Summary

Characterisation parameters of cell growth were obtained through a four-parameter sigmoidal Gompertz model, which proved to provide accurate values to evaluate lag phase, exponential growth rates, and maximum cell density at the stationary phase. The use of this mathematical model to fit empirical data has proven to eliminate variability of results due to subjective evaluation of a cell growth curve (Table 5.1), when the number of data points collected is limited to daily measurements over the course of a cell passage. A modified version of the Gompertz model was found to represent hMSC growth curves accurately (Equations 5.5 to 5.8), and it was used to determine and predict growth rate,

doubling time, maximum cell density, duration of lag phase and time to reach the stationary phase.

Isolated hMSC from bone marrow were cultured sequentially for up to five passages, and cell growth curves were generated for each passage (Figures 5.9 to 5.11). Gompertz fits were generated for each passage, and an analysis of the coefficients generated from the fits analyzed. From this analysis, a modified Gompertz model was developed to forward predict the variation of the Gompertz kinetic model parameters as the population doublings, or passage number of the culture increased. The validity of the modified equation was tested with hMSC isolated from two other patients, for which the growth curves for passages one to five were successfully predicted while comparing to the empirical data (Figures 5.13 to .5.16).

The cultures were characterised with surface marker expression of CD90, CD105, and CD166 to determine their undifferentiated state. Results showed that the cells remained undifferentiated until passage five, but that expression of multipotency by expression levels of CD166 was being lost at the end of passage five.

This modelling approach will allow the process engineer to forward predict the cell growth pattern of patient specific cells, as well as to ensure the quality of the final product generated. Processing time, operation schedule, and logistics of the cell expansion process for undifferentiated hMSC will be much improved by the use of this modified mathematical expression, taking the use of hMSC as a therapy for regenerative medicine applications one step closer to reality.

CHAPTER SIX

Conclusions and Future Work

6 CONCLUSIONS AND FUTURE WORK

6.1 Conclusions

The development of an automated cell expansion process for the production of vast number of hMSC in an undifferentiated state has been explored in this thesis. Several parameters affecting isolation and cell growth kinetics have been identified and evaluated, and optimum values for controlled variables during the bioprocess of hMSC have been determined. The knowledge acquired through these studies about the chemical and physical cues that occur during the cultivation of hMSC and their affect on cell growth and differentiation, has led to a quantitative analysis of the growth kinetic variations observed throughout sequential passages. This quantitative analysis resulted in the development of a mathematical expression that forward predicts growth kinetics for up to five passages for a patient-dependent cell population.

Several isolation techniques have been studied in recent years, with the intention to develop a highly selective technique for the isolation of hMSC from bone marrow aspirates. Some of these isolation techniques have given rise to subpopulation of progenitor cells with characteristics that differ from the ones exhibited by hMSC, such as MIAMI (D'Ippolito et al., 2004) or MAPC (Jiang et al., 2002). Interestingly, such results have been difficult to reproduce by other groups. It is not therefore unrealistic to believe that some other parameter changes during these novel isolations other than the ones reported, are in part responsible for the growth kinetics and differentiation potential of the cell populations obtained. The effect of extensive centrifugation, magnetic sorting, and the prolonged exposure of cells to environmental conditions during these isolations have not been taken into consideration while performing such isolations. Consequently for most of these studies, only limited cell characterisation of the isolated cells tends to be reported, and no information on cell growth characteristics or proliferative potential is available (Hung et al., 2002; Lagar'kova et al., 2005). The effect of eliminating any environmental stress imposed to hMSC during isolation from bone marrow aspirates by performing Direct isolations was identified and studied in Section 3.2.1. For this purpose,

Ficoll density gradient centrifugation and Direct isolation, were compared. Both techniques were successful for hMSC recovery. A comparison of the performance of the cells recovered from these two methods concluded that Direct isolation exhibited higher recovery yields than density gradient centrifugations, with a 34% increase in cell recovery from bone marrow aspirates. Direct isolation is also a faster method with less centrifugation steps involved, which present itself as an advantage from an operations and automation point of view.

The most common method for subcultivation of hMSC was first developed by Friendstein et al., in 1976 and it is still being used for routine cell expansion protocols. Characterisation of the growth kinetics for hMSC expanded under these culture conditions has been performed in this work, being taken as baseline or control process for all studies. With all the process conditions remaining constant, the effect of culture surfaces for the attachment and proliferation of hMSC *in vitro* were studied with the intention to evaluate any variability added to future results if these were to be performed in vessels of different geometries. Under constant operating parameters of temperature, aeration, humidity, culture medium, and incubation time, growth characteristics were shown to be similar for static cultures regardless of the geometry of the culture vessel (T-flask versus. well-plates) and the dimensions (24, 12, and 6 well-plates) as shown in Figures 3.1 and 3.2.

Microcarrier cultures were also tested as an attractive alternative to increase the cell growth yield with reduced medium requirements and aseptic manipulations. From the three types of microcarriers tested, MicroHex, Cytodex 1, and Cytodex 3, only one of them, Cytodex 3 supported cell attachment and proliferation under an optimised set of process conditions (Section 3.5). However, results for the conditions tested did not show any improvement of hMSC growth over static cultures and so microcarrier cultures were not investigated further. Although the use of Cytodex microcarries has been proven successful for the propagation of other animal-derived stem cells, there has been no reported success in their use in hMSC (Schop et al., 2008).

The scarce number of hMSC obtained from bone marrow aspirates (Reyes et al., 2001; Silva et al., 2003), makes of cell quantities for experimentation a limiting factor. The effect of cryo-preservation was studied on hMSC that had undergone processing steps to create a cell bank versus cells that had been sequentially passaged after isolation from a bone marrow aspirate. Cell banking is an important process that allows storage of a cell source for subsequent experimentation or future us such as transport of cells to a cGMP manufacturing facility, or to retain the cells during a halt in the cell expansion process. The effect of such procedure on cell growth was demonstrated to exhibit some detrimental effect on cell growth rate and maximum cell density reached at the end of the first passage (Section 3.2.2). This effect may not be cumulative, however it has a negative impact on cells seeded right after thawing from storage in liquid nitrogen.

Subcultivation of hMSC was evaluated, confirming a decrease in growth rates and maximum viable cell densities as the passage number increases (Table 3.2) in agreement with results reported by Bruder et al., 1997. A novel quantitative analysis for the expansion of hMSC was performed by using a mathematical Gompertz model (Equation 3.1) that accurately represents the growth kinetics of hMSC. Results were confirmed by experimenting with two different sources of cells from two donors, showing excellent agreement between the empirical data and the mathematical model. The implications of the decrease in growth rate and cell recovery as the cell expansion progresses, was assessed for the overall completion of the process (Table 3.3).

Having established hMSC growth characteristics under baseline culture conditions and a method to quantify cell growth kinetics, comparison of results from cultures exposed to different conditions of growth will be possible. Given the vast number of process parameters involved in the expansion of hMSC, and the uncertainty of their combinatory effects on cell growth characteristics, a design-of-experiments (DOE) approach was not chosen to evaluate optimum values for control parameters of an automated process. Instead, the effect of individual parameters on cell growth kinetics was investigated while keeping all other process conditions as defined by the baseline culture protocol.

Optimum conditions for the cell expansion process of hMSC in automated microwells were characterised. As a result, the optimised values obtained for inoculation cell density, medium exchange strategies, and environmental control proved that the overall time for the cell expansion process was reduced considerably in comparison with the values dictated by the baseline condition for the same set of parameters. Reduction in doubling times of hMSC was found to be mainly attributed to an increase in the frequency of medium exchanges (Figure 4.5), and not to a decrease in inoculation cell density as it had been previously reported by Sekiya et al., 2002. The Gompertz model was found to represent hMSC growth curves accurately, and it was used to quantitatively determine growth rate, doubling time, maximum cell density, duration of lag phase and time to reach the stationary phase. This information was used to determine the duration of a cell expansion process that requires $1x10^8$ of undifferentiated multipotent hMSC from an autologous source for their usage in regenerative medicine applications. Results on Table 4.2 showed that low ICD of 100 cells/cm^2 as well as frequent media addition rates of 6 hours resulted in shorter doubling times when compared to the baseline condition of growth, reducing the overall duration of the cell expansion process from 59 to 30 days.

Having shown that faster media addition rates of 6 hours resulted in a decrease in the overall cell expansion time, the contributing parameters to this result were evaluated. As well as the rapid addition of nutrients and removal of accumulated by-products, the cell monolayer is exposed to environmental variations every time a medium exchange is performed. With the added advantage of an automated platform with temperature and gas control for the cell expansion process, the effect of these parameters on hMSC growth kinetics were evaluated. Environmental variations of pH and temperature during medium exchanges were recorded with the aid of temperature and pH sensors (Section 4.4). The effect of these variations in growth kinetics of hMSC was studied, indicating that repeated exposures to pH step changes from 7.5 to 8.2 were not detrimental to cell growth but they did not contribute to an increase in cell growth rates in the absence of medium exchanges at a similar frequency.

As a result of these studies, an automated platform was used for the cell expansion process of hMSC under optimised feeding strategies of 4 and 12 hours addition rates. The automated platform successfully performed medium exchange operations eliminating the use of open manipulations throughout the duration of one passage. The robotic platform will be further modified to accomplish all the operations involved in sequential subcultivation of autologous hMSC on the basis of these promising results.

The advantage of using the Gompertz model to accurately determine cell growth kinetic parameters was demonstrated. Comparison of growth rate calculations performed with or without this mathematical expression highlighted the advantage of using the Gompertz model. The use of this mathematical model to fit empirical data has proven to eliminate variability of results due to subjective evaluation of a cell growth curve (Table 5.1), when the number of data points collected is limited to daily measurements over the course of a cell passage.

Cell growth kinetic model parameters for growth curves generated over five sequential passages were obtained to study the growth kinetic changes over subcultures of hMSC (Figures 5.9 to 5.11). Gompertz fits were generated for each passage, and an analysis of the coefficients generated from the fits was performed. From this study, a modified Gompertz model was developed to forward predict the variation of the Gompertz kinetic model parameters as the population doublings, or passage number of the culture increased (Equations 5.5 to 5.8). The validity of this modified Gompertz model was tested with hMSC isolated from two other patients, for which the growth curves for passages one to five were successfully predicted when compared to the empirical data (Figures 5.13 to .5.16). Prediction of the cell growth characteristics of hMSC have not been reported previously in the literature. The variability of growth rates depending on the donor or the population doubling of the culture has made such a quantitative approach a challenge when designing a robust cell expansion process. The use of the model reported here, will allow prediction not just of the duration of a cell expansion process, but will also facilitate the cost analysis of such a process prior to completion. The requirements of raw materials such as

media, culture vessels, and staffing requirements will be known for each individual patient-targeted process.

The characterisation of hMSC remains a topic in the developmental stage. Several surface markers have been shown to be expressed on the cytoplasmic membranes of the anchorage-dependent subpopulation of cells obtained from bone marrow aspirates. However, many of the markers being expressed on hMSC are also expressed in other cell lines and/or they have been shown to decrease in expression levels over the cell expansion process. The cultures were characterised with surface marker expression of CD90, CD105, and CD166 to determine their undifferentiated state. These surface markers are characteristic of hMSC and are indicative of their multipotency. Results showed that the cells remained undifferentiated until passage five, but that expression of multipotency by expression levels of CD166 was lost at the end of passage five. This result alone is not indicative of a differentiating cell population, since the levels of expression of CD166 decrease with increasing cell density in culture (Yeh et al., 2005).

In conclusion, quantitative results on the hMSC growth kinetics of sequential passages have been presented. The effect of different control parameters on cell growth characteristics have contributed to the design of an automated cell expansion process for the robust expansion of autologous hMSC. A mathematical expression has been developed to forward predict the duration and growth characteristics of hMSC in culture over serial subcultivation. Finally, this model has been shown to accurately predict such parameters of growth for cell cultures originated from different donors.

6.2 Future Work

The results shown in this thesis provide solid bases for the development of a robust automated cell expansion process for autologous hMSC in an undifferentiated state. Many parameters such as ICD, vessel surface characteristics, feeding strategies, pH, and temperature have been optimised for the implementation of such a robotic platform as a tool for cell expansion. Further studies will be able to contribute to a greater understanding of the chemical and

physical parameters controlling cell fate during the cell expansion process of hMSC in an automated process. In particular:

- A first priority should be the further biological characterisation of hMSC at different stages of growth in an automated platform. As studies of the biology of hMSC improve, specific markers for the characterisation of these cells will become available. Also functionality studies of the differentiation potential and performance *in vivo* should be carried out. These will determine the potential of hMSC, expanded using the procedures developed in this work, for use in regenerative medicine applications.
- Growth studies of hMSC on microcarrier cultures deserves further investigation given the promising results showing attachment to Cytodex 3 spheres. Optimisation of culture parameters and feeding strategies evaluated in this thesis may be applied to microcarrier cultures and lead to the development of an automated process in well-plates or stir-tank bioreactors.
- Feeding strategies that maximise cell growth rate have been shown, proving that faster addition rates were the main contributor towards developing a faster expansion process. However, the factor or factors in the culture media composition contributing to growth rate limitations other than glucose, glutamine, lactate, and glutamate have not been investigated. As analytical tools for biological analysis develop, further studies on the characterisation of media components (as well as the ones provided for the chemically undefined serum) and their contribution to cell fate will be of great interest.
- A mathematical model to forward predict hMSC characteristics has been developed. Future work with this modelling tool should investigate possible correlations of the expressions obtained for the coefficients a, b, X_0, and t_0 of the modified Gompertz model (Equations 5.1 and 5.5 to 5.8) not just as a function of passage number but also as a function of process parameters such as frequency of medium exchanges, pH levels, or any other factor that can be controlled and can influence growth.
- Further adjustment of environmental conditions within the Tecan platform used for these studies will allow for a high throughput of experimental conditions and ensure the development and operation of a robust cell

expansion process for hMSC cultures. Studies carried over sequential passages with hMSC will demonstrate the feasibility of a fully automated process that will add robustness and will eliminate any requirement for manual interventions.

REFERENCES

Abdallah BM, Haack-Sorensen M, Burns JS, Elsnab B, Jakob F, Hokland P, Kassem M. Maintenance of differentiation potential of human bone marrow mesenchymal stem cells immortalized by human telomerase reverse transcriptase gene in despite of extensive proliferation. *Biochem Biophys Res Commun,* (2005) 326:527-538

Amstein C, Hartman P. Adaptation of plastic surfaces for tissue culture by glow discharge. *J Clin Microbiol*., (1975) 2(1):46-54

Arkin S, Naprstek B, Guarini L, Ferrone S, Lipton JM. Expression of intercellular adhesion molecule-1 (CD54) on hematopoietic progenitors. *Blood* (1991) 77(6):948-953

Baksh D, Davies J, Zandstra P. Adult human bone marrow-derived mesenchymal progenitor cells are capable of adhesion-independent survival and expansion. *Experimental Hematology,* (2003) 31:723-732

Baksh D, Song L, Tuan R. Adult mesenchymal stem cells: characterization, differentiation, and application in cell and gene therapy. *J. Cell. Mol. Med.,* (2004) 8(3):301-316

Ball S, Shuttleworth A, Kielty C. Direct cell contact influences bone marrow mesenchymal stem cells. *Int. J. of Biochemistry and Cell Biology,* (2004) 36:714-727

Banfi A, Bianchi G, Notaro R, Luzzatto L, Cancedda R, Quarto R. Replicative aging and gene expression in long-term cultures of human bone marrow stromal cells. *Tissue Eng.,* (2002) 8:901-910

Bapat S, Mali A, Koppikar C, Kurrey N. Stem and progenitor-like cells contribute to the aggressive behavior of human epithelial of ovarian cancer. *Cancer Res.,* (2005) 65(8):3025-3029

Barrilleaux B, Phinney DG, Prockop DJ, O'Connor K. Review: Ex Vivo Engineering of Living Tissues with Adult Stem Cells. *Tissue Eng*., (2006) 12(11):3007-3019

Barry FP, Boynton RE, Haynesworth S, Murphy JM, Zaia J. The monoclonal antibody SH-2, raised against human mesenchymal stem cells, recognizes an epitope on endoglin (CD105). *Biochem. Biophys. Res. Commun*., (1999) 265(1):134–139

Bernard C, Connors D, Barber L, Jayachandra S, Bullen A, Cacace A. Adjunct Automation to the Cellmate: Cell Culture Robot. *J. of the Association for Laboratory Automation* (2004) 9(4):209-217

Bianchi G, Banfi A, Mastrogiacomo M, Notaro R, Luzzatto L, Cancedda R. Quarto R, Ex vivo enrichment of mesenchymal cell progenitors by fibroblast growth factor 2. *Experimental Cell Res.*, (2003) 287:98-105

Blanch HW, Clark DS. Biochemical Engineering, *Marcel Dekker,* (1997) 702pp

Bodziak ML, Grefrath PL, Price PJ, Jayme DW. *In Vitro* (1985) 21:47A

Bongso A, Richards M. History and perspective of stem cell research. *Best Practice Res. Clinical Obstetrics Gynaecology*, (2004) 18(6):827-842

Bruder SP, Jaiswal N, Haynesworth S. Growth kinetics, self-renewal, and the osteogenic potential of purified human mesenchymal stem cells during extensive subcultivation and following cryopreservation. *J of Cellular Biochemistry* (1997) 64:278-294.

Burt SM, Carter TJ, Kricka LJ. Thermal characteristics of microtitre plates used in immunological assays. *J. Immunol Methods* (1979) 31:231-236.

Caplan AI, Bruder SP. Cell and molecular engineering of bone regeneration. In 'Textbook of Tissue Engineering' (Lanza R, Langer R, Chick W, eds), *Georgetown Landes,* (1996) pp. 603:18

Caplan AI. Mesenchymal stem cells. *J. Orthop. Res.*, (1991) 9:641-650

Caplan, AI, Bruder SP. Mesenchymal stem cells: building blocks for molecular medicine in the 21st century. *Trends Mol. Med.*, (2001) 7:259-264

Castro-Malaspina H, Gay RE, Resnick G, Kapoor N, Meyers P, Chiarieri D, McKenzie S, Broxmeyer HE, Moore MA. Characterization of human bone marrow fibroblast colony-forming cells (CFU-F) and their progeny. *Blood*. (1980) 56(2):289-301

Chapman T. Automation on the move, *Nature,* (2003) 421:661-666

Cheng L, Hammond H, Ye Z, Zhan X, Dravid G. Human adult marrow cells support prolonged expansion of human embryonic stem cells in culture. *Stem Cells*, (2003) 21(2):131-142

Chu L, Robinson DK. Industrial choices for protein production by large-scale cell culture. *Current Opinion in Biotechnology,* (2001) 12:180-187

Clark B, Keating A. A Biology of bone marrow stroma. *Ann NY Acad Sci* (1995) 770:70-78

Cole RJ, Paul J. The effects of erythropoietin on haem synthesis in mouse yolk sac and cultured foetal liver cells. *J. Embryol. Exp. Morphol.*, (1966) 15:245-260

Colter D, Class R, DiGirolamo C, Prockop D. Rapid expansion of recycling stem cells in cultures of plastic-adherent cells from human bone marrow. *Proc. Natl Acad. Sci., USA* (2000) 97:3213-3218

Conget PA, Minguell JJ. Phenotypical and functional properties of human bone marrow mesenchymal progenitor cells. *J. Cell Physiol.,* (1999) 181:67-73

Crespi CL, Thilly WG. Continuous cell propagation using low-charge microcarriers. *Biotechnol. Bioeng,.* (1981) 23:983-993

D'Amour KA, Agulnick AD, Eliazer S, Kelly OG, Kroon E, Baetge EE. Efficient differentiation of human embryonic stem cells to definitive endoderm. *Nat. Biotechnol.*, (2005) 23(12):1534-1541

Deans R, Moseley A, Mesenchymal stem cells: biology and potential clinical uses. *Experimental Hematology*, (2000) 28:875-884

Deasy B, Jankowski R, Payne T, Cao B, Goff J, Greensberger J, Huard J. Modeling stem cell population growth: incorporating terms for proliferative heterogeneity. *Stem Cells*, (2003) 21:536-545

Deguchi Y, Kehrl JH. Selective expression of two homeobox genes in CD34-positive cells from human bone marrow. *Blood*, (1991) 78(2):323–328

DiGirolamo CM, Stokes D, Colter D, Phinney DG, Class R, Prockop DJ. Propagation and senescence of human marrow stromal cells in culture: a simple colony-forming assay identifies samples with the greatest potential to propagate and differentiate. *Br. J. Haematol.,* (1999) 107(2):275-281

D'Ippolito G, Schiller PC, Ricordy C, Roos BA, Howard GA. Age-related osteogenic potential of mesenchymal stromal cells from human vertebral bone marrow. *J. Bone Miner Res*., (1999) 14(7):1115-1122

D'Ippolito G, Diabira S, Howard G, Menei P, Ross B, and Schiller P. Marrow-isolated adult multilineage inducible (MIAMI) cells, a unique population of postnatal young and old human cells with extensive expansion and differentiation potential. *J. of Cell Science* (2004) 117 (14): 2971-2981

Drapper J, Smith K, Gokhale P, Moore H, Maltby E, Johnson J, Meisner L, Zwaka T, Thomson J, Andrews P. Recurrent gain of chromosomes 17q and 12 in cultured human embryonic stem cells. *Nature biotechnology* (2004) 22:53-54

Elequin, FT, Muggia, FM, Ghossein, NA, Schreiber KA. A quick method for concentration and processing cancer cells from serous fluids and fineneedle nodule aspirates. *Acta Cytol* (1977) 21:596–599

Evans M. Isolation and maintenance of murine embryonic stem cells in Essentials of Stem Cell Biology (Lanza P, Gearhart J, Hogan B). *Elsevier* (2006) 269-273

Ferrari, G, Cusella G, Angelis D, Colletta M, Paolucci E, Stornaiuolo A, Cossu G, Mavilio F. Muscle regeneration by bone marrow derived myogenic progenitors. *Science,* (1998) 279:1528–1530

Fickert S, Fiedler J, Brenner RE. Identification of subpopulations with characteristics of mesenchymal progenitor cells from human osteoarthritic cartilage using triple staining for cell surface markers. *Arthritis Res. Therapy,* (2004) 6(5):R422-432

Fink T, Adildtrup L, Fogd K, Abdallah B, Kassem M, Ebbessen P, Zachar V. Induction of adipocyte-like phenotype in human mesenchymal stem cells by hypoxia. *Stem Cells,* (2004) 22:1346-1355

Frauenschuh S, Reichmann E, Ibold Y, Goetz PM, Sittinger M, Ringe J. A microcarrier-based cultivation system for expansion of primary mesenchymal stem cells. *Biotechnol. Prog.,* (2007) 23:187-193

Freshney RI. Culture of Animal Cells: A Manual of Basic Technique. *John Wiley and Sons, New York,* (1994) 153-157

Friedenstein A, Gorskaja J, Lulagina N. Fibroblast precursors in normal and irradiated mouse hematopoietic organs. *Exp. Hematol.,* (1976) 4(5):267-274

Friedenstein, AJ, Chailakhjan, RK, Lalykina KS. The development of fibroblast colonies in monolayer cultures of guinea- pig bone marrow and spleen cells. *Cell Tissue Kinetics,* (1970) 3(4):393-403

Gaus G, Demir-Weusten AY, Schmitz U, Bose P, Kaufmann P, Huppertz B, Frank H. Extracellular pH modulates the secretion of fibronectin isoforms by human trophoblast. *Acta Histochemica,* (2002) 104(1):51-63

Gebb C, Lundgren B, Clark J, Lindskog U. Harvesting and subculturing cells growing on denatured-collagen coated microcarriers (Cytodex 3). *Dev Biol Stand,* (1983)55:57-65

Grinell F. Cellular adhesiveness and extracellular substrata. *Int. Review of Cytology,* (1978) 53:65-144

Gronthos S, Graves S, Ohta S, Simmons PJ. The Stro-1+ fraction of adult human bone marrow contains the osteogenic precursors. *Blood,* (1994) 84(12):4164-4173

Gronthos S, Simmons PJ. The growth factor requirements of STRO-1-positive human bone marrow stromal precursors under serum-deprived conditions in vitro. *Blood,* (1995) 85(4):929-940

Gronthos S, Zannettino ACW, Hay SJ, Shi S, Graves SE, Kortesidis A, Simmons PJ. Molecular and cellular characterization of highly purified stromal stem cells derived from human bone marrow. *J. of Cell Science,* (2003) 116:1827-1835

Grzelak A, Rychlik B, Bartosz G. Light-dependent generation of reactive oxygen species in cell culture media. *Free Radical Biology and Medicine,* (2001) 30(12):1418-1425

Haseltine WA. The emergence of regenerative medicine: A new field and a new society. *J. Regen. Med.,* (2001) 2(4):17-23

Hayashia T, Hayashib I, Shinoharaa T, Morishitaa Y, Nagamuraa H, Kusunokia Y, Kyoizumia S, Seyamac T, Nakachia K. Radiation-induced apoptosis of stem/progenitor cells in human umbilical cord blood is associated with alterations in reactive oxygen and intracellular pH. *Mutation Res.,* (2004) 556(1-2):83-91

Hayflick H, Moorehead PJ. The serial cultivation of human diploid cell strains. *Exp. Cell Res.,* (1961) 25:585-621

Hayflick L. The limited in vitro lifetime of human diploid cell strains. *Exp. Cell Res.,* (1965) 37:614-636

Haynesworth SE, Baber MA, Caplan AI. Cell surface antigens on human marrow-derived mesenchymal cells are detected by monoclonal antibodies. *Bone*, (1992) 13(1):69–80

Hevehan DL, Papoutsakis ET, Miller WM. Physiologically significant effects of pH and oxygen tension on granulopoiesis. *Experimental Hematology*, (2000) 28(3):267-275

Honczarenkoa M, Lea Y, Swierkowskia M, Ghiranb I, Glodeka AM, Silberstein LE. Human Bone Marrow Stromal Cells Express a Distinct Set of Biologically Functional Chemokine Receptors. *Stem Cells,* (2006) 24(4):1030-1041

Horita A, Weber LJ. Skin penetrating property of rugs dissolved in dimethylsufoxide (DMSO) and other vehicles. *Life Sciences.,* (1964) 3:1389-1395

Horwitz EM, Blanc KL, Dominici M, Mueller I, Slaper-Cortenbach I, Marini FC, Deans RJ, Krause DS, Keating A. Clarification of the nomenclature for MSC: The International Society of Cellular Therapy position statement. *Cytotherapy* (2005) 7(5):393-395

Horwitz EM, Prockop DJ, Fitzpatrick LA, Koo WWK, Gordon PL, Michael N, Sussman M, Orchard P, Marx JC, Pyeritz RE, Brenner MK. Transplantability and therapeutic effects of bone marrow-derived mesenchymal cells in children with osteogenesis imperfecta. *Nature Med* (1999) 5:309-313

Horwitz EM. Stem cell plasticity: The growing potential of cellular therapy. *Archives of Medical Res.,* (2003) 34(6):600-606

Hudis M. Plasma Treatment of Solid Materials. Techniques and Applications of Plasma Chemistry (Eds. Hollahan JR, Bell AT.) *John Wiley and Sons,* (1974) 113-147

Hung S, Chen N, Hsieh S, Li H, Ma H, Lo W. Isolation and characterization of size-sieved stem cells from human bone marrow. *Stem Cells,* (2002) 20:249-258

in‘t Anker PS, Scherjon SA, Kleijburg-van der Keur C, de Groot-Swings GMJS, Claas FHJ, Fibbe WE, Kanhai HHH. Isolation of mesenchymal stem cells of fetal or maternal origin from human placenta. *Stem Cells,* (2004) 22:1338-1345

Ishii M, Koike C, Igarashi A, Yamanaka K, Pan H, Higashi Y, Kawaguchi H, Sugiyama M, Kamata N, Iwata T, Matsubara T, Nakamura K, Kurihara H, Tsuji K, Kato Y. Molecular markers distinguish bone marrow mesenchymal stem cells from fibroblasts. *Biochem and Biophy Res. Commun.,* (2005) 332(1):297-303

Jaenisch R, Young R. Stem cells, the molecular circuitry of pluripotency and nuclear reprogramming. *Cell,* (2008) 132(4):567-582

Jaiswal N, Haynesworth SE, Caplan AI, Bruder SP. Osteogenic differentiation of purified, culture-expanded human mesenchymal stem cells in vitro. *J. Cell. Biochem.,* (1997) 64(2):295–312

Jaiswal RK, Jaiswai N, Gruder SP, Mbalaviele G, Marshak DR, and Pittenger MF. Adult human mesenchymal stem cell differentiation to the osteogenic or adipogenic lineage is regulated by mitogen-activated protein kinase. *J. of Biological Chemistry* (2000) 275(13):9645-9652

Javazon EH, Beggs KJ, Flake AW. Mesenchymal stem cell: paradoxes of passaging. *Experimental Hematology,* (2004) 32(5):414-425

Jiang Y, Jahagirdar BN, Reinhardt RL, Schwartz RE, Keene CD, Ortiz-Gonzalez XR, Reyes M, Lenvik T, Lund T, Blackstad M, Du J, Aldrich S, Lisberg A, Low WC, Largaespada DA, Verfaillie CM. Pluripotency of mesenchymal stem cells derived from adult marrow. *Nature,* (2002) 418:41-49

Jiang Y, Vaessen B, Lenvik T, Backstad M, Reyes M, Verfaillie CM. Multipotent progenitor cells can be isolated from postnatal murine bone marrow, muscle, and brain. *Experimental Haematology,* (2002) 30(8):896-904

Jiang Y, Vaessen B, Lenvik T, Blackstad M, Reyes M, Verfaillie CM. Multipotent progenitor cells can be isolated from postnatal murine bone marrow, mucle, and brain. *Experimental Hematology,* (2002) 30(8):896-904

Joannides A, Fiore-Heriche C, Westmore K, Caldwell M, Compston A, Allen N, Chandren S. Automated Mechanical Passaging: A novel and efficient method for human embryonic stem cell expansion. *Stem Cells,* (2006) 24(2):230-235

Kang TJ, Yeom J, Lee H, Rho SH, Han H, Chae G. Growth kinetics of human mesenchymal stem cells from bone marrow and umbilical cord blood. *Acta Haematol* (2004) 112(4):230-233

Katz-Jaffe MG, Trounson AO, Cram DS. Mitotic errors in chromosome 21 of human preimplantation embryos are associated with non-viability. *Molecular Human Reproduction,* (2004) 10:143-147

Keating A, Berkahn L, Filshie R. A phase I study of the transplantation of genetically marked autologous one marrow stromal cells. *Hum. Gene Theraphy,* (1998) 9(4):591-600

Keenan J, Pearson D, Clynes M. The role of recombinant proteins in the development of serum-free media. Cytotechnology (2006) 50(1-3):49-56

Kempner ME, Felder RA. A review of cell culture automation. *J. Of Association for Laboratory Automation,* (2002) 7(2):56-62

Kenda-Ropson N, Lenglois S, Miller AOA. Microsupport with two-dimensional geometry (2D-MS). 4. Temperature-induced detachment of anchorage-dependent CHO-K1 cells from cryoresponsive MicroHex((R)) (CryoHex). *Cytotechnology,* (2002) 39(3):163–170

Kenda-Ropson N, Mention D, Motte V, Genlain M & Miller AOA. Microsupport with two-dimensional geometry (2D-MS). In situ determination of the growth kinetics of anchorage-dependent cells by laser diffraction particle sizing (LDPS). *Cytotechnology* (2002) 37(1):49–53

Kenda-Ropson N, Mention D, Motte V, Genlain M, and Miller AOA. Microsupport with two-dimensional geometry (2D-MS). In situ determination of the growth kinetics of anchorage-dependent cells by Laser Diffraction Particle Sizing (LDPS). *Cytotechnology,* (2001) 37(1):49-53

Kino-Oka M, Ogawa N, Umergaki R, Taya M. Bioreactor design for successive culture of anchorage-dependent cells operated in an automated manner. *Tissue Eng.* (2005) 11(3-4):535-545

Kirschstein R, Skirboll L. Stem cells: Scientific Progress and Future Research Directions. *National Institutes of Health Resource for Stem Cell Research,* June:(2001), </info/scireport/2001report>

Koller MR, Emerson SG, Palsson B. Large-scale expansion of human stem and progenitor cells from bone marrow mononuclear cells in continuous perfusion cultures. *Blood,* (1993) 82(2):378-384

Kopen GC, Prockop DJ, Phinney D. Marrow stromal cells migrate throughout forebrain and cerebellum, and they differentiate into astrocytes after injection into neonatal mouse brains. *Proc. Natl Acad. Sci., USA* (1999) 96(19):10711-10716

Krause DS, Theise ND, Collector MI, Henegariu O, Hwang S, Gardner R, Neutzel S, Sharkis SJ. Multi-organ, multi-lineage engraftment by a single bone-marrow derived stem cell. *Cell* (2001) 105(3):369-377

Largar'kova MA, Lyakisheva AV, Filonenko ES, Volchkov PY, Rubtsova KV, Gerasimov YV, Chailakyan RK, Kiselev SL. Characteristics of human bone marrow mesenchymal stem cells isolated by immunomagnetic selection. *Bulletin of Experimental Biology and Medicine,* (2006) 141(1):112-116

Lazarus HM, Haynesworth SE, Gerson SL, Rosenthal NS, Caplan AI. Ex vivo expansion and subsequent infusion of human bone marrow-derived stromal progenitor cells (mesenchymal progenitor cells): implications for therapeutic use. *Bone Marrow Transplant*, (1995) 16(4): 557-564

Lenglois S, Moser M, Miller AOA. Microsupport with two-dimensional geometry (2D-MS). 5. EDTA-mediated detachment of CHO-K1 cells and VERO cells from MicroHex. *Cytotechnology*, (2004) 44(1-2):47-54

Li L, Xie T. Stem cell niche: Structure and function. *Annu. Rev. Cell Dev. Biol.,* (2005) 21:605–631

Liu S, Dontu G, Wicha MS. Mammary stem cells, self-renewal pathway and carcinogenesis. *Breast Cancer Res.,* (2005) 7(3):86–95

Lodie TA, Blickarz CE, Devarakonda TJ, He C, Dash AB, Clarke J, Gleneck K, Shihabuddin L, Tubo R. Systematic analysis of reportedly distinct populations of multipotent bone marrow-derived stem cells reveals a lack of distinction. *Tissue Eng.,* (2002) 8(5):739–751

Lundholt BK, Scudder KM, Pagliaro L. A simple technique for reducing edge effect in cell-based assays. *J. Biomol. Screen.,* (2003) 8(5):566-570

Malda J, Frondoza CG. Microcarriers in the engineering of cartilage and bone. *Trends Biotechnology*, (2006) 24(7):299-304

Mangi A, Noiseux N, Kong D, He H, Rezvani M, Ingwall J, and Dzau V. Mesenchymal stem cells modified with Akt prevent remodelling and restore performance of infacted hearts. *Nature Medicine,* (2003) 9:1195-1201

Marek H, Le Y, Sweirkowski M, Ghuran I, Glodex AM, Silberstien LE. Human bone marrow stromal cells express a distinct set of biologically Functional Chemokine Receptors. *Stem Cell*s, (2006) 24(4):1030-1041

Mareschi K, Ferrero I, Rustichelli D, Aschero S, Gammaitoni L, Aglietta M, Madon E, Fagioli F. Expansion of mesenchymal stem cells isolated from pediatric and adult donor bone marrow. *J. Cell Biochem.* (2006) 97(4):744-754

Martin JA, Klingelhutz AJ, Moussavi-Harami F, Buckwalter JA. Effects of oxidative damage and telomerase activity on human articular cartilage chondrocyte senescence. *J. Gerontology: Biological Sciences Medical Sciences* (2004) 59:324-336

Martin MJ, Muotri A, Gage F, Varki A. Human embryonic stem cells express an immunogenic nonhuman sialic acid *Tech. Reports Nature Medicine,* (2005) 11(2):228-232

Martin-Rendon E, Watt S. Stem Cell Plasticity. *Brit. J. Haematology,* (2003) 122(6):877-891

Mason C, Hoare M. Regenerative medicine bioprocessing: the need to learn from the experience of other fields. *Regenerative Med.,* (2006) 1(5);615-623

Mason C. The time has come to engineer tissues and not just tissue engineer. *Regenerative Med.,* (2006) 1(3):303–306

Melero-Martin JM, Dowling M, Smith M, Al-Rubeai M. Optimal in-vitro expansion chondroprogenitor cells in monolayer culture. *Biotechnology and Bioengineering,* (2006) 93(3):519-533

Mezey E, Chandross KJ, Harta G, Maki RA, McKercher SR. Turning blood into brain: cells bearing neuronal antigens generated in vivo from one marrow. *Science,* (2000) 290(5497):1779-1782

Miller WM, Blanch HW, Wilke CR. A kinetic analysis of hybridoma growth and metabolism in batch and continuous suspension culture: effect of nutrient concentration, dilution rate and pH. *Biotechnology and Bioengineering,* (1988) 32(8):947-965

Minami R, Yokota S, Teplitz RL. Gradient separation of normal and malignant cells. II. Application to in vivo tumour diagnosis. *Acta Cytol*, (1978) 22(6):584–588

Mineault M, Batra SK. Concise review: recent advances on the significance of stem cells in tissue regeneration and cancer therapies. *Stem Cells,* (2006); 24(11):2319–2345

Mironov V, Visconti RP, Markwald RR: What is regenerative medicine? The emergence of applied stem cell and development biology. *Expert Opin. Biol. Ther*., (2004) 4(6):773–781

Moussavi-Harami F, Duwayri Y, Martin JA, Moussavi-Harami F, Buckwalter J. Oxygen effects on senescence in chondrocytes and mesenchymal stem cells: consequences for tissue engineering. *The Iowa Orthopaedic J.,* (2004) 24:15-20

Muschler GF, Nakamoto C, Griffith L. Engineering Principles of Clinical Cell-Based Tissue Engineering. *J. Bone Joint Surg. Am.,* (2004) 86-A(7):1541-1558

Nealon AJ, Willson KE, Pickering SC, Clayton TM, O'Kennedy RD., Titchener-Hooker NJ, Lye GJ. Use of operating windows in the assessment of integrated robotic systems for the measurement of bioprocess kinetics. *Biotechnol. Prog.,* (2005) 21(1):283-291

Nerbauer M, Fischbach C, Bauer-Kreisel P, Lieb E, Hacker M, Tessmar J, Schulz M, Goepferich A, Blunk T. Basic fibroblast growth factor enhances PPARgamma ligand-induced adipogenesis of mesenchymal stem cells. *FEBS Letters,* (2004) 577(1):277-283

Ochsenbien-Kolble N, Bilic G, Hall H, Huch R, Zimmermann R. Inducing proliferation of human amnion epithitelial and mesenchymal cells from prospective engineering of membrane repair. *J. Perinat. Med.* (2003) 31:287-294

Ohgushi H, Caplan AI. Stem cell technology and bioceramics: from cell to gene engineering. *J. Biomed. Materials. Res.,* (1999) 48(6):913–27

Oliver DG, Sanders AH, Hogg RD, Hellman JW. Thermal gradients in microtitration plates. Effects on enzyme-linked immunoassay. *J. Immunol Methods,* (1981) 42(2):195-201

Olsen JV, Ong SE, Mann M. Trypsin cleaves exclusively C-terminal to arginine and lysine residues. *Molecular & Cellular Proteomics,* (2004) 3(6):608-614

Oreffo R, Cooper C, Mason C, Clements M. Mesenchymal stem cells. Lineage, plasticity, and skeletal therapeutic potential. *Stem Cell Reviews,* (2007) 1(2):169-178

Ozturk SS, Palsson BO. Chemical decomposition of glutamine in cell culture media: effect of media type, pH, and serum concentration. *Biotechnol. Prog.,* (1990) 6(2):121-128

Pereira RF, O'Hara MD, Laptev A, Halford KW, Pollard MD, Class R, Simon D, Livezey K, Prockop DJ. Marrow stromal cells as a source of progenitor cells for nonhematopoietic tissues in transgenic mice with a phenotype of osteogenesis imperfecta. *Proc.Natl Acad. Sci. USA* (1998) 95(3):1142-1147

Pharmacia Fine Chemicals, Technical Booklet Series, Uppsala, Sweden. Save with CytodexÔ 1. *Separation News,* (1979) 4:5

Pharmacia Fine Chemicals, Technical Booklet Series, Uppsala, Sweden. Microcarrier cell culture: principles and methods. (1981)

Pharmacia LKB Biotechnology. Microcarrier cell culture principles and methods. (1989)

Phillips DR. Effect of trypsin on the exposed polypeptides and glycoproteins in the Human Platelet Membrane. *Biochemistry,* (1972) 11(24):4582-4588

Phinney DG, Kopen G, Righter W, Webster S, Tremain N, Prockop DJ. Donor variation in the growth properties and osteogenic potential of human marrow stromal cells. *J. Cell Biochem.,* (1999) 75(3):424-435

Pittenger MF, Mackay AM, Beck SC, Jaiswal RK, Doulas R, Mosca JD, Moorman MA, Simonetti DW, Craig S, Marshak DR. Multilineage potential of adult human mesenchymal stem cells. *Science,* (1999) 284(5411):143-147

Pittenger MF, Martin B. Mesenchymal stem cells and their potential as cardiac therapeutics. *Circulation Research,* (2004) 95:9-20

Prockop, DJ. Marrow stromal cells as stem cells for nonhematopoietic tissues. *Science,* (1997) 276(5309):71-74

Quesenberry PJ, Colvin GA, Lambert J. The chiaroscuro stem cell: A unified stem cell theory. *Blood,* (2002) 100(13):4266-4271

Ramsey WS, Herti W, Nowlan ED, Binkowski NJ, Surface Treatments and Cell Attachment. *In Vitro* (1984) 20(10):802-808

Ratajczad MZ, Kucia MM, Majka M, Reca R, Ratajczak J. Heterogeneous populations of bone marrow stem cells – are we spotting on the same cells from the different angles? *Folia Histochemica et Cytobiologica* (2004) 42(3):139-146

Reyes M, Dudek A, Jahagirdar B, Koodie L, Marker PH, Verfaillie CM. Origin of endothelial progenitors in human postnatal bone marrow. *J. Clin. Invest.* (2002) 109(3):337-346

Reyes M, Lund T, Lenvik T, Aguiar D, Koodie L, Verfaillie C. Purification and ex vivo expansion of postnatal human marrow mesodermal progenitors cells. *Blood,* (2001) 98(9):2615-2625

Reyes M, Verfaillie CM. Characterization of multipotent adult progenitor cells, a subpopulation of mesenchymal stem cells. *Ann. N. Y. Acad. Sci.,* (2003) 938:231-233

Romanov YA, Svintsitkaya VA, Smirnov VN. Searching for alternative sources of postnatal human mesenchymal stem cells: Candidate MSC-like cells from umbilical cord. *Stem Cells,* (2003) 21:105-110

Rubio D, Garcia-Castro J, Martin M, Fuente R, Cigudosa J, Lloyd A, Bernad A. Spontaneous human adult stem cell transformation. *Cancer Res.,* (2005) 65(8):3035-3039

Salim A, Nacamuli RP, Morgan EF, Giaccia AJ, Longaker MT. Transient Changes in oxygen tension inhibit osteogenic differentiation and Runx2 expression in osteoblasts. *J. Biological Chem.,* (2004) 279(38):40007-40016

Sanchez-Ramos J, Song S, Cardozo-Pelaez F, Hazzic C, Stedeford T, Willing A, Freeman TB, Saporta S, Janssen W, Patel N,. Cooper DR, Sanberg PR. Adult bone marrow stromal cells differentiate into neural cells in vitro. *Exp. Neurol.,* (2000) 164(2):247-256

Schiller P, D'Ippolito G. Multilineage-inducible cells and uses thereof. (2004) WO 2004/069172 A2, PCT/US2004/002480. Patent USPTO Applicaton #: 20060147426 - Class: 424093700 (USPTO)

Schop D, Janssen FW, Borgart E, de Bruijn JD, van Dijkhuizen-Radersma R. Expansion of mesenchymal stem cells using a microcarrier-based cultivation system: growth and metabolism. *J. Tissue Eng. Regen. Med.* (2008); 2(2-3)126–135

Schwartz RE, Reyes M, Koodie L, Jiang Y, Blackstad M, Lund T, Lenvik T, Johnson S, Hu W, Verfaillie CM. Multipotent adult progenitor cells from bone marrow differentiate into functional hepatocyte-like cells. *J. Clin. Invest.,* (2002) 109(10):1291-1302

Scott R, Gerontas S, Hussain W, Mason C, Veraitch F, Lye G. A Platform for predictive bioprocessing of autologous cells for therapy based on automated microwell cultures. Oral presentation at: Stem Cell Engineering, Coronado, California Jan 2007 (2007)

Sekiya I, Colter DC, Prockop DJ. BMP-6 enhancess chondrogenesis in a subpopulation of human marrow stromal cells. *Biochem. Biophys. Res. Commun.,* (2001) 284(8):411-418

Sekiya I, Larson B, Smith J, Pochampally R, Cui J, Prockop D. Expansion of human adult stem cells from bone marrow stroma: conditions that maximise the yields of early progenitors and evaluate their quality. *Stem Cells,* (2002) 20:530-541

Sen A, Kallos Ms, Behie La. New tissue dissociation protocol for scale-up production of neural stem cells in suspension bioreactors. *Tissue Eng.,* (2004) 10(5-6):904-913

Shan J, Xu J, Zou Q, Wang X, Zhu H. Comparison between microcarrier and ordinary method in culturing human mesenchymal stem cells in seed cell culture of massive bone defect. *Chinese Journal o.f Clinical Rehabilitation,* (2004) 8:4741-4743

Silva WA, Covas DT, Panepucci RA, Proto-Siqueira R, Siufi JLC, Zanette DL, Santos ARD, Zago MA. The profile of gene expression of human marrow mesenchymal stem cells. *Stem Cells,* (2003) 21:661-669

Simmons P, Torok-Storb B. CD34 expression by stromal precursors in normal human adult bone marrow. *Blood,* (1991) 78(11):2848–2853

Sinanan AC, Hunt NP, Lewis MP. Human adult craniofacial muscle-derived cells: neural-cell adhesion-molecule (NCAM; CD56)-expressing cells appear to contain multipotential stem cells. *Biotehcnol. Appl. Biochem*., (2004) 40(1):25-34

Smith JR, Pochampally R, Perry A, Hsu S, Prockop DJ. Isolation of a highly clonogenic and multipotential subfraction of adult stem cells from bone marrow stroma. *Stem Cells,* (2004) 22:823-831

Sotiropoulou PA, Perez SA, Salagianni M, Baxevanis C N, Papamichail M. Characterization of the Optimal Culture Conditions for Clinical Scale Production of Human Mesenchymal Stem Cells. *Stem Cell*s (2006) 24:462–471

Stolzing A, Scutt A. Age related impairment of mesenchymal progenitor cell function. *Aging Cell,* (2006) 5(3):213-224

Stolzing A, Sethe S, Scutt AM. Stressed Stem Cells: Temperature Response in Aged Mesenchymal Stem Cells. *Stem Cells and Development* (2006) 15(4):478-487

Stute N, Holtz K, Bubenheim M, Lange C, Blake F, Zander A. Autologous serum for isolation and expansion of human mesenchymal stem cells for clinical use. *Experimental Hematology*, (2004) 32(12):1212-1225

Taboas JM, Krebsbach PH, Hollister SJ. Mechanobiological regulation of human bone marrow stromal cell differentiation. Summer Bioengineering Conference (June 2003, Sonesta Beach Resort in Key Biscayne, Florida) (2003)

Takahashi K, Tanabe K, Ohnuki M, Narita M, Ichisaka T, Tomoda K, Yamanaka S. Induction of Pluripotent Stem Cells from Adult Human Fibroblasts by Defined Factors *J. Cell*, (2007) 131(5): 861-872

Terstegge S, Laufenberg I, Pochert J, Schenk S, Istkovitz-Eldor J, Endl E,. Brustle O. Automated maintenance of embryonic stem cell cultures. *Biotechnology Bioengineering,* (2006) 96(1)-1:195-201

Thomson, JA, Itskovitz-Eldor J, Shapiro SS, Waknitz MA, Swiergiel JJ, Marshall VS, Jones JM. Embryonic stem cell lines derived from human blastocysts. *Science* (1998) 282(5391):1145-1147

Tuan RS, Boland G, Tuli R. Adult mesenchymal stem cells and cell-based tissue engineering. *Arthritis Res and Ther.* (2003) 5(1):32-45

Tuli R, Tuli S, Nandi S, Wang ML, Alexander PG, Haleem-Smith H, Hozack WJ, Manner PA, Danielson KG, Tuan RS. Characterization of multipotential mesenchymal progenitor cells derived from human trabecular bone. *Stem Cells,* (2003) 21(6):681-693

Van Hemert P, Kilburn DG, van Wezel AL. Homogeneous cultivation of animal cells or the production of virus and virus products. *Biotehcol. Bioeng.,* (1969) 11(5):875-885

Veraitch FS, Scott R, Wong JW, Lye GJ, Mason C. The impact of manual processing on the expansion and directed differentiation of embryonic stem cells. (2008) 99(5):1216-1229

Verfaillie CM. Adult stem cells: assessing the case for pluripotency. *Trends in Cell Biol.,* (2002) 12(11):502-508

Weissman IL Translating stem and progenitor cell biology to the clinic: barriers and opportunities. *Science,* (2000) 287(5457):1442-1446

Westermark B. The deficient density-dependent growth control of human malignant glioma cells and virus-transformed glialike cells in culture. *Int. J. Cancer,* (1974) 12(2):438-451

Wexler SA, Donaldson C, Denning-Kendall P, Rice C, Bradley B, hHows, JM. Adult bone marrow is a rich source of human mesenchymal 'stem' cells but umbilical cord and mobilized adult blood are not. *British. Journal of. Haematology*, (2003) 121(2):368-374

Woodward WA, Chen MS, Behbod F, Rosen JM.. On mammary stem cells. *J. Cell Sci.,* (2005) 118(6):3585–3594.

Wu QF, Wu C, Dong B, Wang LS. Cultivation of human stem cells on macroporous CultiSpher G microcarriers. *J. Exp. Hematol*., (2003) 11(1):15-21

www.malvern.com/LabEng/technology/dynamic_light_scattering/dynamic_light_scattering.htm

Yeh SP Chang JG, Lin CL, Lo WJ, Lee CC, Lin CY, Chiu CF.. Mesenchymal stem cells can be isolated from bone marrow of patients with various haematological malignancies but the surface antigens expression may be changes after prolonged ex vivo culture. *Leukemia*, (2005) 19(8):1505-1507

Young HE, Black AC. Adult Stem Cells, The anatomical record. *Part A, Discoveries in molecular, cellular, and evolutionary biology* (2004) 276(1):75-102

Zhang, H., Lamping, S.R., Pickering, S.C.R., Lye, G.J. and Ayazi-Shamlou, P. Engineering characteriszation of a single well from 24- and 96- well microtitre plates. *Biochem. Eng. J.*, (2008) 40:138-149

Zhao F, Pathi P, Grayson W, Xing Q, Locke B, MaA. T. Effects of oxygen transport on 3-D human mesenchymal stem cell metabolic activity in perfusion and static cultures: Experiments and Mathematical Model. *Biotechnol. Prog.*, (2005) 21(4):1269-1280

Zimmermann S, Voss M, Kaiser S, Kapp U, Waller CF, Martens UM. Lack of telomerase activity in human mesenchymal stem cells. *Leukemia,* (2003) 17:1146-1149

Zohar R, Sodek J, McCulloch CA. Characterisation of stromal progenitor cells enriched by flow cytometry. *Blood,* (1997) 90(9):3471-3481

Zuk, PA, Zhu M, Mizuno H, Huang J, Futrell JW, Katz AJ, Benhaim P, Lorenz HP, Hedrick MH. Multilineage cells from human adipose tissue: implications for cell-based therapies. *Tissue Eng.,* (2001) 7(2):211-228

Zwietering M, Jongenburger I, Rombouts FM, Riet K. Modeling of the Bacterial Growth Curve. *Appl. Env. Microbiology*, (1990). 56(6):1875-1881

APPENDIX I

Relationship between inoculation cell density (ICD in cells/cm^2) and doubling time (Td) for hMSC from Donor X and Donor Y. Data collected for passage 2 for Donors X and Y and for passage 9 for Donor X.

Passage 2 - Donor X		Passage 2 - Donor Y		Passage 9 - Donor X	
ICD	Td (hr)	ICD	Td (hr)	ICD	Td (hr)
6864	84	10000	318	5000	446
3520	77	5000	142	1000	112
704	43	1000	74	100	89
70	33	100	44		
35	30	50	36		

APPENDIX II

Metabolic concentrations of Glutamine, Glutamate, Glucose, and Lactate (g/L) in the spent medium collected during frequent medium exchanges during the cell expansion process of hMSC inoculated at $4x10^3$ cells/cm^2 for the data represented in Figure 4.2.

Date Time	Glutamine	Glutamate	Glucose	Lactate
Feb 9, 2006 3:30PM	2.47	0.00	1.00	0.00
Feb 9, 2006 6:00PM	2.52	0.01	1.06	0.00
Feb 9, 2006 11:10PM	2.41	0.00	0.98	0.00
Feb 11, 2006 9:00AM	2.28	0.01	1.06	0.00
Feb 11, 2006 7:00PM	2.16	0.00	0.99	0.00
Feb 12, 2006 12:00AM	2.67	0.45	1.97	0.02
Feb 12, 2006 6:00AM	2.23	0.00	1.00	0.00
Feb 12, 2006 12:30PM	2.22	0.01	0.99	0.00
Feb 12, 2006, 1:50PM	2.28	0.06	1.08	0.01
Feb 13, 2006 6:15AM	2.49	0.04	1.05	0.01
Feb 14 2006, 12:15PM	2.33	0.01	0.95	0.00
Feb 14 2006, 6:00PM	2.31	0.02	1.01	0.00
Feb 15 2006, 5:40PM	2.37	0.02	1.01	0.00
Feb 16 2006, 5:00PM	2.33	0.05	1.07	0.06
Feb 17 2006, 1:00PM	2.45	0.01	0.99	0.00
Feb 17 2006, 5:00PM	2.61	0.00	1.01	0.00
Feb 19 2006, 12:10AM	2.18	0.02	0.89	0.03
Feb 19 2006, 7:00AM	2.27	0.05	0.94	0.00
Feb 19 2006, 7:10PM	2.32	0.04	0.99	0.00
Feb 20 2006, 12:05AM	2.43	0.09	1.17	0.13
Feb 20 2006, 8:00AM	2.33	0.08	1.01	0.02
Feb 20 2006, 1:10PM	2.32	0.03	0.94	0.00
Feb 20 2006, 11:20AM	2.53	0.00	0.94	0.00
Feb 21 2006, 7:15AM	2.50	0.01	0.88	0.00
Feb 21 2006, 12:15PM	2.56	0.00	0.94	0.00
Feb 21 2006, 6:00PM	2.61	0.05	1.03	0.35
Feb 23 2006, 5:20PM	1.96	0.00	0.41	0.21
Feb 28 2006, 6:00PM	2.12	0.00	0.50	0.04

Metabolic concentrations of Glutamine, Glutamate, Glucose, and Lactate (g/L) in the spent medium collected during medium exchanges performed every 3 days, during the cell expansion process of hMSC inoculated at $4x10^3$ cells/cm^2 for the data represented in Figure 4.2.

Date Time	Glutamine	Glutamate	Glucose	Lactate
Feb 9, 2006 3:30PM	2.47	0.00	1.00	0.00
Feb 11, 2006 9:00AM	1.82	0.15	1.03	0.10
Feb 12, 2006 1:50PM	1.71	0.29	1.15	0.13
Feb 13, 2006 6:15AM	2.42	0.06	1.01	0.25
Feb 14 2006, 4:30PM	2.01	0.07	1.02	0.10
Feb 15 2006, 5:40PM	1.72	0.04	0.82	0.04
Feb 16 2006, 5:00PM	1.64	0.06	0.89	0.21
Feb 17 2006, 5:00PM	1.91	0.00	0.79	0.00
Feb 19 2006, 7:10PM	1.59	0.04	0.72	0.03
Feb 20 2006, 1:10PM	1.42	0.03	0.73	0.29
Feb 21 2006, 3:50PM	2.24	0.06	0.97	0.45
Feb 23 2006, 5:20PM	1.81	0.00	0.64	0.02
Feb 24 2006, 4:00PM	1.65	0.00	0.58	0.35
Feb 28 2006, 6:00PM	1.65	0.00	0.46	0.18

Metabolic concentrations of Glutamine, Glutamate, Glucose, and Lactate (g/L) in the spent medium collected during medium exchanges performed every 3 days, during the cell expansion process of hMSC inoculated at $1x10^2$ cells/cm^2 for the data represented in Figure 4.2.

Date Time	Glutamine	Glutamate	Glucose	Lactate
Feb 9, 2006 3:30PM	2.47	0.00	1.00	0.00
Feb 11, 2006 9:00AM	1.89	0.02	1.02	0.00
Feb 12, 2006 1:50PM	1.79	0.07	1.06	0.00
Feb 13, 2006 6:15AM	2.30	0.08	1.11	0.20
Feb 14 2006, 4:30PM	2.04	0.01	1.02	0.00
Feb 16 2006, 5:00PM	1.72	0.07	1.06	0.00
Feb 17 2006, 5:00PM	2.36	0.00	1.02	0.00
Feb 19 2006, 7:10PM	1.77	0.05	1.01	0.00
Feb 20 2006, 1:10PM	1.54	0.07	1.07	0.01
Feb 21 2006, 3:50PM	2.36	0.07	0.99	0.21
Feb 23 2006, 5:20PM	1.86	0.01	0.84	0.00
Feb 24 2006, 4:00PM	1.62	0.04	0.83	0.00
Feb 28 2006, 6:00PM	1.70	0.00	0.57	0.08

APPENDIX III

The effect of cell growth phase on subcultivation. Cells recovered from passage zero during mid-exponential phase, as well as cells recovered from the same culture during stationary phase were seeded into 24 well-plates at a seeding density of $5x10^3$ cells/cm^2. Growth curves from the two cultures, passage one with inoculum from stationary phase, and passage one with inoculum from mid-exponential phase are shown in figure below.

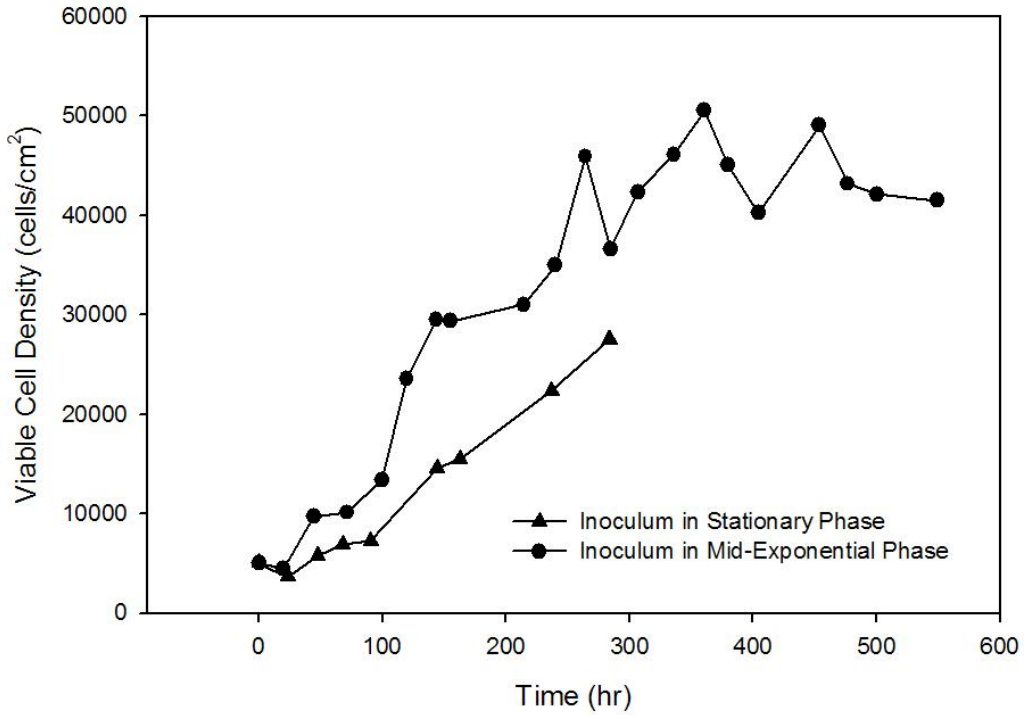

The growth curves generated from each of these cultures indicate a difference in growth, showing slower growth for those cells originated from the stationary phase of growth from the previous passage. This culture also appears to exhibit a longer lag phase during the first 100 hr in culture when compared to the culture seeded from cells originated from the mid-exponential phase from the previous passage.